EXPERIMENTAL AND PETROLOGICAL STUDIES ON AMPHIBOLES IN ULTRABASIC ROCKS

by

R. GRANT CAWTHORN B.Sc. (Dunelm)

Thesis presented for the Degree of Doctor of Philosophy
of the University of Edinburgh in the Faculty of Science.

1973

ABSTRACT

Basic and ultrabasic rocks from many geological environments contain an igneous amphibole. Geochemical evidence suggests that pargasite, kaersutite or hornblende may exist in the upper mantle. Partial melts produced from hydrous and anhydrous ultrabasic material differ. Data show that the subsequent crystallisation of amphibole from hydrous basic magma is important in determining the evolution of certain liquids.

Experimental work on synthetic compositions within the system CaO - MgO - Al_2O_3 - SiO_2 - Na_2O - H_2O in equilibria involving forsterite - calcium-rich pyroxene - orthopyroxene - amphibole - plagioclase - spinel - liquid - vapour under 5 kb pressure is presented. Two previously accepted thermal divide zones, involving forsterite - calcium-rich pyroxene - plagioclase and calcium-rich pyroxene - orthopyroxene - plagioclase, stable under 5 kb under dry conditions were not encountered in the presence of water vapour. Amphibole was not stable with liquids containing less than 3% Na_2O. A thermal maximum for the assemblage forsterite - calcium-rich pyroxene - amphibole - liquid - vapour exists for compositions containing at least 10% normative nepheline. Forsterite - calcium-rich pyroxene - amphibole - vapour co-exist with quartz-normative liquids. Hence, silica-undersaturated liquids may crystallise in this equilibrium to produce silica-oversaturated residua. Forsterite and calcium-rich pyroxene are in reaction relationship with the liquid once amphibole becomes stable. Amphibole and plagioclase are

likely to be the main crystallising phases from andesitic compositions under these conditions. The equilibrium forsterite - calcium-rich pyroxene - orthopyroxene - amphibole - plagioclase - liquid - vapour occurs at 960 $\pm$ 12°C under 5 kb pressure, and contains a plagioclase more calcic than An_{87}. The liquid contains 16.5% normative quartz.

The similarity between this synthetic and other natural experimental studies under comparable conditions suggests that the phase diagrams produced here may be applied to natural material.

Some andesitic and anorthositic compositions project close to the olivine - calcium-rich pyroxene - orthopyroxene - amphibole - plagioclase - liquid - vapour thermal minimum in these diagrams, and they can be related to the postulated parental magmas by crystallisation of amphibole $\pm$ olivine $\pm$ calcium-rich pyroxene. Crystallisation of these phases from a more primitive magma produced at greater depth can explain many of the important chemical and physical characteristics of these two suites.

CONTENTS

CHAPTER 1

INTRODUCTION

Occurrence of amphibole in igneous rocks

Amphibole has been reported as an igneous mineral in rocks ranging from ultrabasic to acidic. It is the intention of this study to consider the role of this mineral in ultrabasic and certain basic compositions only. Generally, amphiboles occur as accessory or subordinate minerals in basic compositions (Brown, 1967). Because they are stabilised by water pressure, they tend to occur more frequently in intrusive bodies or in late stage volcanic differentiates than in early extrusive material. However, there are several instances of essential amphibole appearing throughout a volcanic sequence in which it is thought to play an important petrogenetic role (Wilkinson, 1961; Aoki, 1963 and 1971; Mason, 1966 and 1968; Baker, 1968; Binns et al., 1970; Borley et al., 1971). It is usually found in alkaline basaltic provinces.

As a result of the explosive nature of these eruptions, nodules and blocks of cumulus material, thought to be co-magmatic with the volcanic liquids, are often observed to contain amphibole together with a variety of other minerals (Wager, 1962; Yamazaki et al., 1966; Baker, 1968; LeMaitre, 1969; Aoki, 1970; Lewis, 1973).

Amphibole is a frequent constituent of ultrabasic material, although in many instances it is difficult to demonstrate whether it is igneous or metamorphic. Those

containing an igneous amphibole may be divided into three groups.

1) Layered intrusive bodies

The most simply explained amphibole-bearing ultrabasic rocks are of the type described by Hawkins (1965 and 1970) and Cattermole (1969). The lower divisions of layered basic intrusions from Caernarvonshire contain cumulus olivine and augite and intercumulus amphibole. They grade upwards into hornblende gabbros.

Possibly similar to these is the Connemara peridotite (Leake, 1970) which contains an igneous amphibole as well as a metamorphic amphibole formed by the recrystallisation of clinopyroxene. Borisenko (1967) reports pyroxene- and amphibole-bearing ultramafic layers underlying gabbroic rocks in the Ural mountains thought to represent a fractionally crystallised sequence.

Bodies which may have a similar origin, but are of a different shape, are the stock-like intrusions in Alaska (Ruckmick & Noble, 1959), where a central core of peridotite grades outwards into pyroxenite- and amphibole-rich layers. A metasomatic origin for these layers is possible, but fractional crystallisation is equally plausible. Nakamura (1971) describes a similar intrusion from Japan.

Some of the bodies of the appinitic suite of Scotland and Ireland belong to this group, although the suite covers a wide range of compositions and mineral assemblages (Hall, 1967; Westoll, 1968).

2) Nodules

Nodules of ultrabasic material containing amphibole have been reported from a variety of volcanic provinces. The spinel peridotite, hornblende peridotite and gabbro nodules reported by Aoki (1963, 1968 and 1970) are interpreted as the result of fractional crystallisation of an alkali basaltic magma at various depths.

Some of the nodules described by Baker (1968) and LeMaitre (1969) fall into this category. Blocks from volcanics in the Auvergne, France are often composed almost entirely of hornblende (Collée, 1963; F. Conquéré, personal communication). Amphibole peridotite nodules are also observed in the Carboniferous volcanic sequence of Fifeshire (N.A. Chapman, in preparation); in the Red Sea volcanics (Gass et al., 1965), in tuffs from Ireland (Coe, 1966), from Nevada (Trask, 1969), from Arizona (Best, 1970) and Northern Tanzania (Dawson et al., 1970). These have been discussed by Dawson & Smith (1973).

3) Upper mantle

Various occurrences of amphibole peridotite bodies have been interpreted as samples of upper mantle. Inclusions reported by Varne (1970) from a cinder cone in Aden are thought by him to be representative upper mantle. Whether such instances should be included in this section or regarded as nodules is debatable, but they all tend to support the argument that amphibole may be involved in certain igneous processes.

Hornblende peridotite - spinel peridotite assemblages

from St. Peter and St. Paul Rocks in the Atlantic have been described by Melson & Jarosewich (1967) and Tilley & Long (1967). These may be a mylonitised, recrystallised fragment of virgin or barren upper mantle.

Conquéré (1971) described an amphibole, olivine, orthopyroxene rock from Caussou, France intruding spinel lherzolite. He suggested that this may be the result of localised melting or metasomatism, and that the whole complex was a mobilised wedge of upper mantle.

A hornblende peridotite - gabbro complex near Finero, Northern Italy has been interpreted by Lensch (1968) as an upturned slice of upper mantle, while Vogt (1962) regarded it as an alpine-type metamorphosed peridotite. These alternatives are questioned (Cawthorn, in preparation) and an origin by fractional crystallisation preferred.

Many orogenic areas contain ophiolite complexes, a series of interbanded peridotites (or serpentinites), pillow lavas and cherts, which may represent a section through the oceanic crust and uppermost mantle (Moores, 1969 and 1970; Church & Stevens, 1971; Coleman, 1971; Dewey & Bird, 1971; Williams, 1971). It is often difficult to interpret initial igneous mineral assemblages because of metamorphism and tectonism. However, it is suggested that amphibole is an igneous material within some of the heterogeneous banded ultramafic horizons (Church & Stevens, 1971).

Stability of amphibole

Rubey (1951) presented some calculations which suggested that the interior of the earth was gradually degassing, losing mainly water. It was not until 1964 that Oxburgh postulated the existence of amphibole in the mantle on other geochemical grounds, which could act as a source for this water. Since then the stability limits of amphibole, both by itself and in various mineral assemblages, have been the subject of much investigation.

Boyd (1959) studied the low-pressure stability of synthetic pargasite, and various other amphibole end-member compositions have been investigated subsequently (Greenwood, 1963; Ernst, 1966; Gilbert, 1966 and 1968; Kushiro & Erlank, 1970) at temperatures up to the beginning of melting or decomposition. J.R Holloway (in press) studied the stability of pargasite at pressures from 1.2 - 8 kb, with varying partial pressures of water. The data suggest that some amphiboles may be stable at igneous temperatures under water pressures of less than 1 kb. As such pressures may easily be exceeded even in the necks of volcanos (Fudali & Melson, 1972) the minimum depth above which amphibole becomes unstable is extremely shallow.

The maximum depth at which it is stable is of importance in terms of interpreting such properties in the mantle as the low velocity zone, and in geochemical and petrological processes. Nishikawa et al. (1971) have studied the upper stability limits of a natural amphibole and conclude that the $\frac{dT}{dP}$ of its breakdown curve becomes negative at about 28 kb.

At higher pressures its thermal stability rapidly decreases.

Kushiro (1970) investigated the stability of amphibole in ultrabasic assemblages and concluded that amphibole lherzolite is stable up to the solidus only to 18 kb and 1000°C.

Comparison with anhydrous ultrabasic mineral assemblages (O'Hara, 1967) suggests that the amphibole lherzolite stability range replaces the spinel lherzolite facies and also overlaps into the plagioclase and garnet lherzolite stability fields.

Kushiro (1970) and Nishikawa et al. (1971) experimented under water-saturated conditions, and Kushiro (1970) suggested that under water-undersaturated conditions the thermal stability of amphibole might decrease.

Lambert & Wyllie (1968 and 1972) studied the stability of amphibole in basic compositions and found an upper stability limit similar to that reported by Kushiro (1970). Wyllie (1970) discussed how small water contents may affect the beginning of melting of basic and ultrabasic material, but implied there was no significant change relative to the water-saturated conditions in the stability limits of amphibole.

D.H. Green & Ringwood (1967a), investigating the gabbro to eclogite transition, performed some exploratory runs with basic compositions in the presence of small amounts of water. Their data suggest that amphibole is stable up to at least 17 kb and 1100°C, indicating an increase in its thermal stability relative to the water-saturated conditions.

Products of partial melting of amphibole-bearing mineral assemblages

Yoder & Tilley (1962) presented hydrous melting data for a range of basic compositions under various pressures. They concluded that the first liquid formed in the pressure range 2 - 10 kb would be extremely feldspathic. Subsequent work by Holloway & Burnham (1972) suggested that liquids in equilibrium with olivine, clinopyroxene and amphibole derived from a basaltic source may be andesitic. They also suggested that amphibole may have a higher stability limit under water-undersaturated than water-saturated conditions, although this has been questioned by Cawthorn et al. (1973).

T.H. Green & Ringwood (1968) carried out preliminary investigations into liquids produced by melting of basic material in the presence of a small, but uncontrolled, content of water. Amphibole was found together with pyroxenes and plagioclase at 10 kb and 1000°C. Calculations implied the residual liquid might be andesitic.

Using synthetic material, Kushiro (1972) has reported amphibole together with a garnet websterite assemblage at 1000°C and 20 kb, and shows that at a slightly higher temperature very similar compositions may produce quartz-normative liquids in equilibrium with lherzolite.

Bultitude & Green (1967) and D.H. Green (1969 and 1971) have suggested that under water-undersaturated conditions orthopyroxene may be stable in natural silica-undersaturated compositions under total pressures of about 20 kb. This appears to be in direct conflict with the data of Kushiro (1972) which suggests that orthopyroxene melts

incongruently at this pressure in the presence of excess water. In reconciliation, Green (1971) suggested that the addition of a small water pressure causes an increase in the orthopyroxene stability field relative to the anhydrous system, but as water pressure approaches total pressure there is an extremely rapid decrease in its stability. This hypothesis lacks controlled experimental evidence. Two alternative explanations are possible. If silica were extremely soluble in hydrous vapour relative to the other oxides under the conditions of the experiments of Kushiro (1972) the remaining bulk composition (liquid plus solid phases) would be less siliceous than implied by the projection of the composition in his Figs. 1 and 4. This would cause an apparent expansion of the forsterite stability field in these diagrams. Bultitude & Green (1967) and Green (1969) carried out experiments with natural material using platinum and graphite capsules. Solution of iron into the platinum is expected, and the reducing conditions of the graphite container may cause iron droplet precipitation. Removal of iron from the bulk composition would cause the degree of silica-saturation of the remaining material to increase, resulting in the early appearance of orthopyroxene. Open capsules were used for most of the runs and so contamination or escape of material is possible, thereby affecting the bulk composition. It is not possible to decide which, if either, of these alternatives explains the conflict.

Purpose of the experimental work

The previous sections suggest that amphibole is likely to occur in the upper mantle, and that it may influence the composition of magmas either by its involvement in partial melting or fractional crystallisation processes.

Previous studies have concentrated on the phase equilibria of certain specific compositions in the presence of water under various pressures. It is not possible to predict the crystallisation history under hydrous conditions of any random composition from these data. The intention of this study, therefore, is to investigate the stability of amphibole over a wide range of compositions and to map the phase relationships so that such predictions become possible, and liquid evolution paths may be inferred. It is then proposed to re-examine the distinctive characteristics of calc-alkaline and anorthositic magmas to see if the results of this study may contribute to a model for their formation.

CHAPTER 2

EXPERIMENTAL WORK - I

COMPOSITIONS, CONDITIONS, REPRESENTATION OF DATA

Choice of chemical system

Evaluating the significance of each individual component of natural materials in the melting relationships of basic and ultrabasic compositions is extremely difficult because of the large numbers of components involved, some of which are present only in small, but perhaps crucial quantity, e.g. TiO_2, Cr_2O_3, Na_2O, K_2O, CO_2, H_2O, P_2O_5, S. For this reason, simplified systems are often used to elucidate the effects of various components. The 4-component system CaO - MgO - Al_2O_3 - SiO_2 has been studied widely, as analogues of most of the common minerals of proposed upper mantle models and those found in basic rocks can be synthesised in this system.

The awareness of the possible influence of water on equilibrium phase relationships has led to the extension of this system to 5 components by the addition of water (Yoder & Chinner, 1960; Yoder, 1965 and 1966; Yoder & Dickey, 1971; Ford & O'Hara, 1972). Amphibole has been synthesised in some of these experiments, but, as reported by Yoder & Chinner (1960), its composition probably lies within the tremolite - tschermakite - gedrite - anthophyllite volume. Amphiboles found as igneous minerals in basic and ultrabasic rocks belong to the pargasite group and contain essential soda.*

Hence, a part of the 6-component system CaO - MgO -

---

* Soda refers to Na_2O.

Isobaric invariant equilibria in a 6-component system may also be demonstrated in a pseudoternary diagram if three projection phases can be found. In this study it is possible to project some of the run data from forsterite, orthopyroxene and vapour into the plane C - A - N to display the stability relationships between clinopyroxene,* amphibole, plagioclase and spinel in forsterite-orthopyroxene-vapour-saturated equilibria. As olivine and orthopyroxene are ubiquitous phases in the upper mantle this projection is of specific interest in consideration of partial melts from a hydrous mantle.

---

* Clinopyroxene refers to any calcium-rich pyroxene. Diopside is used only when the formula CMS_2 is implied. Orthopyroxene is calcium-poor pyroxene. Enstatite is used for the composition MS.

Al_2O_3 - SiO_2 - Na_2O - H_2O, henceforth referred to as C - M - A - S - N - H, has been chosen to study the equilibrium melting relationships involving synthetic amphibole lherzolite and related mineral assemblages.

Experimental conditions

Kushiro (1972) has studied part of this 6-component system in the pressure range 13 - 35 kb, with particular emphasis on the compositions of the liquids produced by partial melting of forsterite-orthopyroxene-bearing assemblages. However, as such primitive magmas are unlikely to be erupted unmodified, constraints upon the evolution of these liquids at lower pressures require investigation.

Studies on subsystems in C - M - A - S - H by Yoder (1965) on anorthite - diopside - water, by Yoder (1966) on anorthite - forsterite - water, by Yoder & Dickey (1971) on part of the join diopside - pyrope - water, and by Ford & O'Hara (1972) on enstatite - grossular - water have been conducted at 5 kb water pressure. This provides an excellent framework for examining the effect of adding soda to this system.

Compositions containing C - M - A - S - N can be prepared with acceptable accuracy by a gel technique (see Appendix B). Precise control of water content during experimental runs is extremely difficult. Water-saturated conditions were used in all the previously mentioned studies. Similar conditions were chosen for this work so results would be directly comparable.

The experimental procedure and operating conditions are explained in Appendix B.

Representation of data

The main purpose of experimental work is to provide a framework of data within which the crystallisation sequence of various compositions may be predicted. Tables of experimental data for individual compositions convey little idea of how variation of composition affects melting behaviour. Some form of diagrammatic representation is required in which crystallisation sequences can be portrayed and compared with data from other relevant studies.

In multi-component systems two diagrammatic schemes have been developed for presenting phase equilibria involving basaltic liquids. Projection of compositions into the basalt tetrahedron was initially discussed by Yoder & Tilley (1962) and developed by O'Hara (1965) and Clarke (1970). Recalculation of compositions into the system analogous to C - M - A - S was suggested by O'Hara (1968) and designated XO - YO - R_2O_3 - ZO_2 by Jamieson (1969) who described the principle and effects of the recalculation in some detail. Projections within this system are employed for diagrammatic representation of phase relationships.

In this study, projection of data from soda and water reduces the system to 4 remaining components which may be treated in projection diagrams as described by O'Hara (1968). A detailed discussion of the theoretical arguments and principles is presented in Appendix A.

CHAPTER 3

EXPERIMENTAL WORK - II

RESULTS, PHASE EQUILIBRIA, MINERAL COMPOSITIONS, PROJECTION DIAGRAMS

The experimental procedure is described in Appendix B. The analysis of the gels prepared are given in Appendix D, and the results presented in detail in Appendix E.

Pargasite stability

Ideal pargasite compositions - $NC_4A_3M_8S_{12}H_2$ - have been studied by Boyd (1959) and Holloway (in press). The iron-bearing analogue was studied at various oxygen fugacities by Gilbert (1966), and a natural hornblende was studied to high pressure by Nishikawa *et al.*,(1971). Their results are presented in Fig. 3.1.

The results of this study are also shown in this figure and correlate closely with the data of Holloway (in press), except that nepheline is not observed, and that spinel forms at subsolidus temperatures possibly as a metastable phase growing on nuclei observed in the initial gel. Analyses of the amphibole in this study are presented in Table 3.1, where they are compared with the ideal formula. The extremely small amounts of glass observed at temperatures below the beginning of extensive melting of theoretical pargasite composition may reflect the difference between the ideal and actual composition of the amphiboles. Alternatively, it may be attributable to slight inhomogeneities in the charge.

FIG. 3.1

Stability of amphibole

Results of experimental studies on the stability of various hornblendic amphibole compositions carried out under water-saturated conditions. Materials used by Boyd (1959), J.R. Holloway (in press) and this study were synthetic pargasite compositions; by Gilbert (1966) were synthetic iron-pargasite (highest stability shown here at an oxygen fugacity produced by an iron-wüstite buffer); and by Nishikawa et al. (1971) was a natural hornblende.

Log. scale is used for the abscissa to clarify the low pressure region.

Abbreviations: Amph - amphibole (pargasitic); An - anorthite (terminology of Boyd (1959), mineral contains soda); Cpx - aluminous clinopyroxene; Fa - fayalite; Fe-amph - amphibole (iron pargasitic); Fo - forsterite; Gr - garnet (pyropic); Hb - hornblende; Hc - hercynite; Hd - aluminous hedenbergite; L - liquid; Ne - nepheline; Plag - plagioclase; Sp - spinel (sensu stricto); V - vapour.

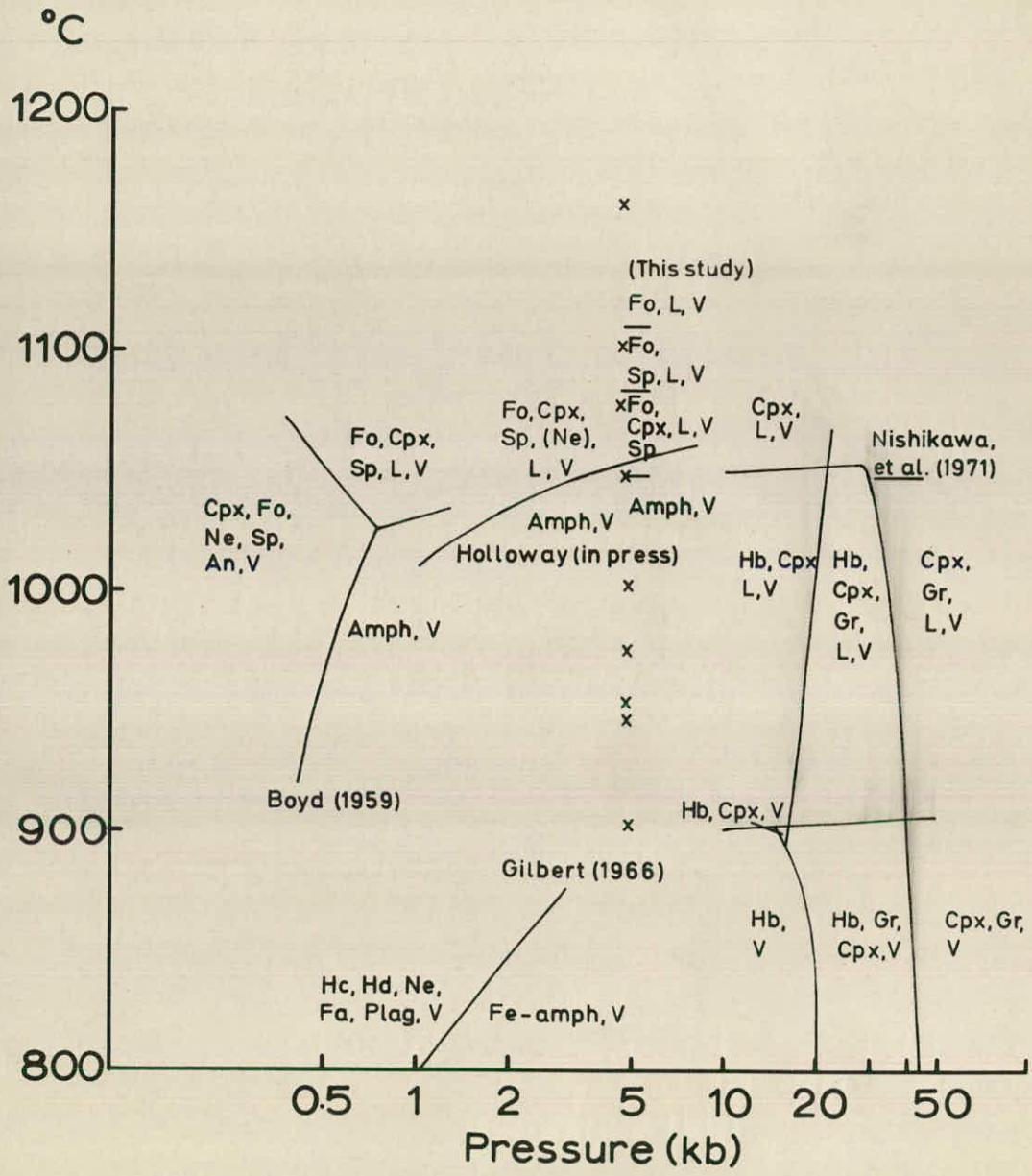
°C
1200
1100
1000
900
800
0.5
1
2
5
10
20
50
Pressure (kb)
(This study)
Fo, L, V
xFo,
Sp, L, V
xFo,
Cpx, L, V
Sp
Fo, Cpx,
Sp, (Ne),
L, V
Fo, Cpx,
Sp, L, V
Cpx, Fo,
Ne, Sp,
An, V
Amph, V
Amph, V
Holloway (in press)
Amph, V
Boyd (1959)
Cpx,
L, V
Nishikawa,
et al. (1971)
Hb, Cpx
L, V
Hb,
Cpx,
Gr,
L, V
Cpx,
Gr,
L, V
Hb, Cpx, V
Gilbert (1966)
Hb,
V
Hb, Gr,
Cpx, V
Cpx, Gr,
V
Hc, Hd, Ne,
Fa, Plag, V
Fe-amph, V

TABLE 3.1

Analysis of amphibole from recrystallised pargasite gel from run 56, temperature 954°C, water pressure 5 kb.

	1	2	3
SiO_2 (wt %)	43.13	44.5	44.4
Al_2O_3	18.30	19.2	19.7
MgO	19.29	19.3	18.9
CaO	13.42	13.9	13.9
Na_2O	3.71	3.3	3.3
H_2O	2.15		
Total	100.00	100.2	100.2

Structural formulae (calculated on 23 oxygen ions)

Si	6.00	6.03	6.01
Al(Tet)	2.00	1.97	1.99
Al(Oct)	1.00	1.09	1.15
Mg	4.00	3.90	3.81
Ca	2.00	2.02	2.02
Na	1.00	0.87	0.87

X + Y site occupancy

7.00	7.01	6.98

1 - Ideal pargasite analysis

2 - Electron microprobe analysis of fine-grained part of charge

3 - Analysis of coarse-grained material occurring near vapour bubbles in the charge.

That spinel is the second phase to crystallise from the pargasite composition is important in the construction of Fig. 3.12e.

Amphibole stability in basaltic compositions

The stability of amphibole in various synthetic basaltic compositions studied here is displayed in Fig. 3.2a. The chosen compositions differ only in silica content and hence their equilibrium phase relationships may be shown in a pseudobinary join, showing difference in silica in weight percent. The C.I.P.W. norms of these compositions are presented in Fig. 3.2b.

The main features of this diagram are:-

1) Forsterite is the near-liquidus mineral even for quartz-normative compositions. Orthopyroxene is not observed despite up to 18% normative enstatite in the most siliceous composition.

2) Clinopyroxene crystallises as the second phase and is followed by amphibole whose thermal stability is sensitive to the bulk composition. A thermal maximum is observed in the equilibrium forsterite - clinopyroxene - amphibole - liquid - vapour for compositions containing about 10% normative nepheline.

3) Forsterite and clinopyroxene are in reaction relationship with the liquid once amphibole becomes stable.

4) Nepheline crystallises from the extremely silica-undersaturated compositions while plagioclase appears in all other compositions.

FIG 3.2

a. Results of experimental runs at 5 kb water pressure on the pseudobinary join:-

$N_{0.36}C_2M_3AS_{4.3}$ - $N_{0.36}C_2M_3AS_{7.9}$

Numbers along the ordinate refer to percent SiO_2 in the anhydrous gels, which are designated by their silica content.

Abbreviations: Amph - amphibole; Cpx - clinopyroxene (alumina-bearing); Fo - Forsterite; Mica - Mica of unidentified composition; Neph - nepheline; Opx - orthopyroxene (alumina-bearing); Plag - plagioclase; Sp - spinel (sensu stricto).

Upper case lettering is used for subsolidus assemblages.

Mineral names overlined indicate reaction relationship with liquid on cooling.

Thin lines indicate soda contents of the liquids.

b. Normative values of compositions studied in this pseudobinary join.

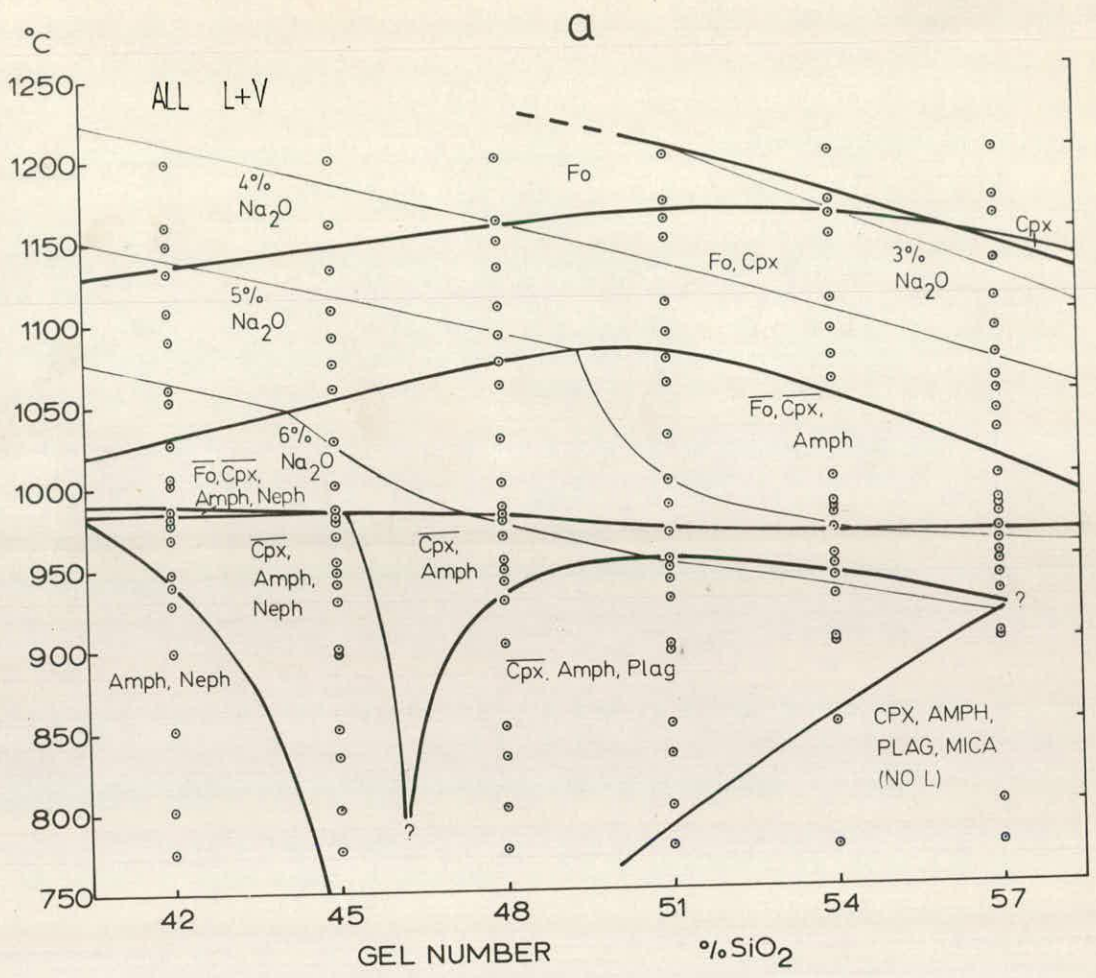
a
°C
ALL L+V
1250
1200
1150
1100
1050
1000
950
900
850
800
750
4% Na2O
5% Na2O
6% Na2O
Fo
Fo, Cpx
Cpx
3% Na2O
Fo, Cpx, Amph
Fo, Cpx, Amph, Neph
Cpx, Amph, Neph
Cpx, Amph
Amph, Neph
Cpx, Amph, Plag
CPX, AMPH, PLAG, MICA (NO L)
?
42
45
48
51
54
57
GEL NUMBER
%SiO2

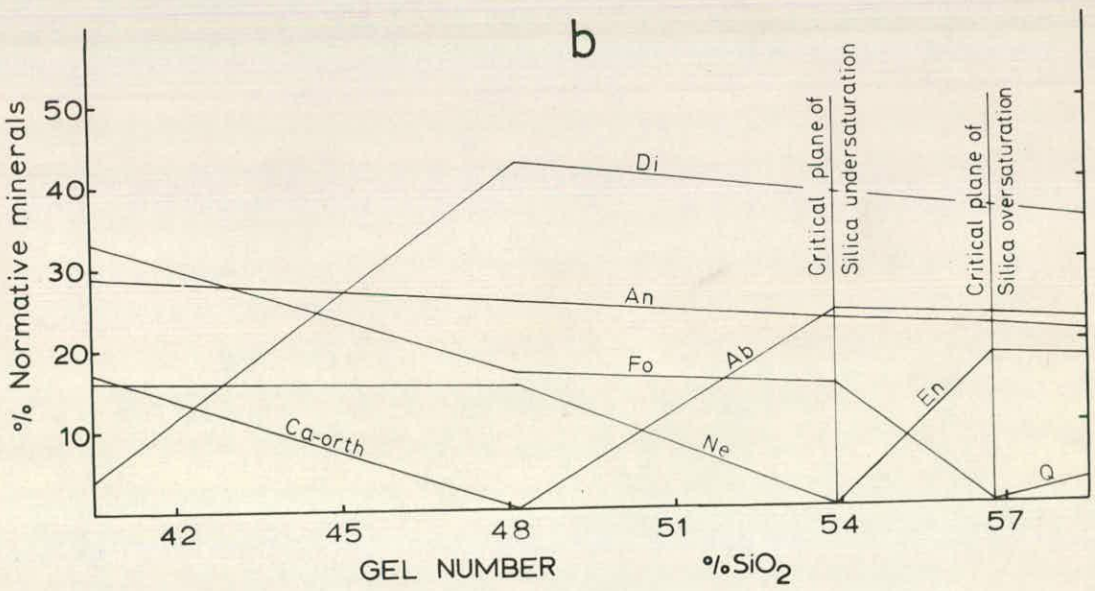
b
% Normative minerals
50
40
30
20
10
Di
An
Fo
Ab
En
Ne
Ca-orth
Q
Critical plane of Silica undersaturation
Critical plane of Silica oversaturation
42
45
48
51
54
57
GEL NUMBER
%SiO2

Superimposed on Fig. 3.2a and all subsequent phase diagrams, are the concentrations of soda in the liquids in the various equilibria. These have been calculated as described in Appendix A, and are of paramount importance in the construction of the projection diagrams.

The critical planes of silica-undersaturation and silica-oversaturation, shown in Fig. 3.2b, may act as thermal divides in the anhydrous system at 5 kb (O'Hara, 1968). The relevant equilibria, forsterite - clinopyroxene - plagioclase and two pyroxenes - plagioclase, are not observed in Fig. 3.2a, and hence these divides may break down under water-saturated conditions.

The hypothesis of Aoki (1970) that amphibole has a higher thermal stability in silica-undersaturated than silica-saturated compositions is supported by the present data (Fig. 3.2a).

Amphibole stability in ultrabasic compositions

Compositions in a second pseudobinary join were used to investigate equilibria involving forsterite, orthopyroxene and liquid. These were prepared by adding to each of the compositions in Fig. 3.2 an equal weight of an enstatite gel. Their C.I.P.W. norms are shown in Fig. 3.3b.

The results are shown in Fig. 3.3a. Forsterite is thought to be the liquidus mineral for all compositions. The important equilibria involving forsterite - two pyroxenes - amphibole - liquid - vapour are observed over a wide range of compositions. Plagioclase is stable only after the

FIG. 3.3

a. Results from experimental runs at 5 kb water pressure on the pseudobinary join:-

$$N_{0.36}C_2M_{9.13}AS_{10.47} - N_{0.36}C_2M_{11.30}AS_{16.20}$$

Gels referred to along the ordinate are prepared from equal weights of gels shown in Fig. 3.2a and enstatite gel.

Abbreviations and explanation as for Fig. 3.2a.

b. Normative values of compositions studied in this pseudobinary join.

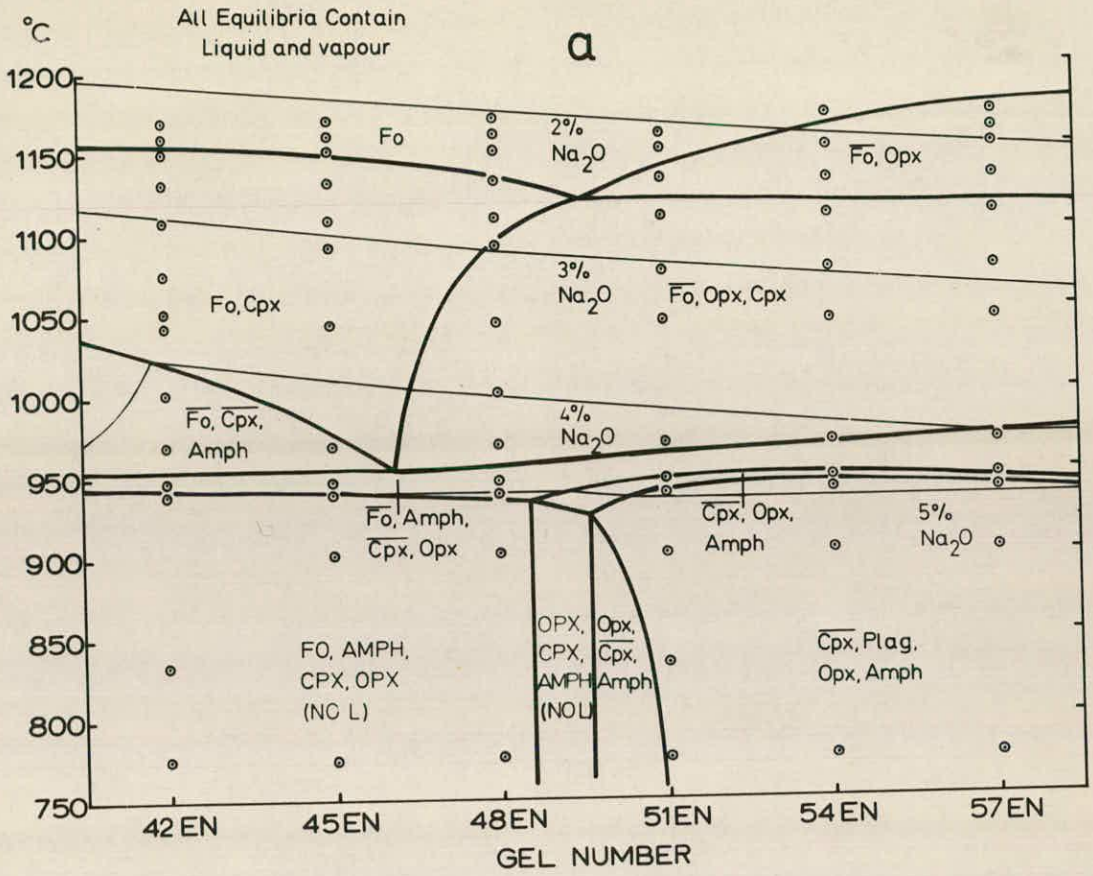
°C
All Equilibria Contain
Liquid and vapour
a
1200
1150
1100
1050
1000
950
900
850
800
750
Fo
2%
Na2O
Fo, Opx
Fo, Cpx
3%
Na2O
Fo, Opx, Cpx
Fo, Cpx,
Amph
4%
Na2O
Fo, Amph,
Cpx, Opx
Cpx, Opx,
Amph
5%
Na2O
FO, AMPH,
CPX, OPX
(NO L)
OPX, Opx,
CPX, Cpx,
AMPH, Amph
(NO L)
Cpx, Plag,
Opx, Amph
42 EN
45EN
48EN
51EN
54 EN
57EN
GEL NUMBER

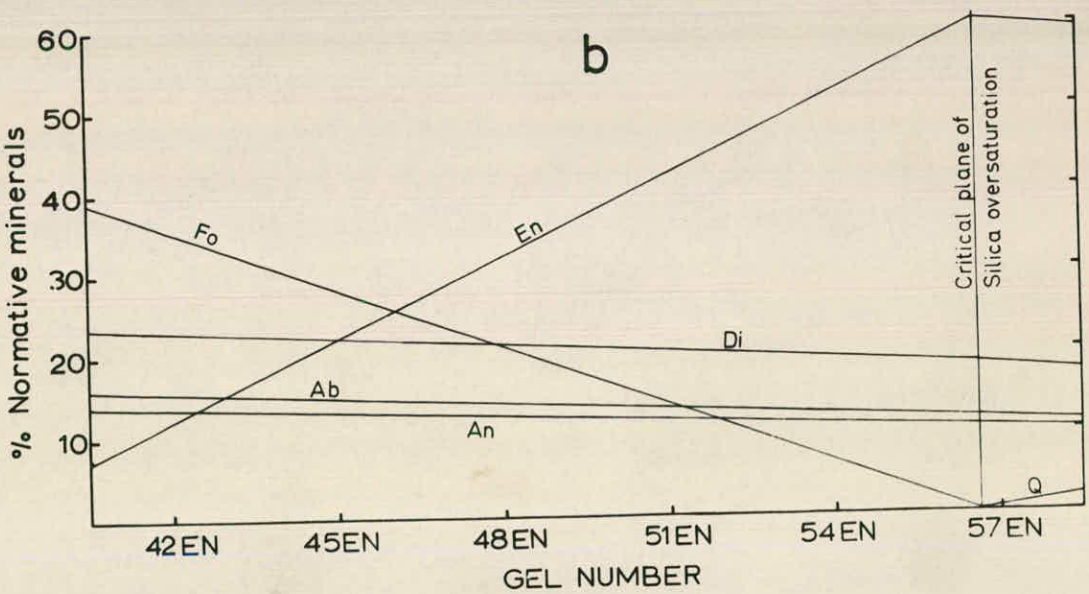
b
% Normative minerals
60
50
40
30
20
10
Fo
En
Di
Ab
An
Q
Critical plane of
Silica oversaturation
42 EN
45EN
48EN
51EN
54 EN
57EN
GEL NUMBER

disappearance of forsterite. Again, the equilibria in the two thermal divides, mentioned in the previous section, are not observed.

Effect of variable soda content on phase relationships

Series of gels were prepared, such that each series of three gels had a fixed C - M - A - S ratio and contained 1, 3 or 6% soda. The effect of variable soda content on various equilibria can be investigated with these compositions.

Gel Series 1

These are designed to delimit the extent of the plagioclase and amphibole stability fields in aluminous-rich liquids, and to yield residual liquids which approach the forsterite - orthopyroxene - plagioclase - amphibole ± spinel - liquid - vapour isobaric invariant equilibrium.

The results and C.I.P.W. norms of the compositions are shown in Figs. 3.4a and 3.4b. The stability of spinel, the liquidus mineral for most compositions, decreases with increasing soda. Forsterite crystallises second from most compositions and is in reaction relationship with the liquid to produce orthopyroxene in the soda-poor charges and amphibole at higher soda contents. The stability of orthopyroxene is limited, and forsterite crystallises at higher temperature even in quartz-normative compositions. The amphibole stability increases with increasing soda content while most other minerals show the reverse trend. Clinopyroxene begins to crystallise after amphibole in the

FIG. 3.4.

a. Results of experimental runs at 5 kb water pressure on gel compositions $C_7M_7A_8S_{24}$ containing various soda levels.

Abbreviations and explanation as for Fig. 3.2a.

b. Normative values of compositions studied in this pseudobinary join.

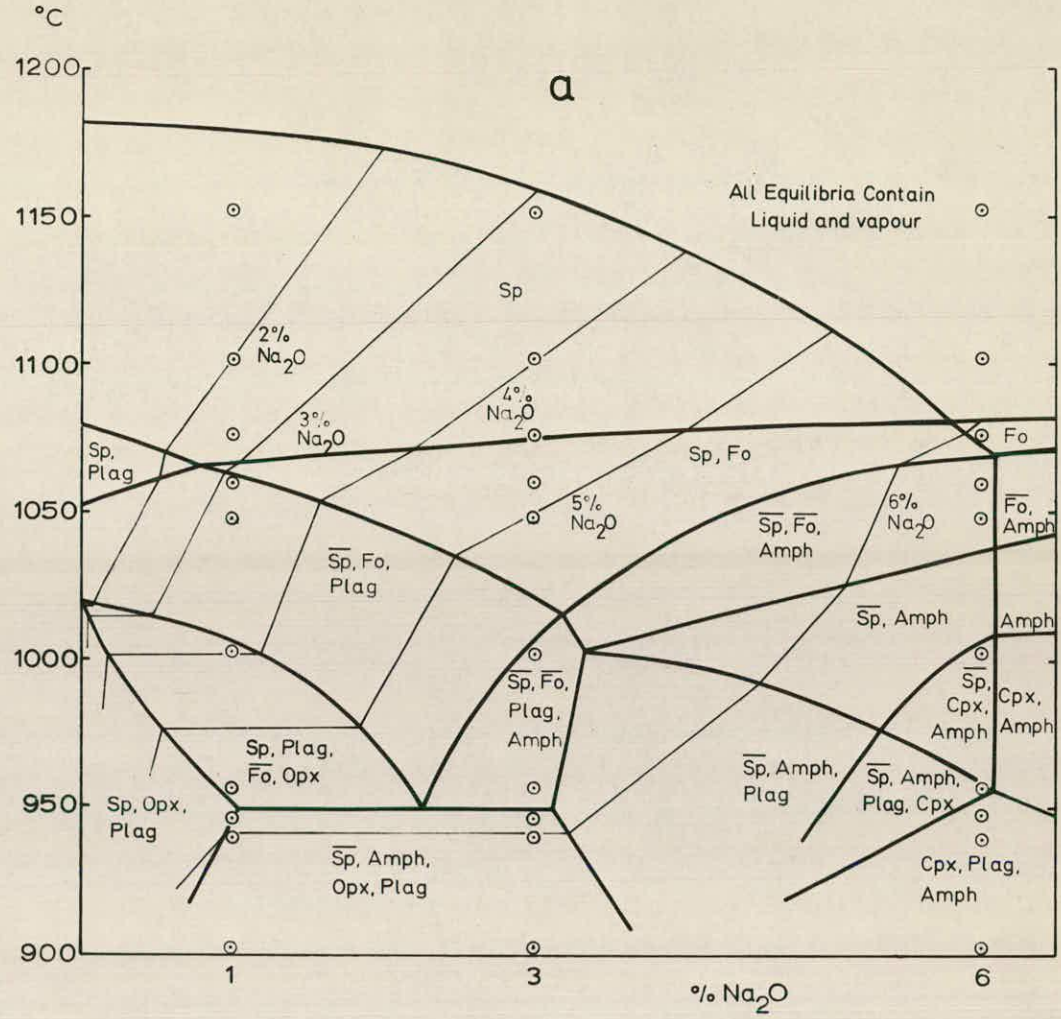

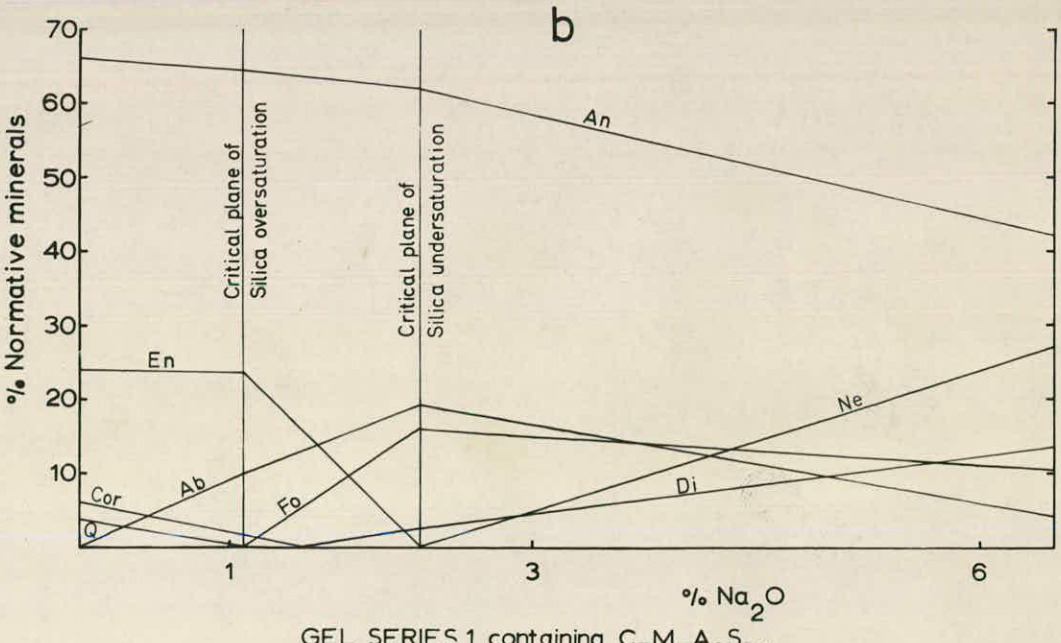

GEL SERIES 1 containing $C_7M_7A_8S_{24}$

high soda region. Hence, pyroxene is not in reaction relationship with the liquid to produce amphibole in this part of the system (contrast with Figs. 3.2a and 3.3a). The temperature of the isobaric invariant equilibrium mentioned above is 952 ± 8°C.

Gel Series 2

Compositions containing up to 3% soda resemble basaltic andesite, see Fig. 3.5b.

The equilibrium phase relationships, Fig. 3.5a, are similar to those of gel series 1 except that spinel has a more restricted stability range in gel series 2. At intermediate to high soda contents amphibole and plagioclase dominate the crystallisation sequence after the early appearance of forsterite. Either spinel or liquid must be metastable in the low temperature equilibrium in the 1 - 3% soda region. Similar arguments to those discussed in connection with pargasite stability apply.

Gel Series 3

These compositions are intended to provide data on the isobaric invariant equilibrium involving forsterite - clinopyroxene - orthopyroxene - amphibole - plagioclase - liquid - vapour.

The results and C.I.P.W. norms are shown in Figs. 3.6a and 3.6b respectively. Forsterite and clinopyroxene appear virtually together and prior to orthopyroxene even in quartz-normative compositions. The crucial equilibrium mentioned above is observed at 960 ± 12°C. There is only a short temperature interval of clinopyroxene crystallisation

FIG. 3.5

a. Results of experimental runs at 5 kb water pressure on gel compositions $C_2M_3A_6S_{12}$ containing various soda levels.

Abbreviations and explanation as for Fig. 3.2a.

b. Normative values of compositions studied in this pseudobinary join.

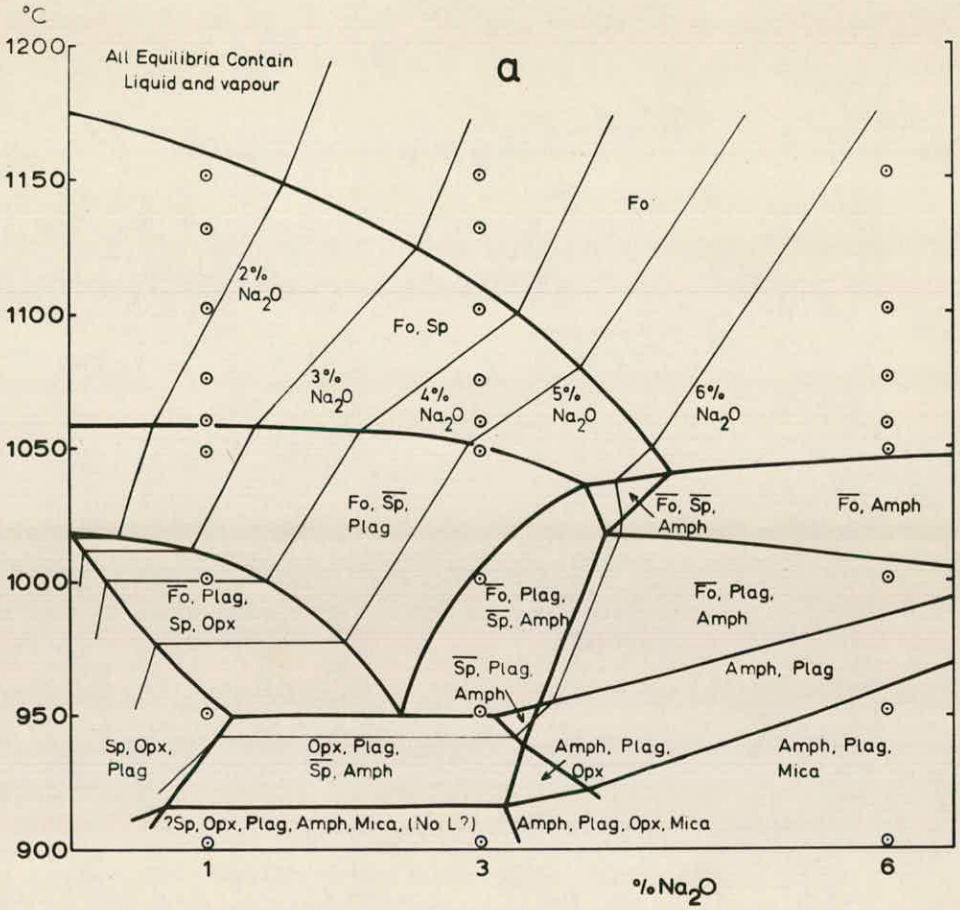

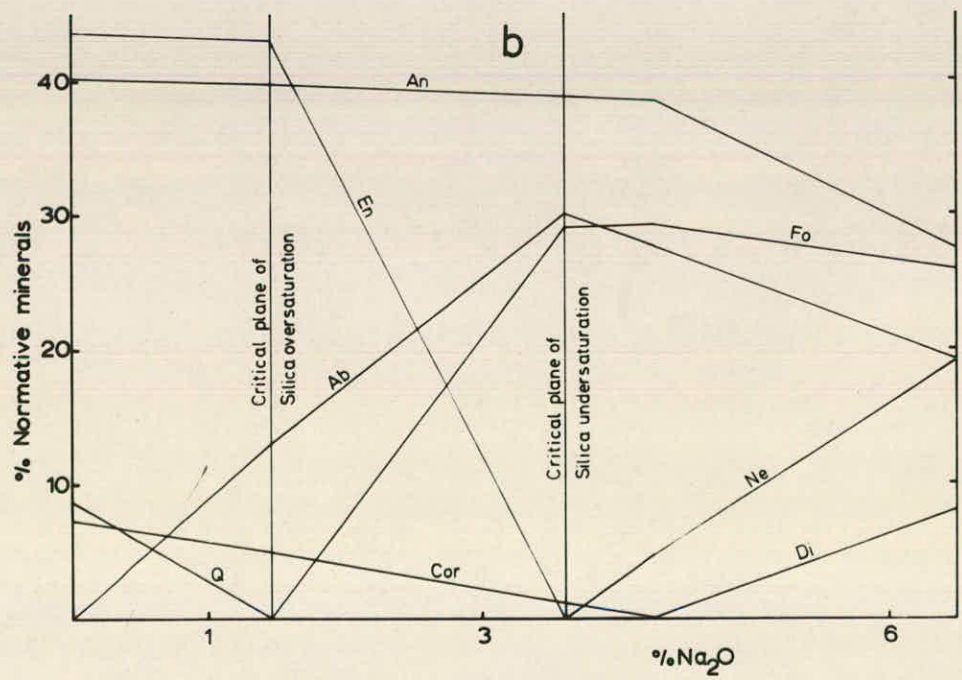

GEL SERIES 2 containing $C_2M_3A_6S_{12}$

FIG.3.6

a. Results of experimental runs at 5 kb water pressure on gel compositions $C_3M_3A_2S_{12}$ containing various soda levels.

Abbreviations and explanation as for Fig. 3.2a.

b. Normative values of compositions studied in this pseudobinary join.

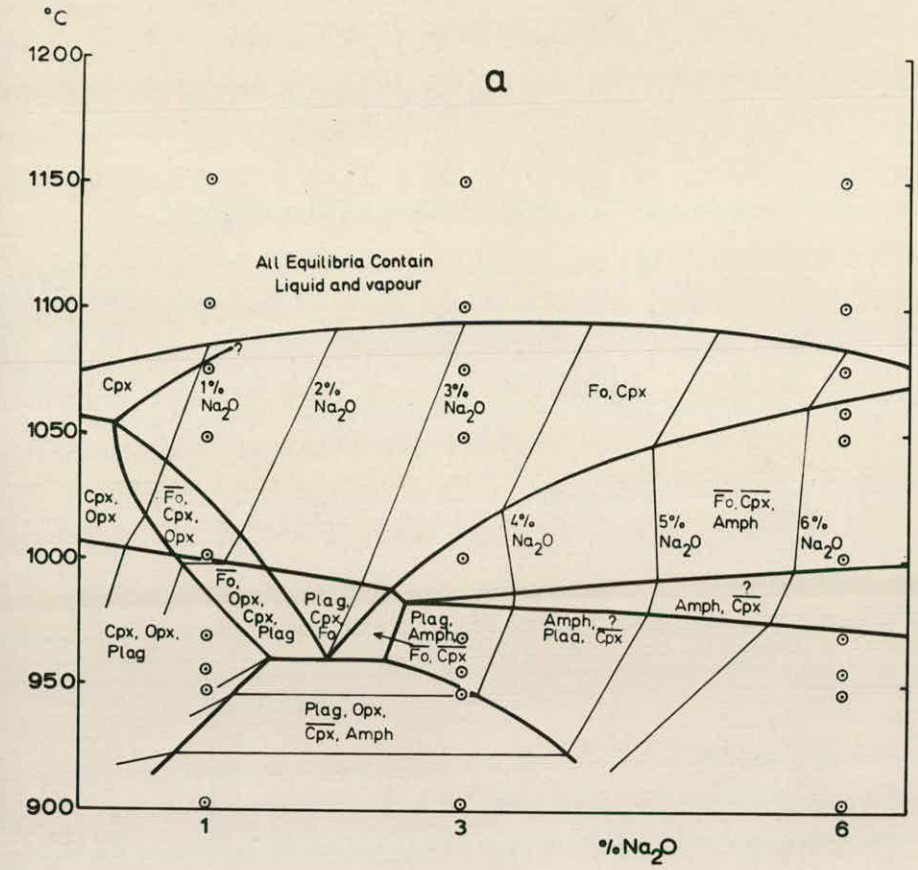

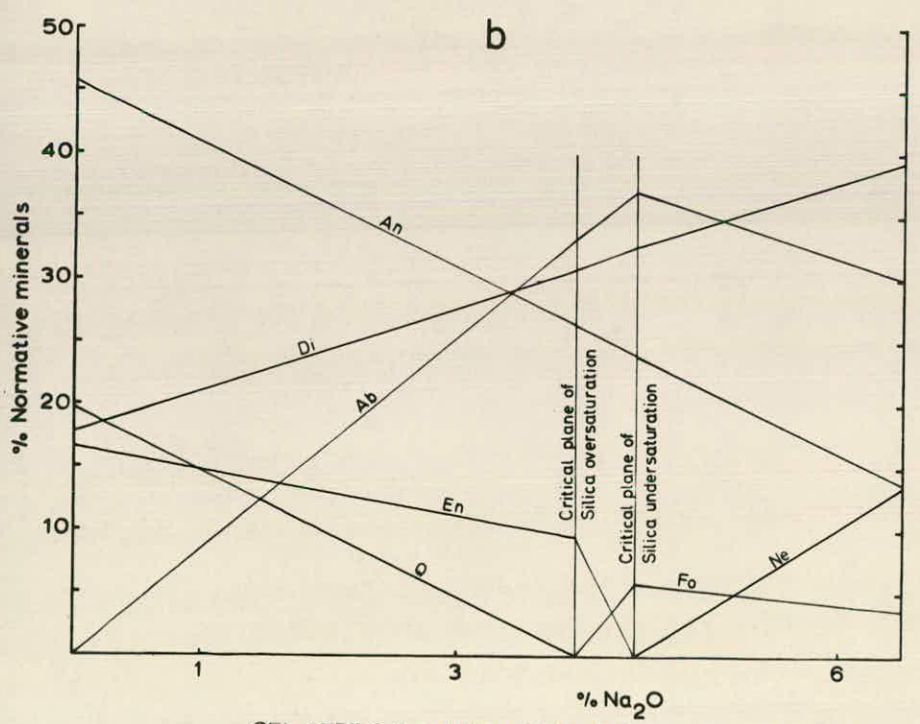

GEL SERIES 3 containing $C_3M_3A_2S_{12}$

before amphibole appears in the high soda region. As these two phases co-exist over a large temperature range clinopyroxene may not be in reaction relationship with the liquid to produce amphibole, but there are no diagnostic data.

Gel Series 6

For soda contents up to 3%, these compositions are similar to andesite, as shown by their C.I.P.W. norms, Fig. 3.7b.

All have a very low liquidus temperature, Fig. 3.7a, implying a proximity to one of the thermal minima in the system. A complex region exists near the isobaric invariant equilibrium of forsterite - two pyroxenes - amphibole - plagioclase - liquid - vapour which is not defined with certainty. There is a comparatively large range of soda contents for which orthopyroxene, not forsterite, is the first magnesian phase to crystallise, but it is restricted to compositions with more than 6% normative quartz. The disappearance of clinopyroxene at low temperature in the soda-rich region suggests that it is in reaction relationship with the liquid to produce amphibole.

Gel Series 7

The compositions are highly corundum-normative, and so do not resemble basic igneous compositions (Fig. 3.8b).

In the low soda region, compositions contain normative quartz, and by the early crystallisation of spinel residual liquids become even more quartz-normative. Hence, there is

FIG. 3.7

a. Results of experimental runs at 5 kb water pressure on gel compositions $CMAS_4$ containing various soda levels.

Abbreviations and explanation as for Fig. 3.2a.

Dashed lines indicate uncertainty in phase relationships.

b. Normative values of compositions studied in this pseudobinary join.

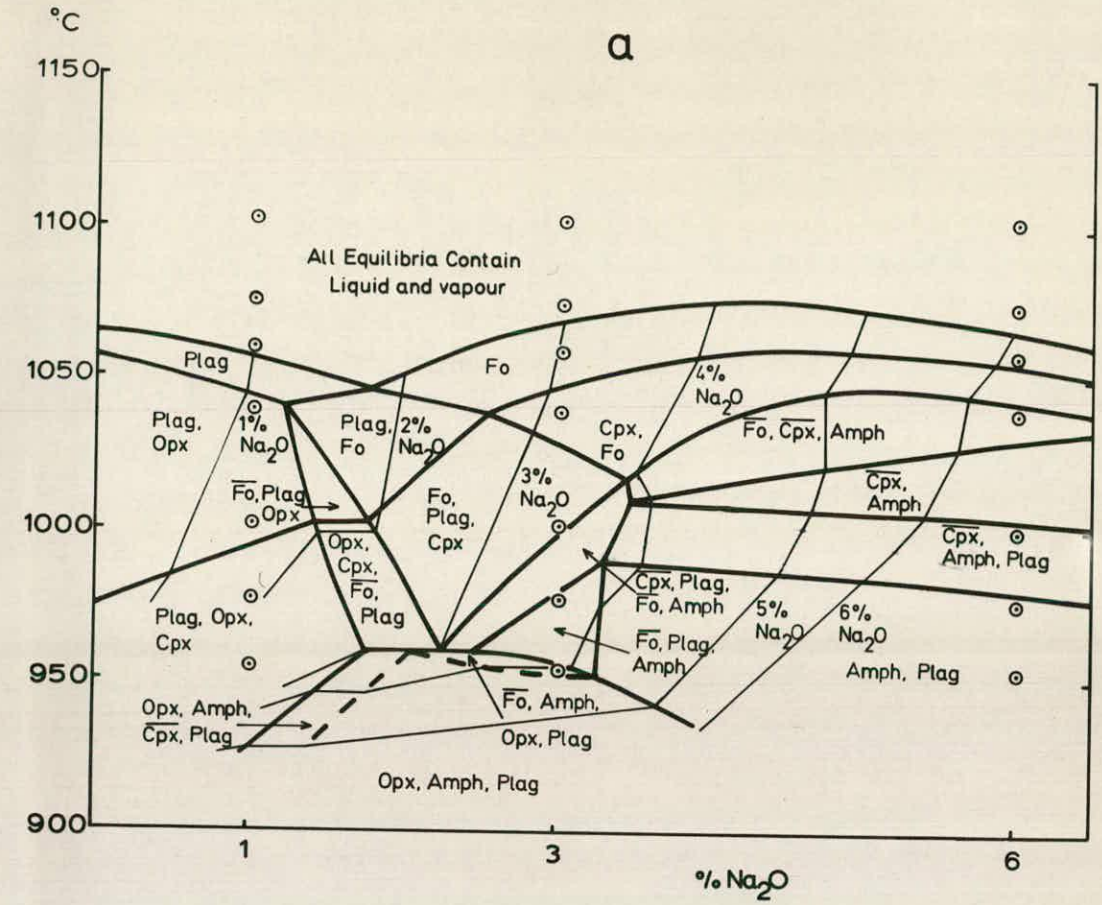

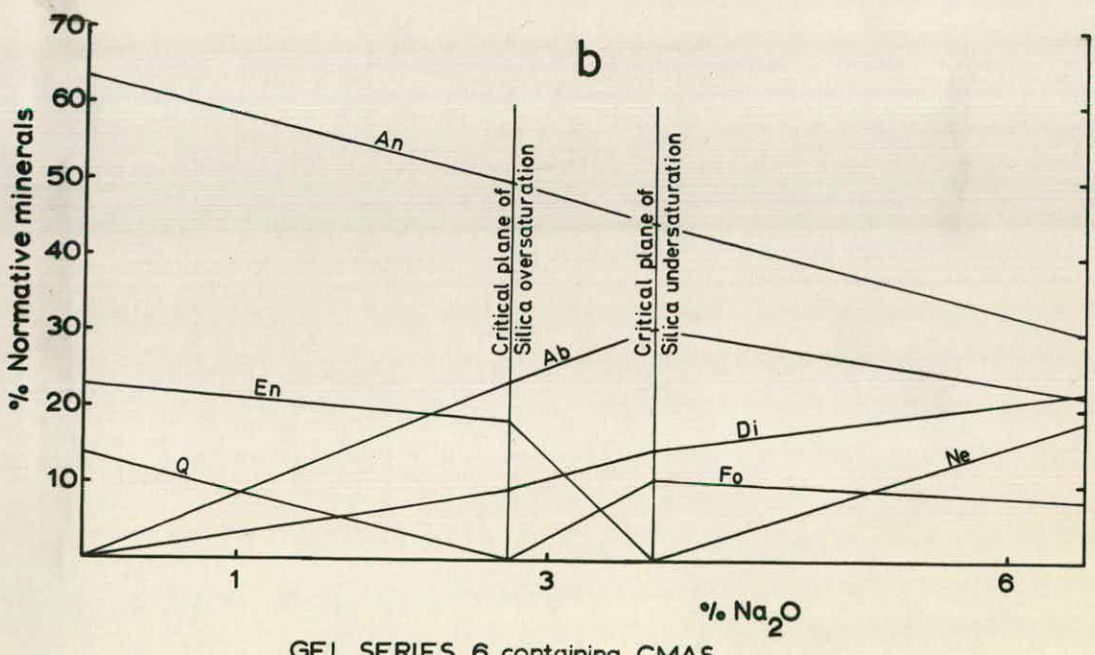

GEL SERIES 6 containing $CMAS_4$

FIG. 3.8

a. Results of experimental runs at 5 kb water pressure on gel compositions $C_2M_5A_4S_{12}$ containing various soda levels.

Abbreviations and explanation as for Fig. 3.2a.

b. Normative values of compositions studied in this pseudobinary join.

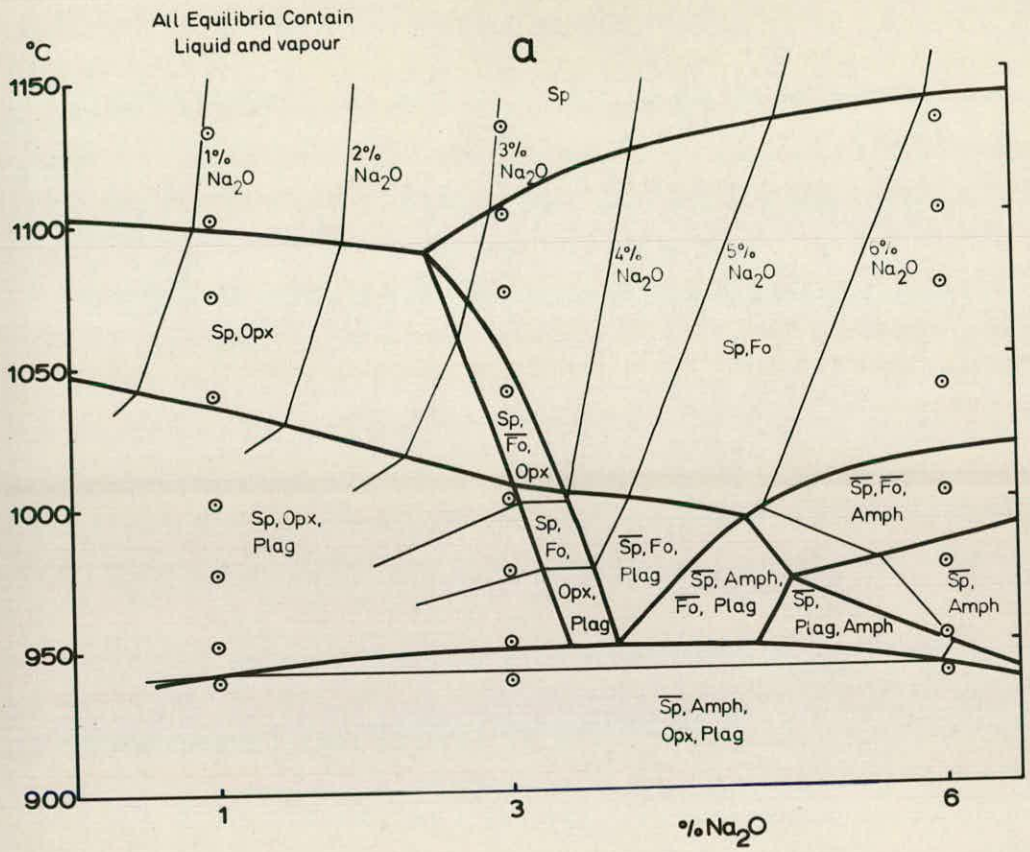

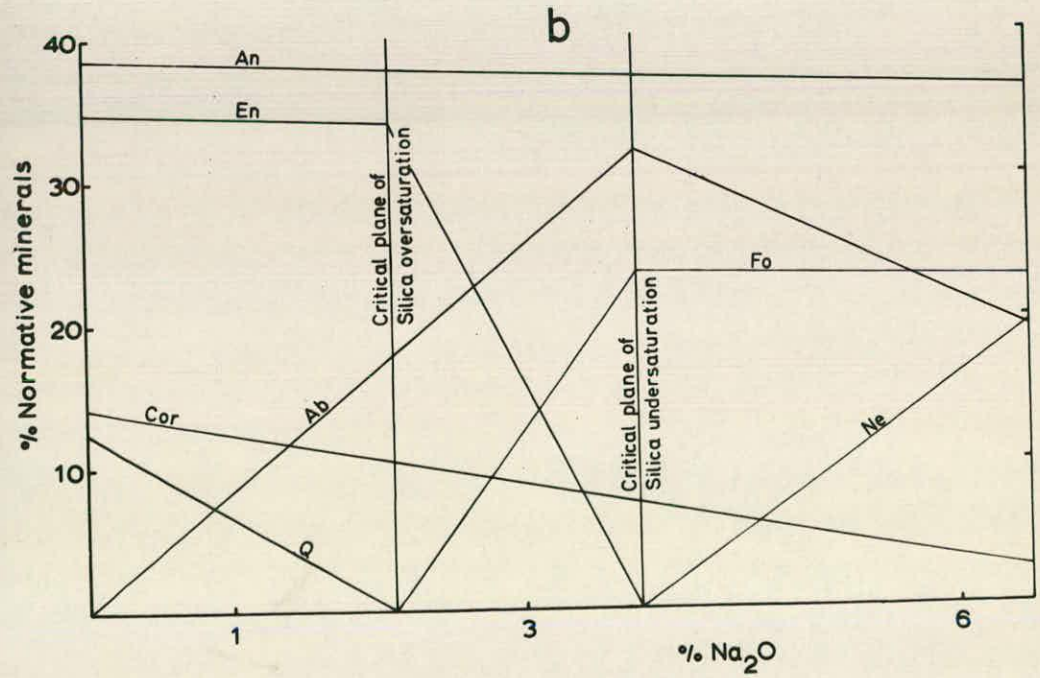

GEL SERIES 7 containing $C_2M_5A_4S_{12}$

a large field of orthopyroxene crystallisation. In other respects, the phase equilibria are similar to those in Figs. 3.4a and 3.5a.

Gel Series 9 and 10

These are both designed to provide data on forsterite - orthopyroxene - vapour-saturated equilibria at various soda levels and are conveniently considered together.

All the compositions have forsterite as liquidus mineral, Figs. 3.9a and 3.10a, despite some of the compositions being quartz-normative, Fig. 3.10b. Orthopyroxene and clinopyroxene appear second and third, the order depending upon the soda content.

Plagioclase has a very restricted stability range as the aluminous phase, being replaced by amphibole as soda content increases. The temperature of the equilibrium forsterite - two pyroxenes - amphibole - liquid - vapour is comparatively independent of soda content, although there is a thermal maximum in this equilibrium at 975 $\pm$ 10°C for liquids containing slightly less than 4% soda. There is a limited range of compositions in gel series 9 which may crystallise in the equilibrium forsterite - two pyroxenes - plagioclase - vapour which is not observed in gel series 10.

Phase compositions

Electron microprobe analysis of certain charges was undertaken to investigate compositional variation of phases in various assemblages.

FIG. 3.9

a. Results of experimental runs at 5 kb water pressure on gel compositions $C_2M_{10}AS_{12}$ containing various soda levels.

Abbreviations and explanation as for Fig. 3.2a.

b. Normative values of compositions studied in this pseudobinary join.

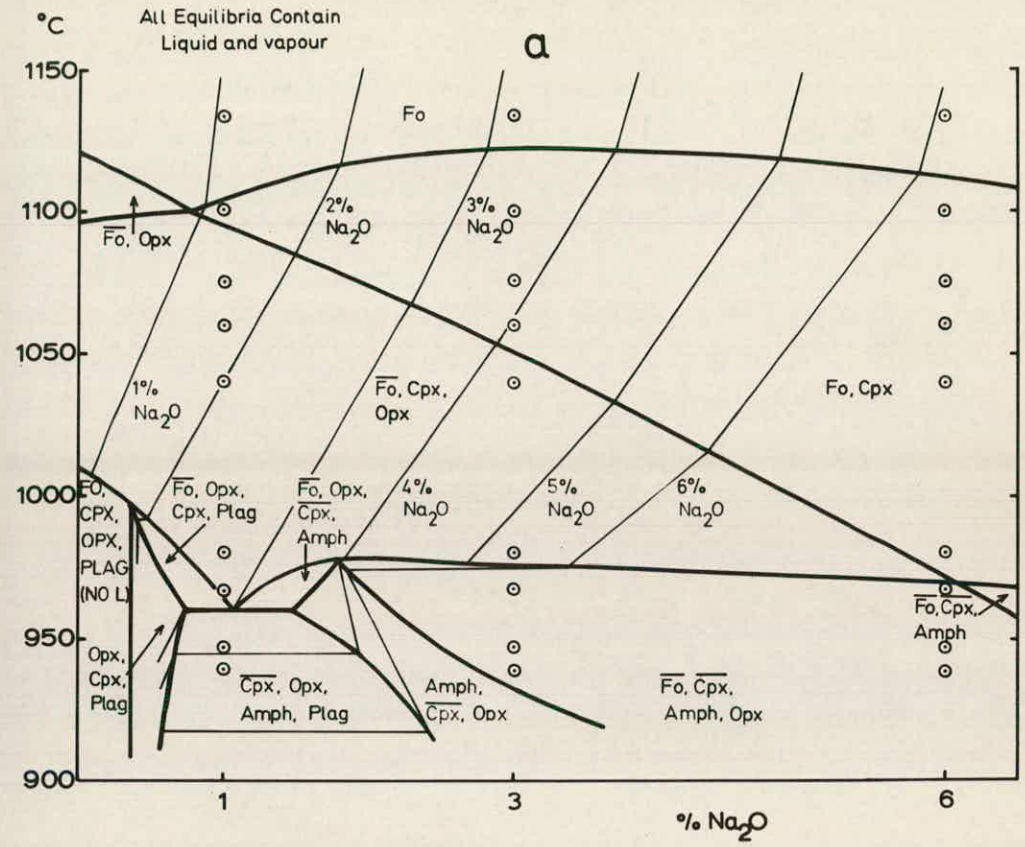

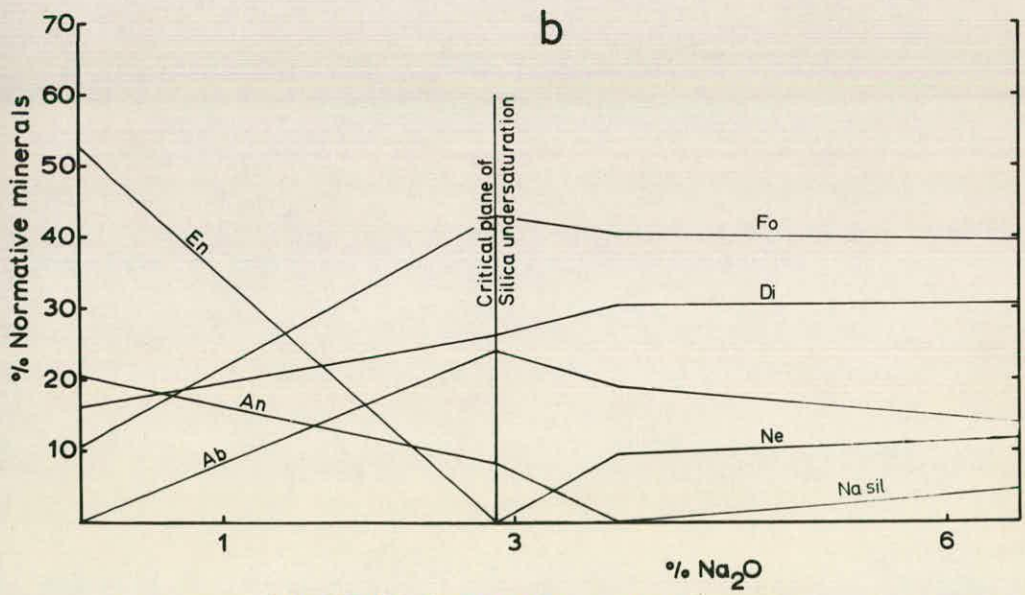

GEL SERIES 9 containing $C_2M_{10}AS_{12}$

FIG. 3.10

a. Results of experimental runs at 5 kb water pressure on gel compositions $C_3M_{18}A_2S_{24}$ containing various soda levels.

Abbreviations and explanation as for Fig. 3.2a.

b. Normative values of compositions studied in this pseudobinary join.

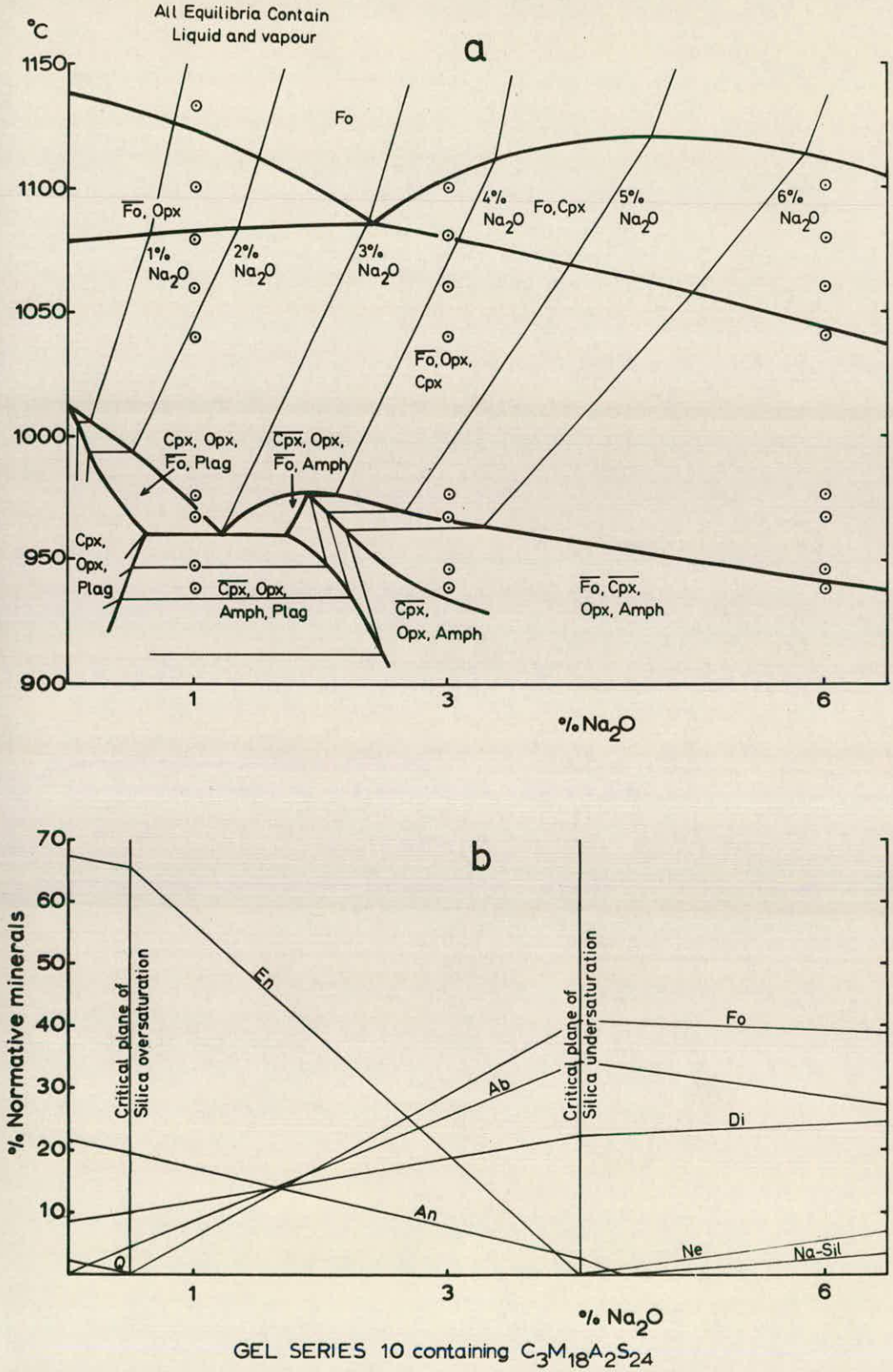

GEL SERIES 10 containing $C_3M_{18}A_2S_{24}$

Glasses

Hydrous glass analyses have been reported by Holloway & Burnham (1972), Kushiro (1972), Modreski (1972) and Cawthorn et al. (1973). Most authors refer to the volatilisation of alkalis during analysis. Magnesium values are extremely low in all reports, and results are thought to be unreliable (Cawthorn et al., 1973).

Electron microprobe analyses of hydrous glasses are presented in Table 3.2 and comparison with calculated compositions substantiate this suggestion. A detailed discussion of the calculation of liquid compositions is located in Appendix A. This method of hydrous glass analysis is regarded as suspect. Discrepancies between analysed and computed compositions may be attributable to the formation of quenching products which alter the composition of the equilibrium liquid.

Amphiboles

The range of amphiboles produced in this study is quite large, as shown by Table 3.3A. Those produced in equilibrium with silica-undersaturated liquids are close to pargasite in composition, analysis 2, while those in equilibrium with silica-rich liquids are themselves more siliceous and lower in alumina, analyses 3 and 4. A sympathetic variation in soda content of the amphibole and co-existing liquid is exemplified by analyses 3 and 4.

Clinopyroxenes

The clinopyroxenes show a considerable range of compositions, see Table 3.3B, especially in their alumina

TABLE 3.2

Compositions of glasses obtained by electron microprobe analysis compared with the predicted composition obtained by calculation.

Electron microprobe analyses

Gel composition	3a	3b	10a	45En
Temperature, °C	968	968	941	1091
Mineral assemblage	Cpx, Opx, Plag.	Fo, Cpx, Amph, Plag.	Cpx, Opx, Amph, Plag.	Fo, Cpx.
SiO_2	55.3	57.7	54.9	56.8
Al_2O_3	18.5	19.8	18.9	15.8
MgO	1.3	1.0	1.4	7.2
CaO	6.9	4.2	7.7	11.9
Na_2O	0.8	0.9	1.0	3.5
Total	82.8	83.6	83.9	95.2
Analyses recalculated to 100%				
SiO_2	66.8	69.0	65.4	59.7
Al_2O_3	22.3	23.7	22.5	16.5
MgO	1.6	1.2	1.6	7.6
CaO	8.3	5.0	9.2	12.4
Na_2O	1.0	1.1	1.2	3.7
Compositions obtained by calculation, normalised to 100% (see Appendix A)				
SiO_2	63.1	60.7	62.3	56.6
Al_2O_3	17.2	18.8	19.1	12.9
MgO	7.2	6.1	5.6	17.6
CaO	10.5	10.4	10.0	10.4
Na_2O	2.0	4.0	3.0	2.5

TABLE 3.3

Compositions and structural formulae of minerals analysed by electron microprobe

A - Amphiboles

Gel composition	Parg	42	9c	10a
Temperature, °C	954	1001	941	941
Co-existing phases	V	Fo,Cpx,L,V	Fo,Cpx, Opx,L,V	Cpx,Opx, Plag,L,V
SiO_2	44.5	42.3	50.0	49.6
Al_2O_3	19.5	19.4	10.0	12.2
MgO	19.1	19.4	21.6	20.6
CaO	13.9	12.4	9.7	10.0
Na_2O	3.3	3.1	4.4	1.9
Total	100.2	96.2	95.7	94.3
Structural formulae				
Si	6.02	5.93	6.99	6.95
Al_{Tet}	1.98	2.07	1.01	1.05
Al_{Oct}	1.12	1.13	0.64	0.97
Mg	3.86	4.05	4.51	4.31
Ca	2.02	1.86	1.45	1.50
Na	0.87	0.84	1.19	0.52
X + Y site content	7.00	7.04	6.60	6.78

(Contd.)

Table 3.3 (Contd.)

B - Clinopyroxenes	1	2	3	4	5	6
Gel Composition	3a	9c	10a	3b	Parg	45En
Temperature, °C	968	941	941	968	1076	1091
Co-existing phases	Opx, Plag, L, V	Fo, Opx, Amph, L, V	Opx, Amph, Plag, L, V	Amph, Plag, L, V	Fo, Sp, L, V	Fo, L, V
SiO_2	54.8	55.0	52.5	56.3	51.8	56.7
Al_2O_3	3.0	3.3	3.7	8.9	8.6	1.0
MgO	18.6	17.7	18.5	14.3	15.0	21.2
CaO	23.7	21.6	19.7	21.0	22.6	22.2
Na_2O	0.1	0.7	0.9	0.6	0.6	0.2
Total	100.2	98.3	95.3	101.1	98.0	101.3
Structural formulae						
Si	1.96	1.99	1.96	1.96	1.87	2.00
Al^{Tet}	0.04	0.01	0.05	0.04	0.13	
Al^{Oct}	0.08	0.13	0.12	0.32	0.24	0.04
Mg	0.99	0.95	1.03	0.74	0.81	1.11
Ca	0.91	0.84	0.79	0.78	0.88	0.84
Na	0.002	0.012	0.016	0.01	0.01	0.003

Table 3.3 (Contd)

C - Orthopyroxenes

Gel composition	3a	10a
Temperature, ^{o}C	968	941
Co-existing phases	Cpx,Plag,L,V	Cpx,Amph,Plag,L,V
SiO_2	59.9	57.3
Al_2O_3	3.2	5.0
MgO	36.9	36.8
CaO	1.7	1.3
Na_2O	0.03	Tr
Total	101.73	100.4
Structural formulae		
Si	1.96	1.91
Al^{Tet}	0.04	0.09
Al^{Oct}	0.08	0.11
Mg	1.84	1.83
Ca	0.06	0.05

D - Forsterites

Gel composition	45En	42	Ideal
Temperature, ^{o}C	1091	1000	analysis
Co-existing phases	Cpx,L,V	Sp,Cpx,L,V	
SiO_2	43.5	44.1	42.7
Al_2O_3	0.11	0.9	
MgO	57.2	57.0	57.3
CaO	0.31	0.01	
Na_2O	0.07	0.23	
Total	101.19	102.24	100.0

TABLE 3.4

Composition of liquids in the equilibrium Forsterite - 2 pyroxenes - Al-phase - Liquid - Vapour at varying soda levels; calculated from the projection diagrams, Figs. 3.12 - 3.14; recalculated to 100%.

	1	2	3	4	5
SiO_2	57.7	58.9	61.7	61.5	61.0
Al_2O_3	20.9	20.4	19.7	18.4	17.7
MgO	8.0	6.9	5.6	6.4	6.8
CaO	13.4	12.8	10.0	9.7	8.5
Na_2O	0	1.0	3.0	4.0	6.0
Normative minerals					
q	19.1	18.0	16.5	11.3	2.2
an	57.0	51.2	40.2	32.3	21.4
ab	0	8.5	25.4	33.9	50.8
di	7.3	9.6	7.5	12.4	16.2
en	16.6	12.7	10.4	10.1	9.4
Plagioclase composition (mole proportions)					
%an		85.8	61.3	48.8	29.6

1 calculated from Figs. 3.12a and 3.14a at 0% soda
2 " " Figs. 3.12b and 3.14b at 1% soda
3 " " Figs. 3.12d and 3.14c at 3% soda
4 " " Figs. 3.12e and 3.14d at 4% soda
5 " " Figs. 3.12g and 3.14e at 6% soda

content. Analysis 1 approximates to the mineral in the equilibrium forsterite - two pyroxenes - plagioclase - liquid - vapour, and contains 3.0% Al_2O_3. Analyses 2, 3 and 4 refer to pyroxenes in equilibrium with sodic liquids and are themselves richer in soda. Clinopyroxenes in equilibrium with silica-undersaturated liquids show high alumina contents, analysis 5. At high temperature, the pyroxene has a composition quite close to that of ideal diopside, analysis 6.

Orthopyroxenes

Because of the fairly limited stability range of orthopyroxene few charges including orthopyroxene were analysed. The analyses indicate the likely compositions in the equilibria forsterite - two pyroxenes - liquid - vapour with either plagioclase or amphibole, analyses 1 and 2 respectively, in Table 3.3C. Al_2O_3 contents of the orthopyroxene appear slightly higher than in the co-existing clinopyroxene.

Forsterites

The stoichiometry of forsterite renders analysis to find its composition superfluous. However, it serves as an estimate on the likely accuracy of the other mineral analyses. The two analyses presented in Table 3.3D suggest an absolute error of $\pm$ 1% on major oxides.

Projection Diagrams

The composition of liquids in various equilibria are not immediately obtained from the phase diagrams presented in the previous sections. The projection diagrams in this section are intended to demonstrate the characteristics of these liquids, and to provide a method for calculating liquid compositions.

Forsterite - vapour-saturated equilibria in the pseudoquaternary volume CS - MS - A - N

The principle of these projections is discussed in Appendix A.

All the compositions used in this study are projected from forsterite and soda into the plane CS - MS - A, Fig. 3.11 (located in wallet at the back of the thesis for use as a transparent overlay on Fig. 3.12). Various relevant mineral tie-planes and joins are also included.

Fig. 3.12a demonstrates the forsterite - vapour-saturated phase relationships in the plane CS - MS - A, data being taken from Yoder & Dickey (1971) and Ford & O'Hara (1972). The important observations are that the forsterite - clinopyroxene - plagioclase - liquid - vapour cotectic curve no longer contains a thermal divide, which is stable up to 8 kb under anhydrous conditions (O'Hara, 1968). Liquids may migrate across the critical plane of silica-undersaturation from critically undersaturated compositions by forsterite - clinopyroxene - spinel crystallisation.

Corundum-normative residua cannot be produced from a diopside-normative parent liquid except by the crystallisation

of a calcic, low-alumina orthopyroxene.

Fig. 3.12b indicates the effect of the addition of 1% soda to liquids in the above equilibria. Data are derived from Figs. 3.6a, 3.7a, 3.9a and 3.10a using equilibria containing 1% soda in the liquid, not 1% soda in the bulk compositions (see Appendix A). The location of cotectic curves for adjacent soda levels are included for comparison. Because of the shift in the position of the plagioclase projection point (see Appendix F) it is not always possible to decide from inspection how liquid compositions in comparable equilibria change with increasing soda content of the liquid.

Increasing soda content to 2% does not introduce any new minerals, Fig. 3.12c, but at the 3% soda level, Fig. 3.12d, amphibole becomes stable in the isobaric invariant equilibrium forsterite - two pyroxenes - plagioclase - liquid - vapour.

The amphibole stability field rapidly increases with increasing soda content. Fig. 3.12e refers to liquids containing 4% soda. The range of stability of the equilibrium forsterite - clinopyroxene - plagioclase - liquid - vapour contracts rapidly for soda levels over 3% and at 5% soda is no longer observed, Fig. 3.12f. At higher soda levels the equilibrium forsterite - orthopyroxene - plagioclase - liquid - vapour is replaced by one containing amphibole as the aluminous phase, Fig. 3.12g. There may be a nepheline stability field in silica-undersaturated compositions (Fig. 3.2a), but there are insufficient data to locate it.

FIG. 3.11

(Located in wallet at the back of thesis)

Projection from or towards forsterite and soda into the plane CS - MS - A (weight percent) of all the compositions used in this study.

FIG. 3.12

Projections of phase equilibria determined in Figs. 3.1 - 3.10 from forsterite and vapour for liquids containing fixed soda contents. Fig. 3.12a contains 0% soda, Figs. 3.12b - 3.12g contain 1 - 6% soda. Relevant invariant points from adjacent soda content diagrams are included for comparison.

Abbreviations: Ab - albite; Di - diopside; En - enstatite; Gross - grossularite; Py - pyrope; Fo-An pp. - forsterite-anorthite piercing point; other abbreviations as for Fig. 3.2a.

Clinopyroxene - vapour-saturated equilibria in the pseudoquaternary volume CA - M - S - N

These are analogous to the data in Fig. 3.12, except that clinopyroxene-bearing assemblages are considered here. There are fewer data available and the location of the phase boundaries is less certain.

Compositions used and mineral tie-planes are presented in Fig. 3.13 (to be found in the wallet at the back of the thesis).

The boundaries in Fig. 3.14a for soda-free compositions are estimated from the data of Ford & O'Hara (1972). The addition of 1% soda is shown in Fig. 3.14b to have little influence on the relative phase stabilities. The isobaric invariant equilibrium forsterite - two pyroxenes - amphibole - plagioclase - liquid - vapour is located in Fig. 3.14c for liquids containing 3% soda. This liquid composition, like the liquids in the equilibrium forsterite - two pyroxenes - plagioclase - liquid - vapour in Figs. 3.14a and 3.14b, is distinctly quartz-normative. The equilibrium clinopyroxene - orthopyroxene - plagioclase - liquid - vapour is observed in these three diagrams, but does not contain a thermal maximum.

Further increases in the soda content cause the reduction and eventual elimination of the forsterite - clinopyroxene - plagioclase - liquid - vapour equilibria, Figs. 3.14d and 3.14e, for liquids containing 4% and 6% soda respectively. A nepheline stability field is expected in the silica-undersaturated compositions.

FIG. 3.13

(Located in wallet at the back of the thesis)

Projection from or towards diopside and soda into the plane CA - M - S (weight percent) of all compositions used in this study which crystallise clinopyroxene.

FIG. 3.14

Projections of the phase equilibria determined in Figs. 3.1 - 3.10 from diopside and vapour for liquids containing fixed soda contents. Fig. 3.14a contains 0% soda, Figs. 3.14b - 3.14e contain 1, 3, 4 and 6% soda respectively. Relevant invariant points from adjacent soda content diagrams are included for comparison.

Abbreviations as for Fig. 3.12.

The thermal divide in the equilibrium forsterite - clinopyroxene - amphibole - liquid - vapour, Fig. 3.14e, allows nepheline-normative liquids to crystallise these phases and produce a quartz-normative residual liquid.

As explained in Appendix A, it is possible to calculate a liquid composition if its location in two different projection diagrams is known. This has been done for liquids in equilibrium with forsterite - two pyroxenes - aluminous phase - vapour at different soda contents, and the results are presented in Table 3.4.

Forsterite - orthopyroxene - vapour-saturated equilibria in the pseudoternary plane C - A - N

Compositions which show the early appearance of these mineral phases are projected into Fig. 3.15. Data from these and from the liquid compositions calculated in Table 3.4 enable the phase boundaries in this system to be constructed, as shown in Fig. 3.15.

Two isobaric invariant points are shown, the composition of the liquid with forsterite - two pyroxenes - amphibole - plagioclase - vapour is known fairly precisely, while the location of the liquid in equilibrium with forsterite - orthopyroxene - plagioclase - spinel - amphibole - vapour is less certain.

Corundum-normative liquids are unlikely to be produced in any melting or crystallisation sequence involving forsterite - two pyroxenes - amphibole except perhaps at very high soda content. The position of the diopside - albite join suggests that peralkaline liquids (containing

FIG. 3.15

Projection from forsterite, enstatite and vapour into the plane C - A - N (weight percent). Compositions are designated by the gel series number, and the soda content in parentheses, e.g. 7(3) refers to gel from series 7 containing 3% soda. G is the projection of compositions in the pseudobinary join 42EN - 57EN (Fig. 3.4). 0%, 1% etc. refer to liquid compositions in the equilibrium forsterite - two pyroxenes - aluminous phase - liquid - vapour with that soda content (Table 3.4).

Abbreviations as for Fig. 3.12.

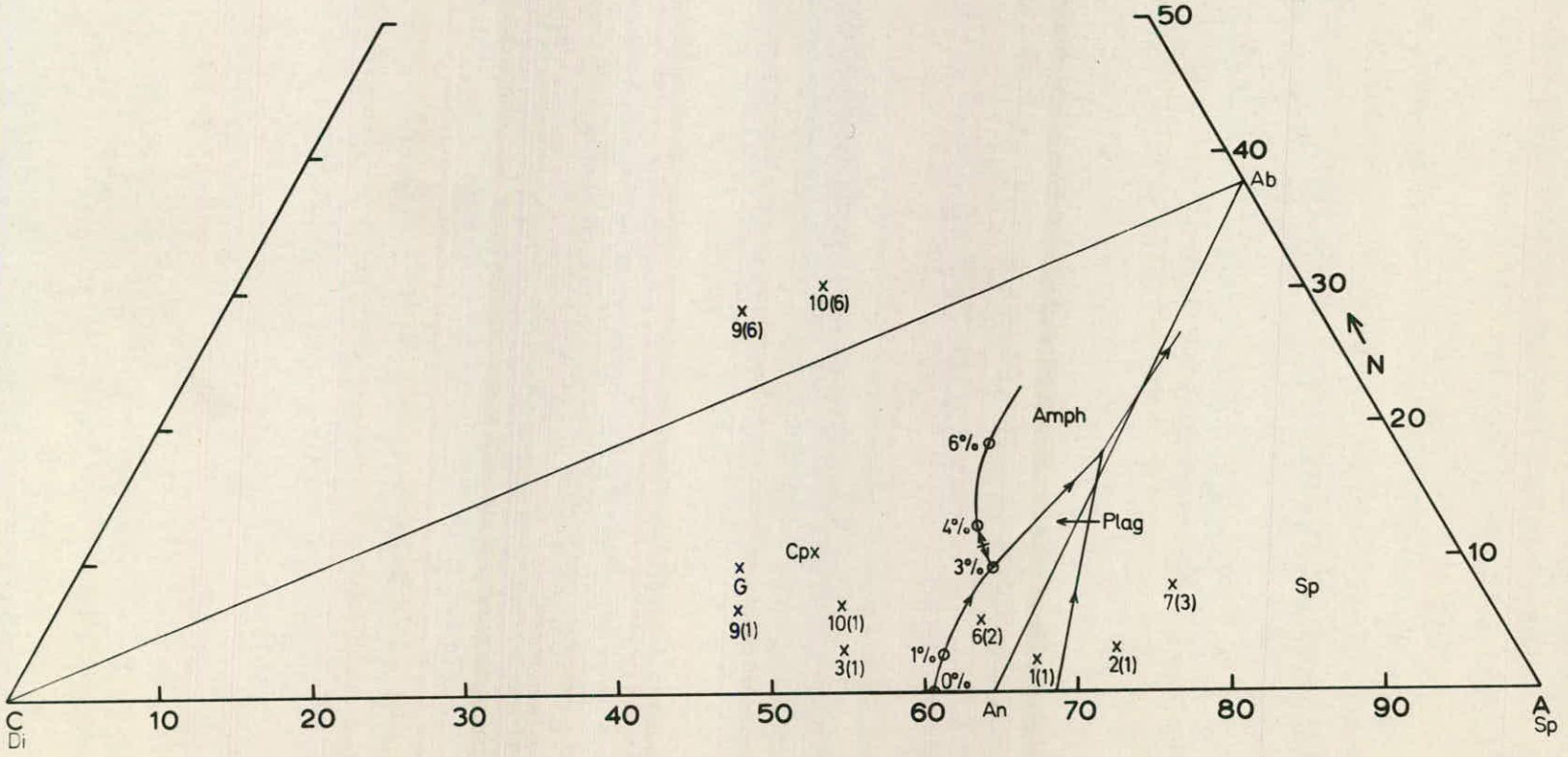
50
40
Ab
30
N
20
10
A
Sp
C
Di
10
20
30
40
50
60
An
70
80
90
Amph
Plag
Cpx
Sp
6%
4%
3%
1%
0%
9(6)
10(6)
G
9(1)
10(1)
3(1)
6(2)
7(3)
1(1)
2(1)

normative soda metasilicate) are unlikely to be produced by partial melting of such an assemblage, unless the bulk rock is itself peralkaline.

Compositions of liquids in the equilibrium forsterite - two pyroxenes - aluminous phase - vapour in the normative basalt tetrahedron

Comparison of liquid compositions produced from these equilibria under 5 kb water pressure with liquids formed in similar equilibria in the absence of water, reveals their distinctive characteristics.

Figs. 3.16, 3.17 and 3.18 are projections within the basalt tetrahedron, and indicate that the hydrous liquids are generally richer in normative feldspar and lower in diopside and significantly more quartz-normative than liquids produced under anhydrous conditions.

Solid solution in minerals

The extent of solid solution in minerals and mineral tie-planes may be indicated by projection diagrams. Figs. 3.19 and 3.20 show the variation of plagioclase, pyroxenes and amphibole in equilibrium with liquids containing 2% and 4% soda. Fig. 3.21 shows similar results in a forsterite - orthopyroxene - vapour-saturation projection into the plane C - A - N. (The orthopyroxene composition is assumed to be enstatite - sensu stricto - in this projection technique.) Mineral compositions are obtained by electron microprobe analysis and, for the feldspars, by the geometrical limitations explained in Appendix F.

FIG. 3.16

Projection from plagioclase (anorthite) into the plane clinopyroxene (diopside) - olivine (forsterite) - quartz (weight percent) within the basalt tetrahedron. 0%, 1% etc. refer to liquid compositions in the equilibrium forsterite - two pyroxenes - aluminous phase - liquid - vapour with that soda content. Data for synthetic and natural systems at atmospheric pressure are estimated from Clarke (1970).

Abbreviations as for Fig. 3.12.

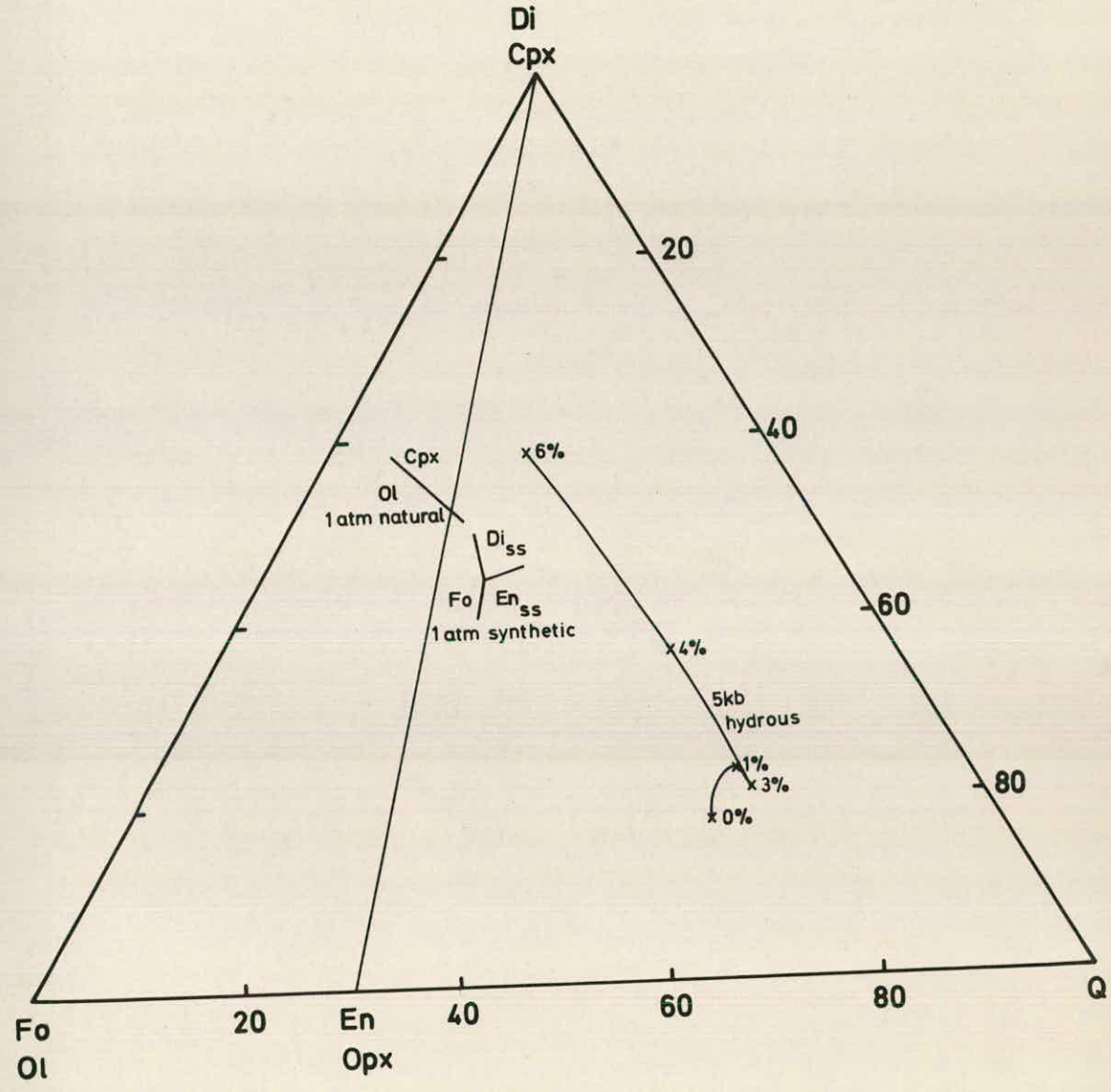
Di
Cpx
20
40
60
80
Cpx
Ol
1 atm natural
Di ss
Fo
En ss
1 atm synthetic
6%
4%
5kb
hydrous
1%
3%
0%
Fo
Ol
20
En
Opx
40
60
80
Q

FIG. 3.17

Projection from clinopyroxene (diopside) into the plane plagioclase (anorthite) - olivine (forsterite) - quartz (weight percent) within the basalt tetrahedron. 0%, 1% etc. refer to liquid compositions in the equilibrium forsterite - two pyroxenes - aluminous phase - liquid - vapour with that soda content. Data for synthetic and natural systems at atmospheric pressure are from Clarke (1970). Locus of liquid compositions in the isobaric anhydrous invariant equilibria involving olivine - two pyroxenes - aluminous phase - liquid is taken from O'Hara (1968), from 1 atm. - 8 kb.

Abbreviations as for Fig. 3.12.

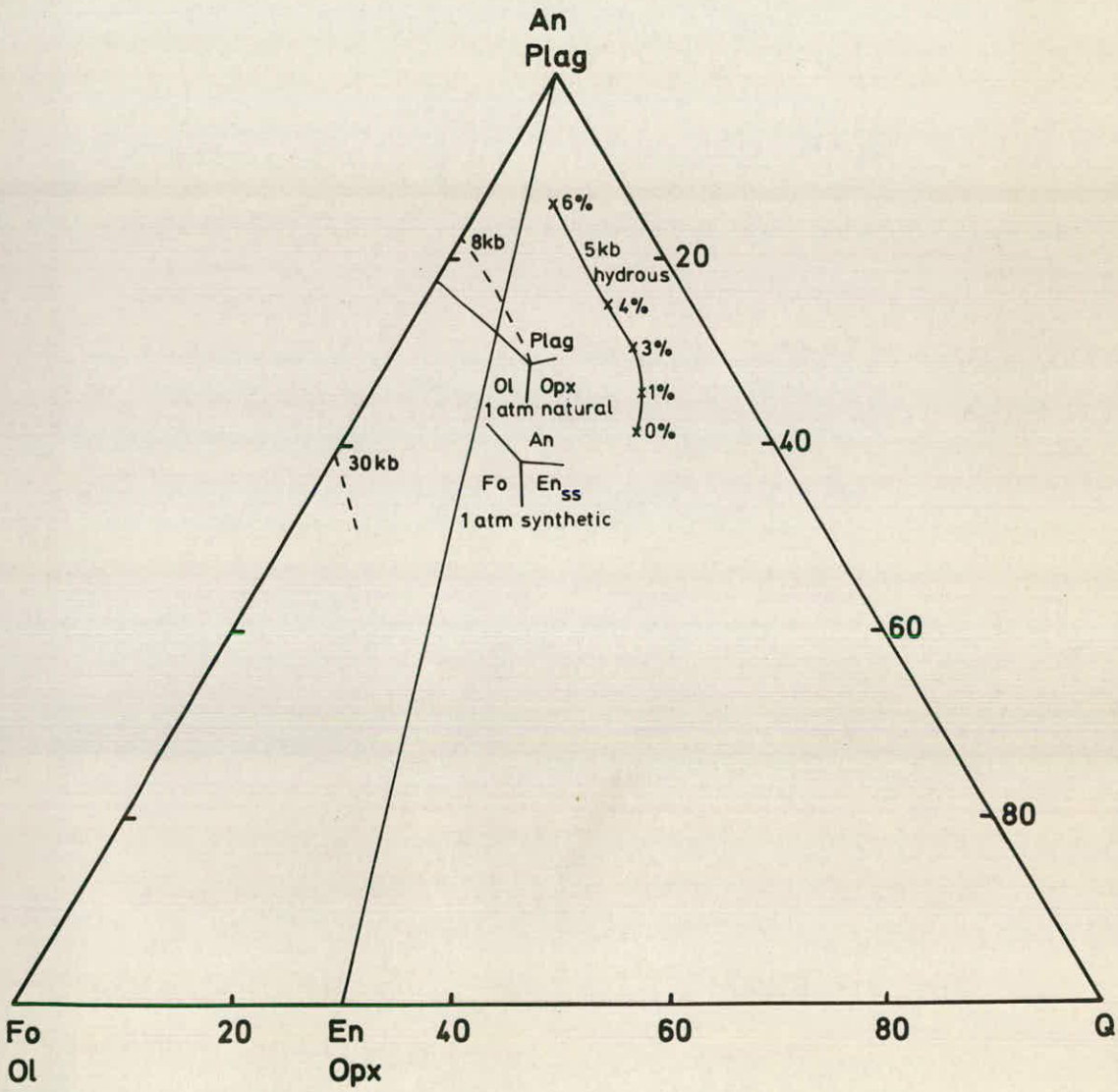
An
Plag
6%
8kb
5kb
hydrous
20
4%
Plag
3%
Ol
Opx
1%
1 atm natural
0%
An
30kb
40
Fo
En
ss
1 atm synthetic
60
80
Fo
Ol
20
En
Opx
40
60
80
Q

FIG. 3.18

Projection from olivine (forsterite) into the plane plagioclase (anorthite) - clinopyroxene (diopside) - quartz (weight percent) within the basalt tetrahedron. 0%, 1% etc. refer to liquid compositions in the equilibrium forsterite - two pyroxenes - aluminous phase - liquid - vapour with that soda content. Data for synthetic and natural systems at atmospheric pressure are from Clarke (1970).

Locus of liquid compositions in the isobaric anhydrous invariant equilibria involving olivine - two pyroxenes - aluminous phase - liquid is taken from O'Hara (1968), from 1 atm. - 8 kb.

Abbreviations as for Fig. 3.12.

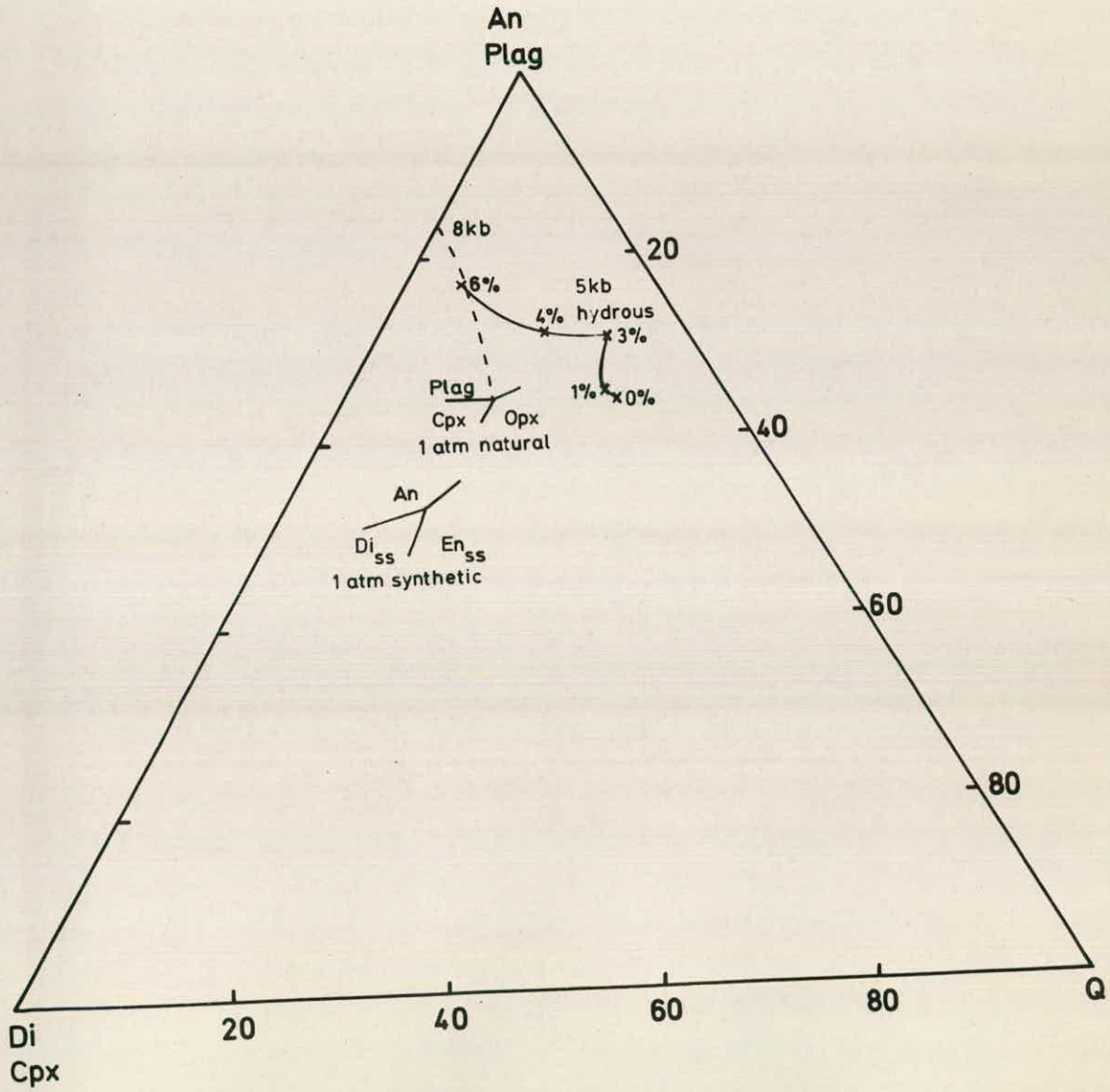
An
Plag
8kb
20
6%
5kb
4%
hydrous
3%
Plag
1%
0%
Cpx
Opx
1 atm natural
An
Di ss
En ss
1 atm synthetic
40
60
80
Q
Di
Cpx
20
40
60
80

FIG. 3.19

Mineral composition and solid solution limits.

Projection from or towards forsterite, soda and vapour into the plane CS - MS - A (weight percent). Liquid compositions containing 2% and 4% soda in the equilibrium forsterite - two pyroxenes - aluminous phase - liquid - vapour (designated L2 and L4) are taken from Figs. 3.12c and 3.12e and estimated from 3.14d.

Estimated solid solution limits of minerals in equilibrium with the liquids at 2% soda (long dashes) and 4% soda (short dashes) are shown.

Mineral compositions are taken from Table 3.3.

A1 refers to amphibole in Table 3.3A number 2

A2 " 3

A3 " 4

C1 refers to clinopyroxene in Table 3.3B number 5

C2 " 2

C3 " 3

C4 " 1

O1 refers to orthopyroxene in Table 3.3C number 1

O2 " 2

Abbreviations as for Fig. 3.12.

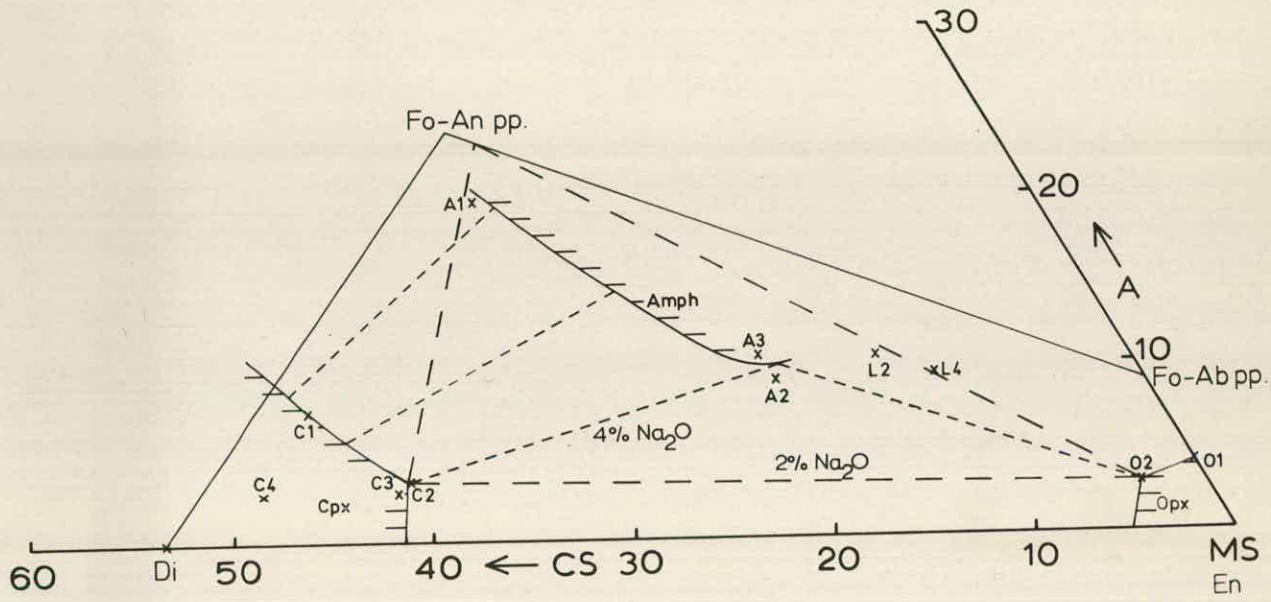
30
Fo-An pp.
20
A
A1
Amph
A3
10
Fo-Ab pp.
L2
L4
A2
C1
4% Na2O
2% Na2O
O2
O1
C4
C3
C2
Cpx
Opx
60
Di
50
40
CS
30
20
10
MS
En

FIG. 3.20

Mineral composition and solid solution limits. Projection from or towards diopside, soda and vapour into the plane CA - M - S (weight percent). Abbreviation and explanation as for Fig. 3.19.

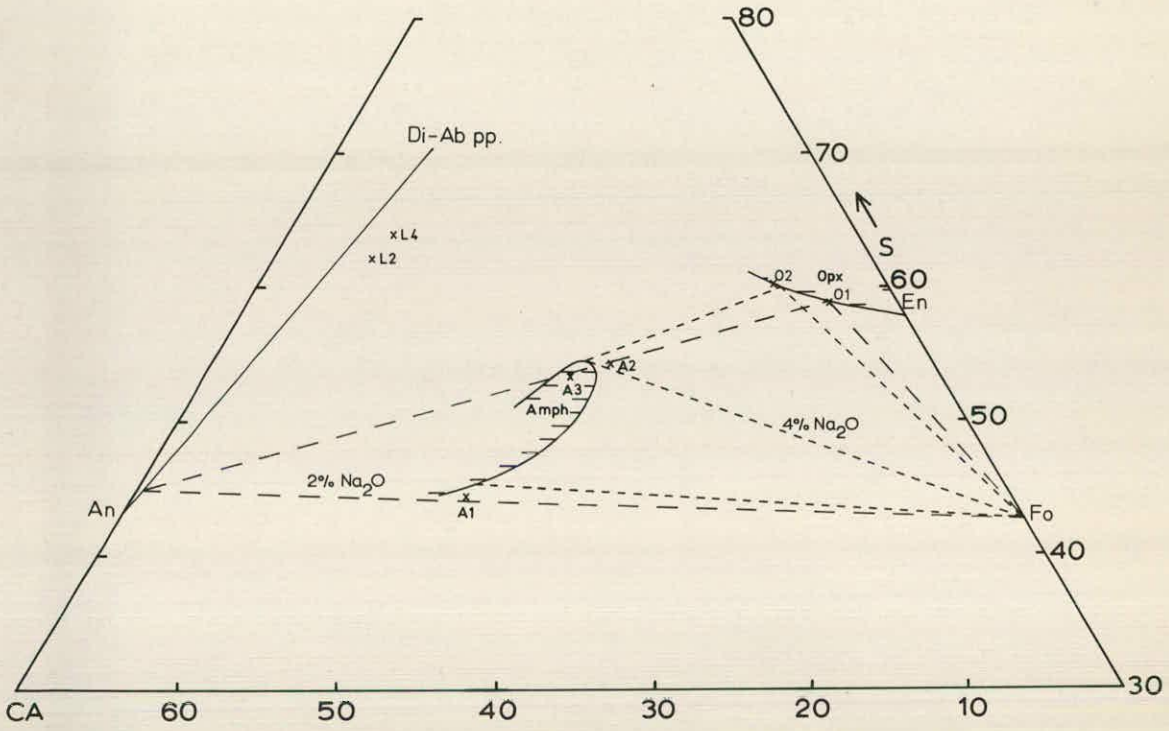
Di-Ab pp.
xL4
xL2
An
CA
60
50
40
30
20
10
80
70
60
50
40
30
S
En
Fo
O2
Opx
O1
A2
A3
Amph
A1
4% Na2O
2% Na2O

Fig.3.21

Mineral compositions and solid solution limits. Projection from forsterite, enstatite and vapour into the plane C - A - N (weight percent).

Abbreviations and explanation as for Fig. 3.19.

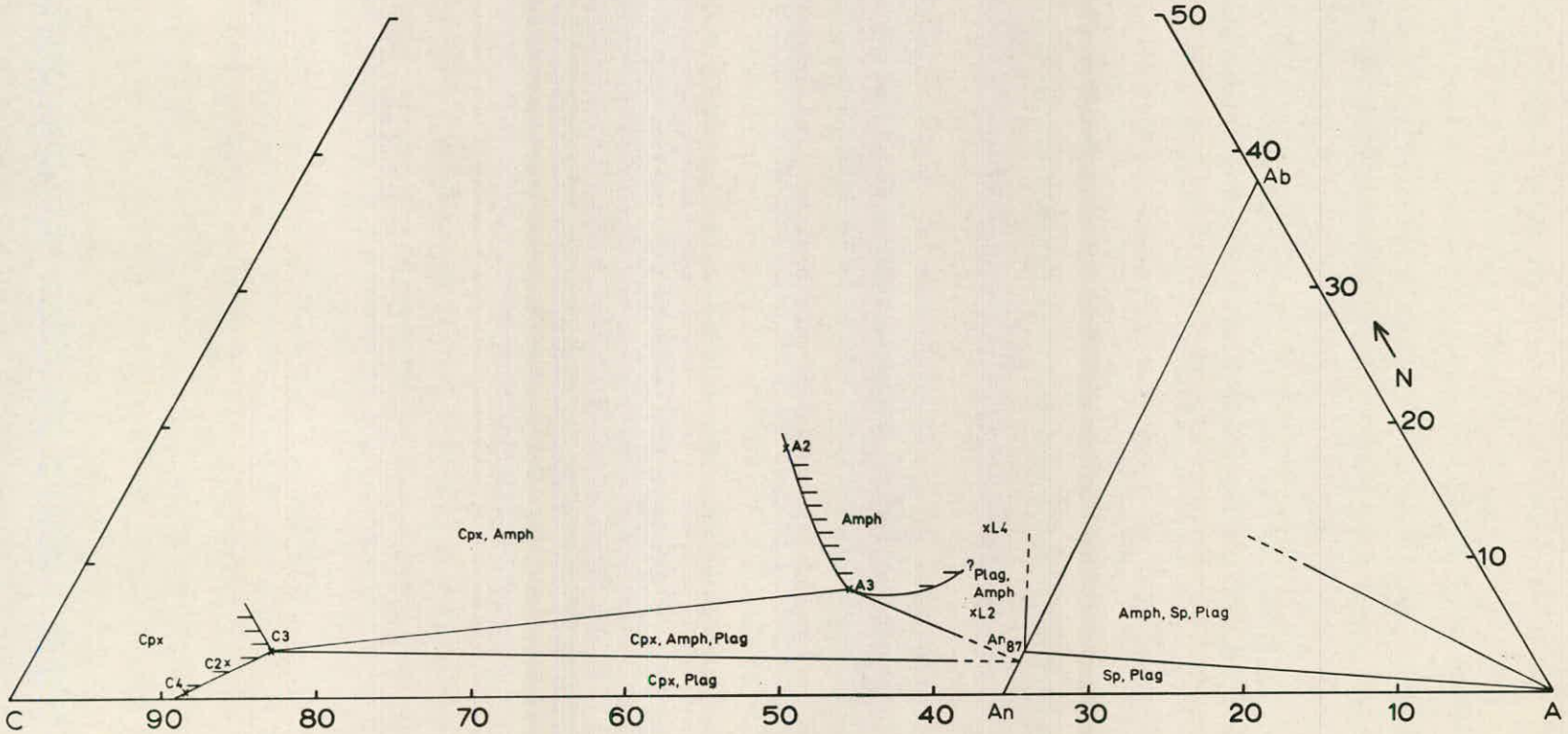
50
40
Ab
30
N
20
10
A2
Amph
xL4
Cpx, Amph
?
Plag,
Amph
xL2
A3
Amph, Sp, Plag
Cpx
C3
C2x
C4
Cpx, Amph, Plag
An87
Cpx, Plag
Sp, Plag
C
90
80
70
60
50
40
An
30
20
10
A

The liquid in equilibrium with forsterite - two pyroxenes - aluminous phase - vapour at 2% and 4% soda are also shown. The liquid at 2% soda projects inside the co-existing mineral tie-triangle on Fig. 3.19 but outside it on Fig. 3.20. Hence, forsterite must be in reaction relationship with this liquid in this equilibrium. The liquid at 4% soda projects outside the relevant tie-triangles on both Figs. 3.19 and 3.20, indicating that both forsterite and clinopyroxene are in reaction relationship with the liquid.

Conclusions

In this synthetic system the possible effect on liquid composition of amphibole stability has been investigated under 5 kb water pressure. A close control of soda content in the bulk compositions and in the residual liquids makes it possible to predict crystallisation sequences of various simple basic oompositions over a range of soda contents. These crystallisation sequences and the change in residual liquid compositions may be visualised in a series of projection diagrams. Quartz-normative, feldspar-rich liquids may be produced in equilibrium with forsterite - two pyroxenes - amphibole under these conditions.

CHAPTER 4

CORRELATION OF RESULTS FROM SYNTHETIC AND NATURAL MATERIALS

Projection of natural compositions into the phase diagrams

The results and diagrams presented in Chapter 3 may only be relevant to geological problems if natural materials exhibit comparable phase relationships under similar conditions.

Experimental work on the phase relationships of natural material at 5 kb pressure under hydrous conditions has been presented by Yoder & Tilley (1962), Holloway & Burnham (1972), Eggler (1972a) and Cawthorn et al. (1973). The crystallisation sequences for the compositions studied are presented in Table 4.1, and the projections of the compositions are shown in Figs. 4.1 and 4.2.

In order to compare these results with those of the synthetic study the soda content is removed from the compositions for exactly the same reason as in the projection of the synthetic compositions (Appendix A). The range of soda contents of the natural materials is from 2.1 - 4.3%. Treatment of the potash content is slightly more complicated. Precisely how small concentrations of K_2O affect the relative stabilities of minerals found in these studies cannot be predicted. The addition of small quantities of soda causes little change in the relative stability of the minerals, although there is a general lowering of temperatures of crystallisation. As potash does not enter any of the solid phases to any appreciable

TABLE 4.1.

Crystallisation sequences of natural materials under 5 kb pressure in the presence of water

1	2	3	4
Ol in 1120°C	Ol in 1090°C	Ol in 1090°C	Cpx in 1040°C
Cpx in 1090°C	Cpx in 1050°C	Cpx in 1040°C	Amph in 960°C
Amph in 970°C	Amph in 1020°C	Amph in 1030°C	Sphene in 890°C
Ol out 970°C	Ol out 980°C	Ol out 980°C	Plag in 870°C
Cpx out 930°C	Cpx out 980°C	Cpx out 940°C	Cpx out 840°C
Sphene in 870°C	Plag in 940°C	Plag in 860°C	
Plag in 820°C			

5	6	7	8
Ol in 980°C	Opx in 1040°C	Ol in > 1090°C	Ol in >1130°C
Opx in 980°C	Cpx in 1030°C	Cpx in >1090°C	Cpx in 1120°C
Ol out 980°C	Plag in 1010°C	Mt in 1090°C	Amph in 1060°C
Cpx in 970°C	Amph in 940°C	Amph in 1020°C	Ol in 960°C
Amph in 940°C		Plag in 900°C	Plag in 930°C
Plag in 920°C			

9	10	11	12
Ol in 1130°C	Ol in 1120°C	Ol in 1070°C	Cpx in 1050°C
Cpx in 1120°C	Cpx in 1120°C	Cpx in 1070°C	Amph in 1030°C
Amph in 1050°C	Amph in 1040°C	Amph in 1040°C	Plag in 940°C
Ol out 960°C	Ol out 970°C	Ol out 990°C	
Plag in 930°C	Plag in 930°C	Plag in 940°C	

Data obtained by interpolation from diagrams. Uncertainty in temperatures estimated to be ± 20°C.

1. Olivine tholeiite, Yoder & Tilley (1962)
2. High-alumina basalt, Yoder & Tilley (1962)
3. Alkali basalt, Yoder & Tilley (1962)
4. Oxidised hawaiite, Yoder & Tilley (1962)
5. Andesite, Eggler (1972a), water-saturated conditions
6. Andesite, Eggler (1972a), charges containing 4% H_2O in melt.
7. Olivine tholeiite, Holloway & Burnham (1972)
8. Basanitoid, 209, Cawthorn et al. (1973)
9. Basanitoid, 184, Cawthorn et al. (1973)
10. Alkali basalt, 286, Cawthorn et al. (1973)
11. Basaltic andesite, 201, Cawthorn et al. (1973)
12. Basaltic andesite, 198, Cawthorn et al. (1973).

FIG.4.1

Projection from olivine, alkalis and vapour into the plane CS - MS - A (weight percent) of all natural compositions studied under 5 kb water pressure. Phase relationships for synthetic liquids containing 3% and 5% soda are taken from Figs. 3.12d and 3.12f. At 3% soda plagioclase is the aluminous phase, while with 5% soda amphibole crystallises. The stability field of spinel has been excluded for clarity. Crystallisation sequences and sources of data are given in Table 4.1.

Crystallisation sequence designation: open triangle - olivine in, clinopyroxene in, amphibole in, olivine out, clinopyroxene out, plagioclase in; open circle - olivine in, clinopyroxene in, amphibole in, olivine out, plagioclase in; inverted open triangle - olivine in, clinopyroxene in, amphibole in, plagioclase in; open square - clinopyroxene in, amphibole in, plagioclase in; solid square - olivine in, orthopyroxene in, olivine out, clinopyroxene in, amphibole or plagioclase in, plagioclase or amphibole in.

Abbreviations as for Fig. 3.12.

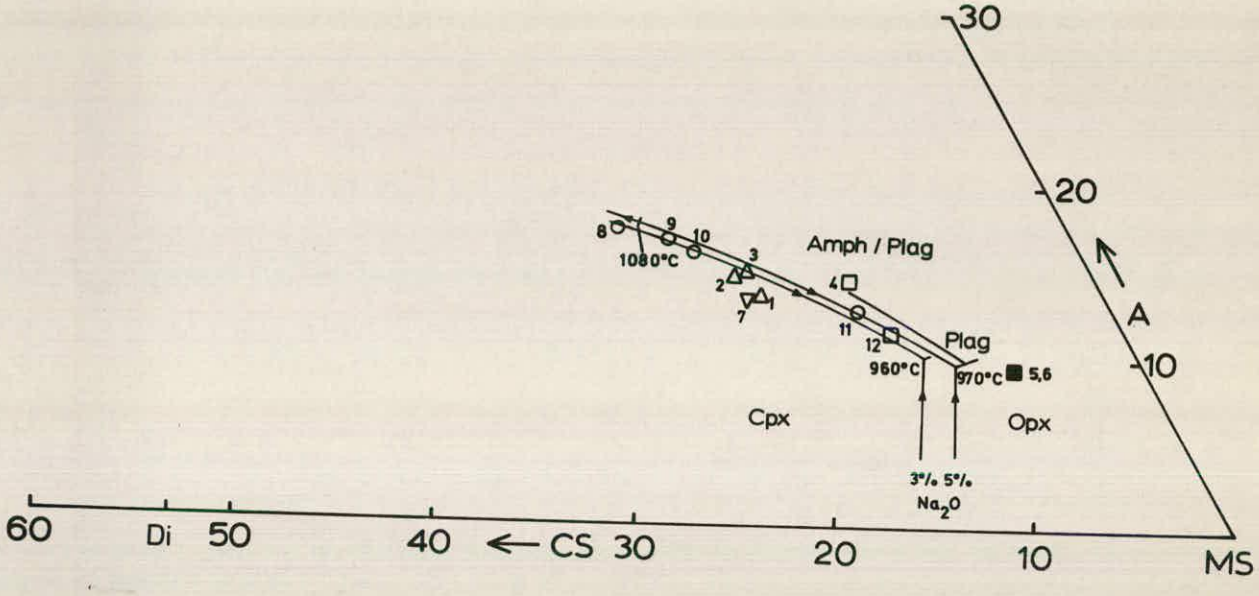
30
20
10
A
MS
60
Di
50
40
CS
30
20
10
Amph / Plag
Plag
Cpx
Opx
1080°C
960°C
970°C
5,6
3% 5%
Na_2O
1
2
3
4
7
8
9
10
11
12

FIG. 4.2

Projection from clinopyroxene, alkalis and vapour into the plane CA - M - S (weight percent) of all compositions studied under 5 kb water pressure. Phase relationships for synthetic liquids containing 3% and 6% soda are taken from Figs. 3.14c and 3.14e. Crystallisation sequences and sources of data are given in Table 4.1.

Crystallisation sequence designation as for Fig. 4.1.

Abbreviations as for Fig. 3.12.

The clinopyroxene - forsterite - amphibole - liquid - vapour peritectic curve for natural materials is estimated to lie slightly to the forsterite-rich side of the curve for synthetic materials.

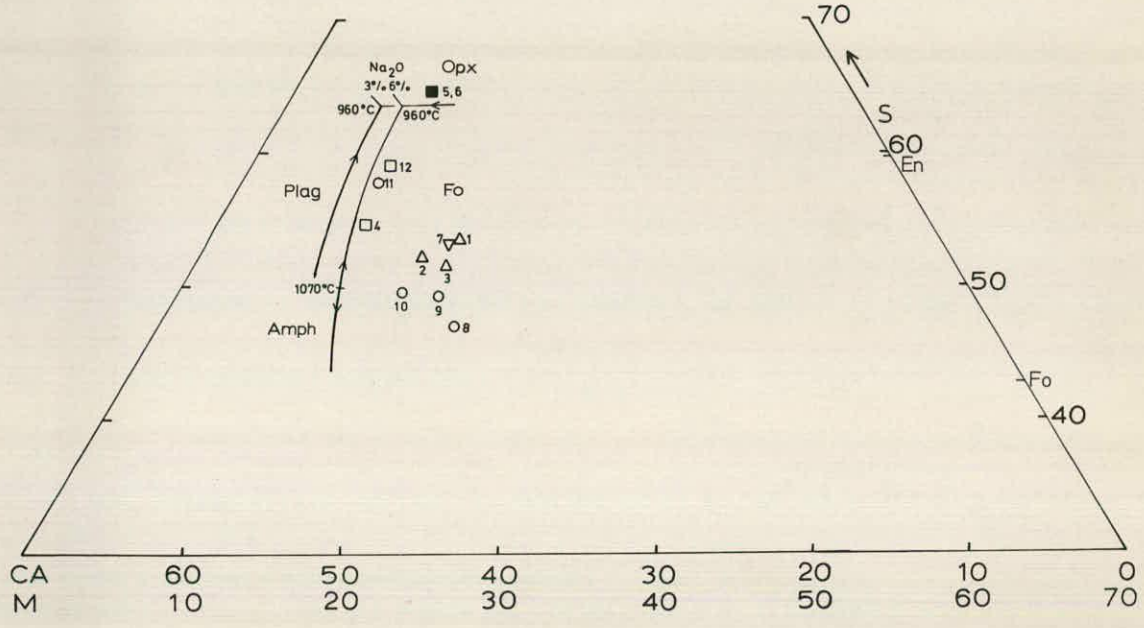
Na2O
3%
6%
Opx
5,6
960°C
960°C
Plag
12
11
Fo
4
7
1
2
3
1070°C
10
9
8
Amph
70
S
60
En
50
Fo
40
CA
M
60
10
50
20
40
30
30
40
20
50
10
60
0
70

extent, it may have a similar effect. Hence, potash is regarded as an incompatible oxide and is not recalculated into the projection scheme. The range of potash contents in the compositions studied is from 0.14 - 1.69%.

TiO_2 is recalculated in the scheme of O'Hara (1968) and Jamieson (1969) so that ulvo-spinels and other spinels all project at the same point. The data of Yoder & Tilley (1962), Eggler (1972a) and Cawthorn et al. (1973) suggest that spinels are relatively unimportant phases crystallising under 5 kb water pressure, and that TiO_2 is more likely to be incorporated into the amphiboles. Hence, a recalculation scheme in which TiO_2 entered an amphibole structure would be desirable. However, pargasites, basaltic hornblendes and kaersutites project in very similar regions of the XO - YO - R_2O_3 - ZO_2 volume using the scheme of Jamieson (1969), and so it is thought to be sufficiently accurate for the present purposes. Consequently, in the projection of natural compositions in Figs. 4.1 and 4.2 the alkali-free analysis is recalculated using this scheme.

The phase relationships for synthetic material at various soda contents are also shown in Figs. 4.1 and 4.2. The 3% soda relationships indicate the likely liquidus minerals for these natural compositions. The higher soda content relationships demonstrate the subsequent crystallisation of these materials.

The crystallisation sequences predicted from the synthetic data for the natural materials are very similar

to those observed (Table 4.1). Slight differences which are apparent are that most compositions project very close to the olivine - clinopyroxene - amphibole - liquid - vapour peritectic curve in the olivine plus soda projection diagram, while the actual experimental data for the natural samples suggest that there should be a temperature range of very approximately 50°C of olivine plus clinopyroxene prior to the appearance of amphibole. However, the temperatures of appearance of amphibole show a close similarity with those predicted from the synthetic study.

The concentration of soda in residual liquids is of interest in this study, but data are only available from Holloway & Burnham (1972). Their percent crystallinity calculations suggest that amphibole begins to crystallise from a liquid containing about 3% soda. The composition of the basalt which they used is very similar to the gels of series 6 in terms of its projection points (as shown by the overlays, Figs. 3.11 and 3.13). The gels from series 6 show a crystallisation sequence of olivine, then clinopyroxene, followed by amphibole for liquids containing greater than 3.8% soda. The crystallisation sequence of many of the other natural compositions is similar to that of the basalt used by Holloway & Burnham (1972) and so comparable degrees of crystallinity may be predicted prior to the appearance of amphibole. Hence, generally, the soda content of the liquids from the natural materials when amphibole begins to crystallise will be in the range 3 - 5%. This is the range of soda levels over which the amphibole stability field in synthetic materials shows a very rapid

expansion. It is concluded that soda levels in liquids which crystallise amphibole from natural materials are similar, possibly slightly lower, than determined in this synthetic study.

Mineral compositions

Mineral analyses have also been presented by Holloway & Burnham (1972), Eggler (1972b) and Cawthorn et al. (1973). These are compared with the compositions obtained in the synthetic system in Figs. 4.3 and 4.4. The recalculation of these mineral analyses is identical to that for the bulk rock compositions described earlier. The clinopyroxenes and amphiboles show very similar compositions in both the synthetic and natural materials.

D.H. Green & Ringwood (1970) suggest that a hydrous upper mantle might be composed of the assemblage olivine - orthopyroxene - amphibole, termed ampholite. The compositions of various possible upper mantle models are projected into Figs. 4.3 - 4.5. It is evident from these diagrams, especially Fig. 4.5, that such a mineralogy is possible at shallow depths, and examples have been reported by Tilley & Long (1967), although they suggest that this is residual material formed by extraction of some basic liquid.

Effect of variation in P_{Total} and P_{H_2O} on phase relationships

The data of Yoder & Tilley (1962) and Holloway & Burnham (1972) showed that over most of the pressure range 2 - 10 kb the order of crystallisation of basic compositions

FIG. 4.3.

Estimated solid solution limits of minerals formed under 5 kb water pressure, projected from olivine, alkalis and vapour into the plane CS - MS - A (weight percent). The solid solution limits in the synthetic system are taken from Fig. 3.19.

Minerals:

A1 refers to amphibole, Eggler (1972b) Table 1, No.1.

A2 refers to amphibole, Holloway & Burnham (1972), Table 4, No.16.

A3 " No.20.

A4 refers to amphibole, Cawthorn et al. (1973), Table 3, No. 5.

A5 " No. 3.

A6 " No. 4.

A7 " No. 1.

A8 refers to amphibole, Eggler (1972b), Table 1, No. 2.

A9 refers to natural amphibole from ampholite (Tilley & Long, 1967)

C1 refers to clinopyroxene, Holloway & Burnham (1972), Table 4, No. 19.

C2 " No. 15.

C3 refers to amphibole, Cawthorn et al. (1973), Table 3, No. 2.

C4 " No. 4.

C5 " No. 5.

Rocks:

I Pyrolite I, D.H. Green & Ringwood (1963)

II Pyrolite II, D.H. Green & Ringwood (1967)

III Pyrolite III, Ringwood (1966)

IV Pyrolite 4:1 model, D.H. Green & Ringwood (1963)

5 Upper mantle compositions, Nichols (1967)

Abbreviations as for Fig. 3.12.

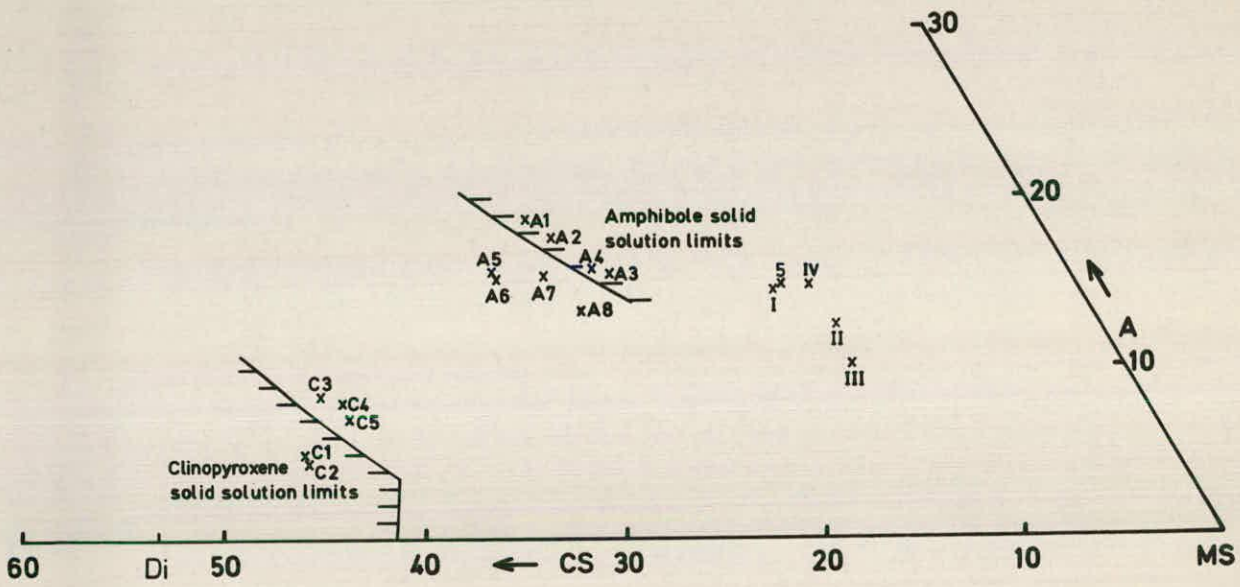
30
20
10
A
Amphibole solid
solution limits
xA1
xA2
xA3
A4
A5
A6
A7
xA8
5
IV
I
II
III
C3
xC4
xC5
xC1
C2
Clinopyroxene
solid solution limits
60
Di
50
40
CS
30
20
10
MS

FIG. 4.4.

Estimated solid solution limits of minerals formed under 5 kb water pressure, projected from clinopyroxene, alkalis and vapour into the plane CA - M - S (weight percent). The solid solution limits in the synthetic system are taken from Fig. 3.20.

Legend as for Fig. 4.3.

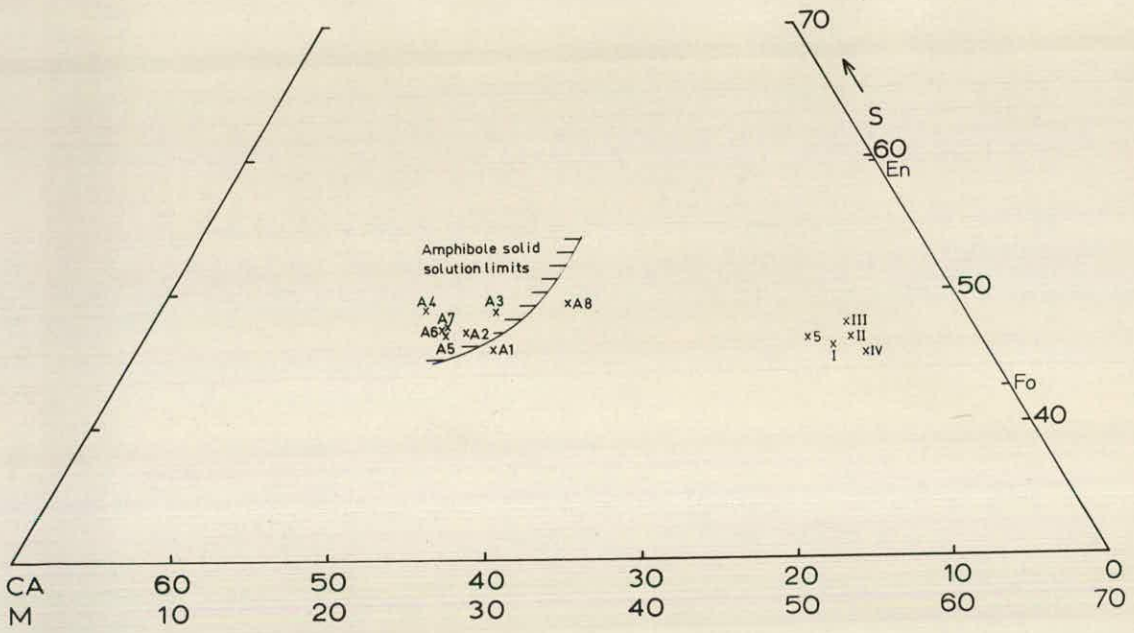
70
S
60
En
50
Fo
40
Amphibole solid
solution limits
A4
A7
A3
xA8
A6
xA2
A5
xA1
xIII
x5
xII
x
I
xIV
CA
M
60
10
50
20
40
30
30
40
20
50
10
60
0
70

FIG. 4.5.

Estimated solid solution limits of minerals formed under 5 kb water pressure, projected from olivine, orthopyroxene and vapour into the plane C - A - N (weight percent). The solid solution limits in the synthetic system are taken from Fig. 3.21.

Legend as for Fig. 4.3.

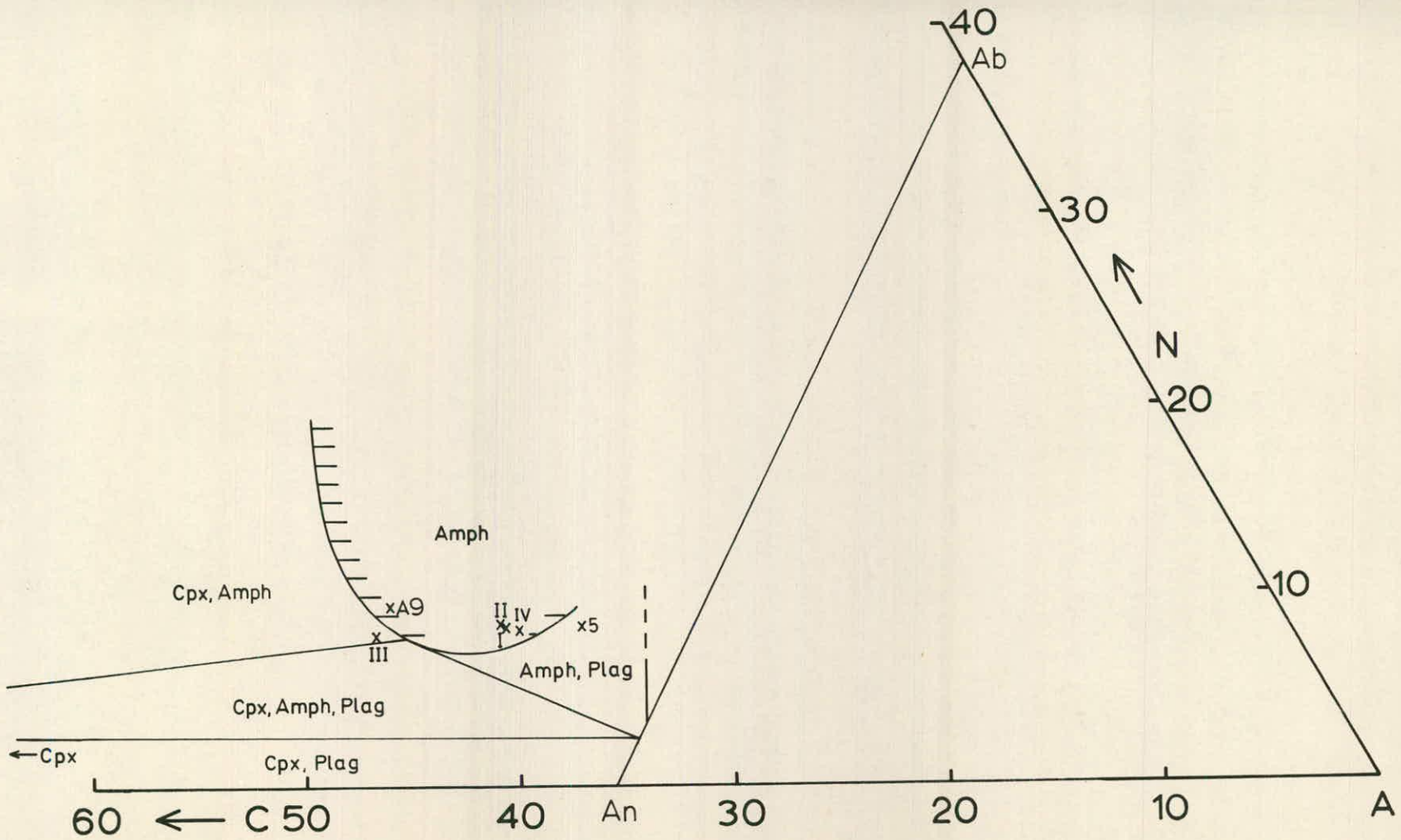
40
Ab
30
N
20
10
Amph
Cpx, Amph
xA9
II IV
x5
III
Amph, Plag
Cpx, Amph, Plag
←Cpx
Cpx, Plag
60 ← C 50
40
An
30
20
10
A

remained the same. Over this range the amphibole stability increases relative to olivine and clinopyroxene. Hence, it is thought that the phase relationships under 5 kb pressure may act as an indicator for phase relationships over a considerable range of pressures. At higher pressure a slightly larger stability field of amphibole at the expense of olivine and clinopyroxene may be envisaged.

The studies of Holloway & Burnham (1972) and Eggler (1972a) were carried out under water-undersaturated conditions, while Yoder & Tilley (1962) and Cawthorn et al. (1973) employed water-saturated conditions. Eggler (1972a) showed that olivine is the liquidus mineral for a quartz-normative composition, although its stability range is very limited. Holloway & Burnham (1972) present data which suggest that a quartz-normative liquid may be produced which does not crystallise orthopyroxene. This indicates that orthopyroxene may melt incongruently at 5 kb in a water-undersaturated environment. There is no evidence, at this pressure, that the orthopyroxene stability field expands relative to the anhydrous situation on the addition of a small amount of water, and then contracts even more rapidly as P_{H_2O} approaches P_{Total} as required by D.H. Green (1971).

Holloway & Burnham (1972) suggest that the thermal stability of amphibole is increased by water pressure less than total pressure. However, the stability of olivine and clinopyroxene will also be increased under these conditions. Hence, the relative stability of amphibole is unaffected by changing the partial pressure of water. Consequently, the phase diagrams presented in Chapter 3, are thought to

apply to either water-saturated or water-undersaturated conditions.

Conclusions

The experimentally determined phase relationships for synthetic material are considered to represent the behaviour of natural material sufficiently accurately for the diagrams derived in Chapter 3 to be used as a basis for discussing certain geological processes in which the presence of water is considered essential.

CHAPTER 5

GEOLOGICAL IMPLICATIONS OF HYDROUS MAGMA GENESIS

Water content of magmas

Nearly all basic magmas contain small proportions of water, as evidenced by the presence of hydrous minerals in the evolved rocks of many suites. However, before crystallisation sequences are likely to be significantly modified by the presence of water compared to the anhydrous course there must be a significant water pressure. J. R. Holloway (in press) has demonstrated that amphiboles become stable at high temperatures for conditions of P_{H_2O} greater than $0.4\ P_{Total}$ for total pressures from 3 - 10 kb. The studies of Hamilton et al. (1964) and this study (Appendix C) indicate that liquids may dissolve 8% - 10% by weight of water under 5 kb pressure. Hence, magmas must contain at least 3% - 4% water if the crystallisation is likely to be influenced by hydrous mineral stability.

This is generally much higher than observed in many basic magmas. However, there is evidence that calc-alkaline and anorthositic magmas may contain substantial amounts of water (Buddington, 1961; Yoder, 1969), and hence it is reasonable to consider models for their evolution invoking hydrous mineral stability.

Calc-alkaline magmas

Evidence of water in calc-alkaline magmas stems from several observations reviewed by Yoder (1969). These include: the explosive nature of most andesitic volcanoes;

presence of hydrous minerals, often in various stages of breakdown; the extremely calcic plagioclase compositions often observed as phenocryst cores in lavas (Lewis, 1969 and 1973); the anomalously high liquidus temperatures at atmospheric pressure producing a crystallisation sequence different from that observed in the natural rocks (Brown & Schairer, 1968 and 1971); and the maintenance of a fairly high oxygen fugacity during fractionation (Osborn, 1959).

The compositions of average andesite, and of allegedly parental magmas of calc-alkaline suites are presented in Table 5.1. They are presented in Figs. 5.1 - 5.6, where they may be compared with the phase relationships under 5 kb water pressure determined from this synthetic study but claimed to approximate to those of natural material. The alkali-free recalculation scheme of Jamieson (1969) is used for the reasons discussed in Chapter 4.

In Fig. 5.1. most of the andesites are seen to project from olivine and orthopyroxene near to the liquid composition in the olivine - orthopyroxene - clinopyroxene - amphibole - plagioclase - liquid - vapour isobaric invariant equilibrium suggesting that they could be the result of partial melting of such an assemblage provided the olivine and orthopyroxene levels are appropriate. The partial melting of an amphibolite mineralogy (D.H. Green & Ringwood, 1970), a possible upper mantle assemblage (see Chapter 4), could also produce such a liquid.

Melting of the upper mantle in the pressure range 2-10 kb is thought unlikely because of the extremely high

FIG. 5.1.

Calc-alkaline compositions.

Projection from olivine, orthopyroxene and vapour into the plane C - A - N (weight percent) of calc-alkaline parental magmas and average andesite compositions. Phase relationships under 5 kb water pressure are taken from Fig. 3.15, and the amphibole solid solution limits from Fig. 3.21.

Circles represent average andesite compositions; crosses - postulated parental magmas of calc-alkaline suites; squares - parental magmas to Japanese basaltic provinces. Compositions and sources of data are given in Table 5.1.

Abbreviations as for Fig. 3.12.

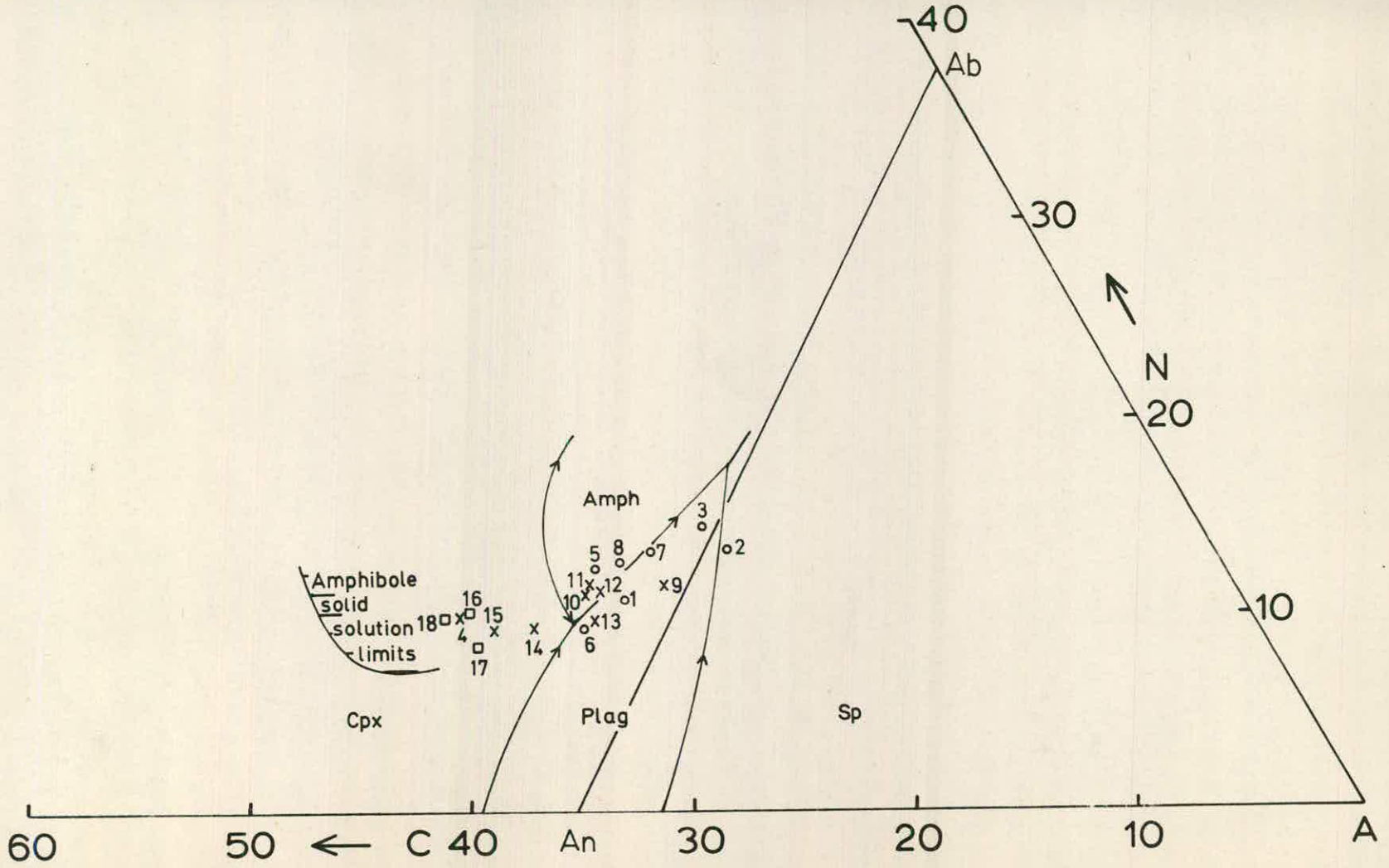
40
Ab
30
N
20
10
Amph
Amphibole
solid
solution
limits
Cpx
Plag
Sp
60
50
C
40
An
30
20
10
A

TABLE 5.1.

Calc-alkaline compositions: alleged parental magmas and average andesites

	1	2	3	4	5	6	7	8	9
SiO_2	58.17	59.59	59.78	51.7	54.9	57.3	59.5	60.8	54.4
Al_2O_3	17.26	17.31	17.19	16.9	17.5	17.4	17.2	16.8	16.5
Fe_2O_3	3.07	3.33	2.45	-	-	-	-	-	1.6
FeO	4.17	3.13	3.65	10.4	8.18	7.3	6.10	5.13	6.4
MgO	3.23	2.75	3.17	6.5	4.71	3.52	3.42	2.15	6.6
CaO	6.93	5.80	6.06	11.0	8.49	8.65	7.03	5.60	7.8
Na_2O	3.21	3.58	3.96	3.1	3.43	2.63	3.68	4.10	3.5
K_2O	1.61	2.04	1.67	0.4	1.10	0.70	1.60	3.25	1.7
TiO_2	0.80	0.77	0.85	-	0.82	0.58	0.70	0.77	1.0

	10	11	12	13	14	15	16	17	18
SiO_2	53.5	56.3	54.9	53.4	49.56	51.7	48.73	48.10	48.11
Al_2O_3	18.3	17.3	18.1	19.0	17.88	18.2	16.52	16.68	15.55
Fe_2O_3	3.2	1.9	3.9	3.2	2.78	-	3.37	3.88	2.99
FeO	5.3	6.3	3.8	5.9	7.26	9.1	8.44	7.75	7.19
MgO	5.5	4.7	5.4	4.0	6.97	5.1	8.24	8.89	9.31
CaO	9.0	7.9	8.6	9.3	9.99	11.1	12.25	10.48	10.43
Na_2O	3.4	3.1	3.4	3.1	2.90	3.0	1.21	2.51	2.85
K_2O	1.1	1.2	0.8	0.8	0.73	0.7	0.23	0.46	1.13
TiO_2	0.4	1.1	0.8	1.1	1.53	1.0	0.63	0.73	1.72

Average compositions

Chayes (1969, Table 1)

1. Average Cenozoic andesite
2. Average andesite after Daly
3. Average Cenozoic andesite in U.S.A.

Taylor (1969, Table 1)

4. Average high-alumina basalt
5. Average low-silica andesite
6. Average low-potash andesite
7. Average andesite
8. Average high-potash andesite

(Table 5.1 Contd.)

Table 5.1 (Contd)

Alleged parental magmas

Best (1969, Table 1)	9. Caledonides
	10. Mount Lassen
	11. Southern California batholith
	12. Crater Lake
	13. Lesser Antilles
	14. High Cascades and Oregon plateau
	15. Aleutian Islands
Kuno (1967)	16. Pigeonitic series, Japan
	17. High-alumina basalt series, Japan
	18. Alkali basalt series, Japan

(Analyses 4-8,15 contain total iron as FeO.)

geothermal gradient required. The alternative interpretation is that a liquid, derived from much greater depth, undergoes extensive crystallisation in this pressure range and produces a liquid whose composition approaches the thermal minimum in this system. Figs. 5.2 and 5.3 provide evidence for rejecting shallow level melting, and supporting the second model. Any partial melt from an ultrabasic upper mantle source ought to have olivine and orthopyroxene as liquidus phases under the conditions of its formation. In both these projection diagrams the calc-alkaline parental magmas do not lie in or at the edge of the orthopyroxene stability field.

The andesite compositions do lie close to the orthopyroxene stability field and so the use of Fig. 5.1 to discuss their phase relationships may be justified, while the parental magmas, not saturated with orthopyroxene,

FIG. 5.2.

Calc-alkaline compositions.

Projection from olivine, alkalis and vapour into the plane CS - MS - A (weight percent) of calc-alkaline parental magmas and average andesite compositions. Phase relationships under 5 kb water pressure for synthetic liquids containing 3% and 5% soda are taken from Figs. 3.12d and 3.12f, and the amphibole solid solution limits from Fig. 3.19.

Circles represent average andesite compositions; crosses - postulated parental magmas of calc-alkaline suites; squares - parental magmas to Japanese basaltic provinces. Compositions and sources of data are given in Table 5.1.

Abbreviations as for Fig. 3.12.

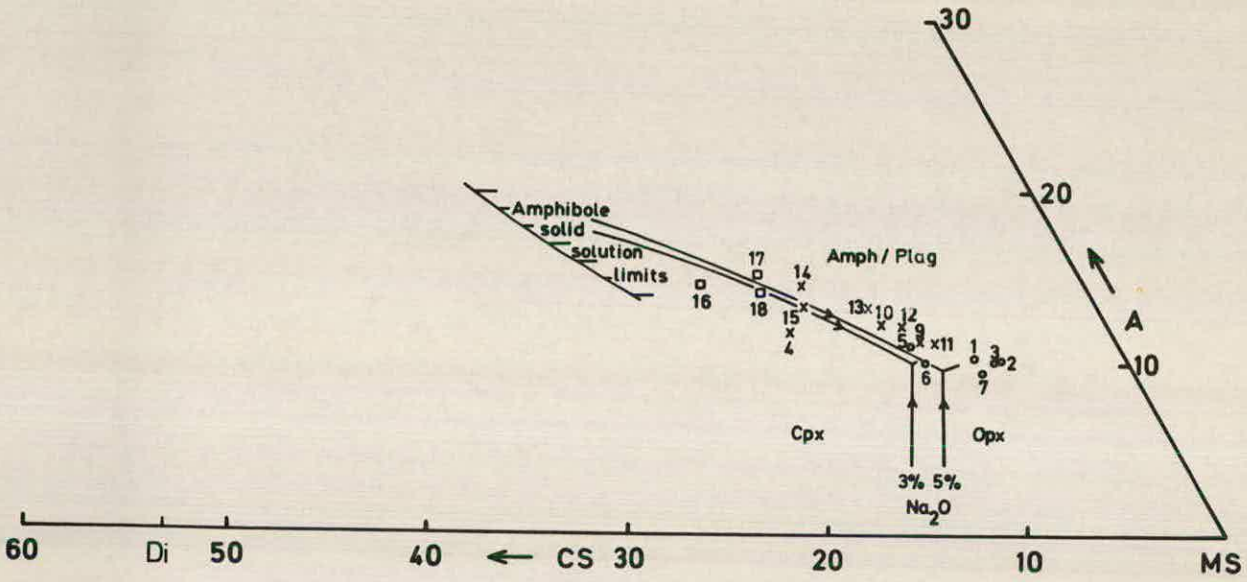
30
20
10
A
Amphibole
solid
solution
limits
Amph / Plag
17
16
18
14
15
4
13
10
12
9
5
8
11
1
3
2
7
6
Cpx
Opx
3%
5%
Na2O
60
Di
50
40
CS
30
20
10
MS

FIG. 5.3.

Calc-alkaline compositions.

Projection from clinopyroxene, alkalis and vapour into the plane CA - M - S (weight percent) of calc-alkaline parental magmas and average andesite compositions. Phase relationships under 5 kb water pressure for synthetic liquids containing 3% and 6% soda are taken from Figs. 3.14c and 3.14e, and amphibole solid solution limits from Fig. 3.20.

Circles represent average andesite compositions; crosses - parental magmas of calc-alkaline suites; squares - parental magmas to Japanese basaltic provinces. Compositions and sources are given in Table 5.1.

Abbreviations as for Fig. 3.12.

should strictly not be considered in Fig. 5.1.

If some primitive hydrous liquid crystallised in the pressure range 2 - 10 kb, its crystallisation course may be controlled by the phase relationships in Figs. 5.2 and 5.3. In Fig. 5.2 the parental magma compositions of various provinces lie close to the range of liquids in equilibrium with olivine - clinopyroxene - amphibole - vapour, and crystallisation along this path would lead towards andesitic liquids. If fractional crystallisation occurred, only amphibole would be formed and the liquids would move directly away from the amphibole composition. As shown in Fig. 5.2, this still leads towards an andesitic liquid.

Fig. 5.3 shows similar relationships, with andesites projecting close to the liquids in the amphibole - two pyroxenes - olivine - liquid - vapour equilibrium, and that these could be derived from the parental magmas either by equilibrium crystallisation of olivine, clinopyroxene and amphibole, or by the removal of amphibole alone, once its stability field has been reached by the fractionating liquids.

The projection of the compositions in the normative basalt tetrahedron are shown in Figs. 5.4 - 5.6. In these compositions it is only possible to compare the natural material with the composition of the liquids in equilibrium with forsterite - 2 pyroxenes - aluminous phase - vapour at various soda contents, and liquids produced in various anhydrous equilibria. In Fig. 5.4, the andesites project close to the hydrous liquid compositions at 3% - 4% soda.

FIG. 5.4.

Calc-alkaline compositions.

Projection from olivine into the planes plagioclase - clinopyroxene - quartz (or nepheline) (weight percent) within the basalt tetrahedron. The locus of the liquids in equilibrium with forsterite - two pyroxenes - aluminous phase - vapour at various soda contents under 5 kb water pressure is presented from Figs. 3.16 - 3.18 (denoted 0% - 3% - 6%). The liquids in equilibrium with olivine - two pyroxenes - plagioclase from 1 atmosphere to 8 kb is taken from Figs. 3.16 - 3.18.

Compositions and sources of data are presented in Table 5.1.

A1, A2 and A3 are synthetic amphibole compositions taken from Table 3.3A, numbers 2, 3 and 4.

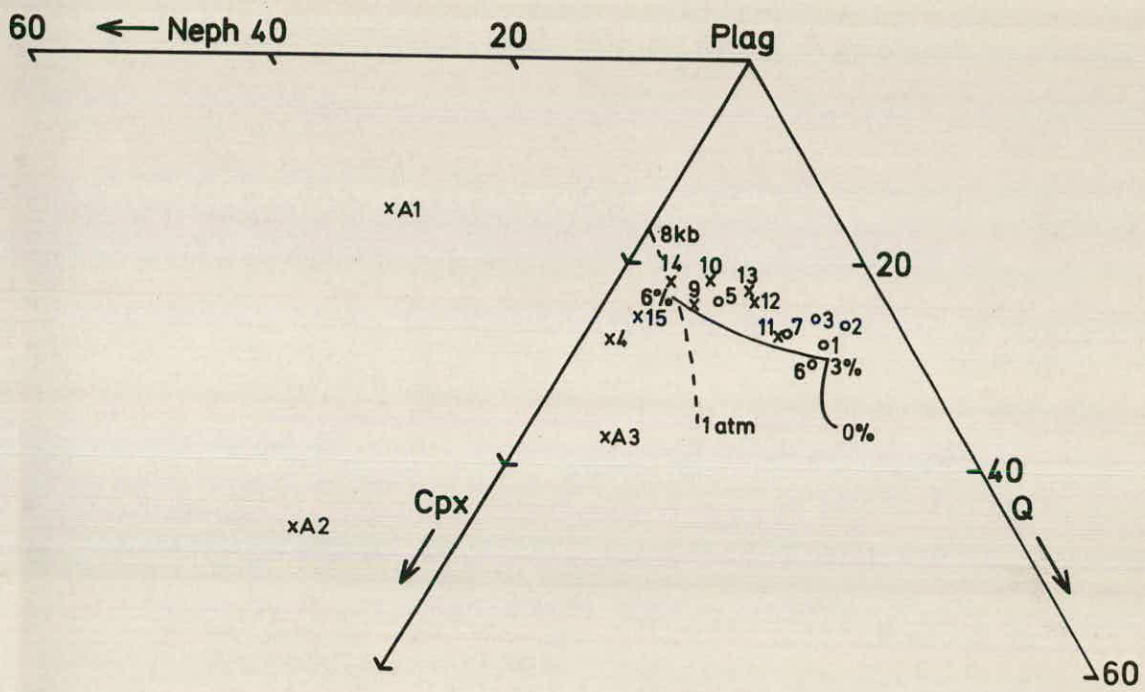
60
Neph 40
20
Plag
xA1
8kb
14
10
13
9
5
12
6%
15
11
7
3
2
1
4
6
3%
0%
1 atm
xA3
20
40
Q
60
Cpx
xA2

FIG. 5.5.

Calc-alkaline compositions.

Projection from clinopyroxene into the planes plagioclase - olivine - quartz (or nepheline) (weight percent) within the basalt tetrahedron.

Legend as for Fig. 5.4.

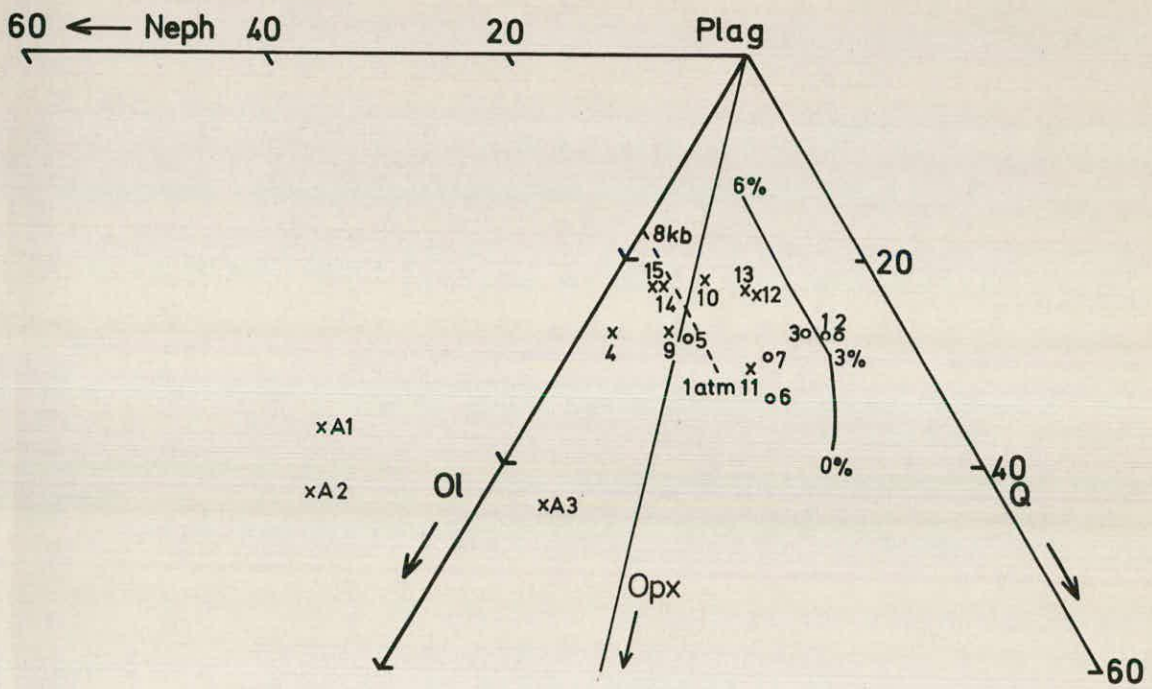
60 ← Neph
40
20
Plag
6%
8kb
15
14
13
12
10
20
12
3%
0%
1atm
11
xA1
xA2
xA3
Ol
Opx
40
Q
60

FIG. 5.6.

Calc-alkaline compositions.

Projection from plagioclase into the planes olivine - clinopyroxene - quartz (or nepheline) (weight percent) within the basalt tetrahedron.

Legend as for Fig. 5.4.

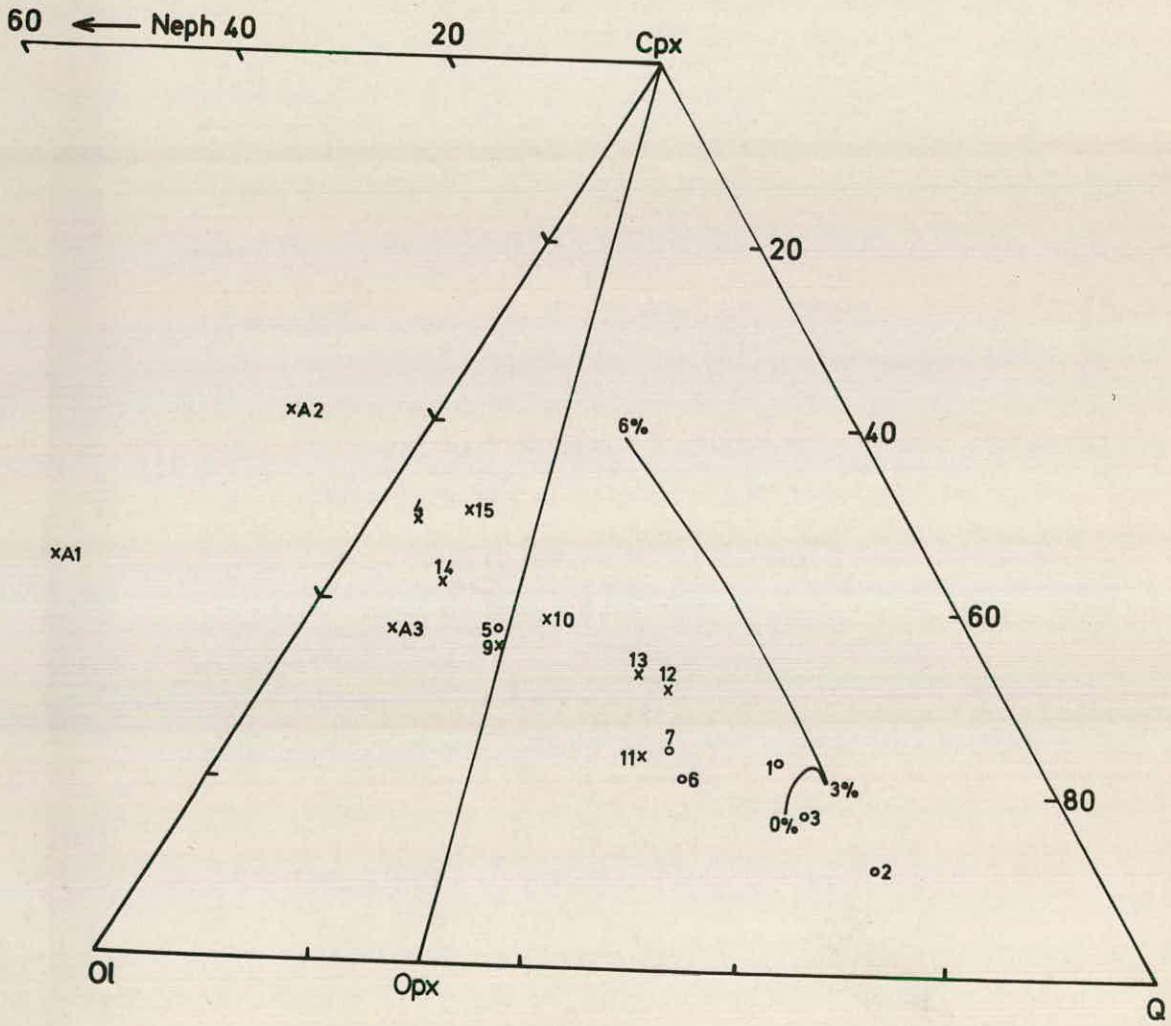
60
Neph 40
20
Cpx
20
40
60
80
Ol
Opx
Q
xA1
xA2
xA3
x15
14
x10
5
9
13
12
7
11
6
1
3%
0%
3
2
6%

The parental magmas appear to project close to these liquid compositions at higher soda levels, but because of the great difference between their soda contents compositions are not comparable. A range of amphibole compositions has been included, but because tie-lines are kinked as they cross from nepheline-normative to enstatite-normative compositions in this projection, it is not easy to demonstrate that their removal from a parental magma composition could produce andesitic derivatives.

The liquid compositions in the anhydrous assemblages forsterite - two pyroxenes - aluminous phase-liquid are also shown and bear no obvious relationship to the andesitic compositions.

Fig. 5.5 demonstrates similar relationships, with the andesitic compositions projecting close to the liquid in equilibrium with forsterite - two pyroxenes - amphibole - plagioclase - liquid - vapour.

In Fig. 5.6 compositions appear more scattered because of the large proportion of the projection phase - plagioclase - in all the compositions. Consequently, small changes in composition cause a large change in the proportions of normative minerals in this diagram. The andesites project in the same region of the diagram as the liquid in the hydrous isobaric invariant equilibrium at 3% soda.

Feldspar compositions

Feldspar crystals in nodules, as xenocrysts, and as cores of phenocrysts in lavas are often extremely calcic (Wager, 1962; Yoder, 1969; Lewis, 1969 & 1973).

Compositions of $An_{>90}$ are reported from these environments. Such compositions are unlikely to be formed by crystallisation under low pressure from the lavas in which they occur.

The data obtained here (Appendix F) suggests that a composition more calcic than An_{87} may crystallise from an andesite-type liquid containing 3% soda under moderate water pressure.

Iron/Magnesium Ratios

One of the characteristics of calc-alkaline volcanic suites is the lack of iron enrichment when compared with tholeiitic provinces (Nockolds & Allen, 1953; Carmichael, 1964). This may be explained by the higher iron/magnesium ratio in amphiboles compared to olivines and pyroxenes crystallising from the same liquid (Holloway & Burnham, 1972; Cawthorn et al., 1973).

Hence, a crystallisation model for calc-alkaline magmas involving moderate water pressure may explain the unusual liquid compositions of andesites, the characteristic iron/magnesium ratio of the suite and the extremely calcium-rich compositions of plagioclase crystals.

Comparison with other models

Calc-alkaline volcanic provinces are characterised by abundant andesitic material. However, this does not mean that it is a primary magma, or the parental magma of the suite. Basaltic material is usually associated with the

andesites, and the andesitic compositions could be the residual products of partial crystallisation of the basalts. The model presented here suggests that all basaltic compositions subjected to crystallisation under several kilobars water pressure will produce an andesitic derivative. Other models which regard andesite as being a primary magma cannot explain the continuum between basaltic and andesitic compositions, or the wide range of basaltic kindreds with which andesite occurs.

Initial wet melting of some basic or ultrabasic source rock may produce andesitic liquids. More extensive melting could produce a range of basaltic compositions. However, if this process were operative, an eruption sequence of andesite followed by basalt would be expected, which is the reverse of that observed.

Consequently, hypotheses suggesting that andesite is the result of direct melting of subducted oceanic plate (T.H. Green & Ringwood, 1966 and 1968; Oxburgh & Turcotte, 1968; Taylor, 1969; Taylor *et al.*, 1969a and b; Fitton, 1971; Holloway & Burnham, 1972) or as a partial melt of hydrous mantle (McBirney, 1969; Yoder, 1969; Kushiro, 1972) are considered inadequate.

An alternative model which provides for the variation in composition from basalt to andesite, proposed by Osborn (1959, 1962 and 1969), involves the removal of magnetite. This has been questioned by Taylor *et al.* (1969a and b) from trace element considerations. Furthermore, there is no reported field evidence of extensive magnetite separation.

Kuno (1968) advocated extensive low pressure fractionation of olivine, pyroxenes and feldspar to produce a trend from basalt to andesite. However, phase relationships in Figs. 5.4 - 5.6 indicate that this is an unlikely process. Further, the degree of crystallinity required to produce an andesite from a basalt ranges from 47% - 98%. Such large degrees of crystallisation would tend to produce very high incompatible trace element concentrations, which are not observed (Taylor, 1969). The absence of evidence for extremely large volumes of these low-pressure cumulates likewise argues against this model.

On geochemical grounds several models invoking fractional crystallisation to produce calc-alkaline magmas have been preferred to direct melting of some source rock. Tilley (1950) considered the possibility of amphibole fractionation to explain the distinctive characteristics of andesites, but rejected this model because of lack of evidence for the involvement of amphibole. Because of the low-pressure decomposition of amphibole, absence of this mineral in lavas is to be expected (Westoll, 1968).

Best & Mercy (1967) suggested that amphibole fractionation could explain the observed variation in the Guadalupe igneous complex, California, while Lewis (1969 and 1973) favours the removal of amphibole and other phases to produce the chemical variation in the Soufrière volcanics, St. Vincent. Brown & Schairer (1971) also envisage fractional crystallisation in the presence of water and high oxygen fugacity, and favour amphibole rather than magnetite as the crystallising material producing the more evolved

members of the calc-alkaline suite.

Anorthositic magmas

There is a variety of types of anorthosite (Isachsen, 1968), but possibly the most intriguing are the massif anorthosites.

The evidence proposed by Buddington (1961) for the presence of water in massif anorthositic magmas includes: extremely coarse grain size of minerals, the formation of which would be aided by great fluidity in the liquid as a result of high water content; the development of gabbro pegmatites; the extensive metasomatism, which has been attributed to volatile-rich fluids escaping from the intrusive magma, of marble horizons adjacent to the Adirondak massif; the shattering and cataclasis of minerals which may be due to the explosive release of hydrous pressure built up in the residual liquids.

Philpotts (1966) drew attention to the similarity between calc-alkaline andesitic compositions and the parental magmas of the anorthosite complex in Southern Quebec. However, not all the provinces containing massif anorthosites are thought to have an andesitic parental magma composition. Such complexes have chill zones which suggest a gabbroic or anorthositic gabbroic parental composition. Examples of these complexes are described by Olmsted (1968) from northwest Wisconsin; by Phinney (1968) from Minnesota; by Emslie (1968) from Michikamau and by Bridgewater & Harry (1968) from southwest Greenland.

The range of parental magma compositions postulated for

various different anorthositic intrusions is quite large, see Table 5.2. These are presented in Figs. 5.7 and 5.8, the projection procedure being the same as described in Chapter 4. The diagrams are analogous to Figs. 5.1 and 5.2 used in the discussion of calc-alkaline magmas and suggest similar controls on crystallisation. The generation of a hydrous basaltic composition, possibly by partial melting within the low velocity zone of the upper mantle, is the first stage of this process. Compositions 2, 3 and 4 in Table 5.2 and Figs. 5.7 and 5.8 are thought to be examples of such hydrous basalts. Crystallisation of these liquids within the pressure range 2 - 10 kb will produce compositions akin to andesites or compositions similar to 5, 6 and 7 in Table 5.2, by the same process as discussed in the previous section. Varying degrees of crystallisation in this pressure regime could produce the range of parental magma compositions shown in these diagrams. In Fig. 5.8, the postulated parental magma from the Mineral Lake intrusion (Olmsted, 1968) does not appear related to the olivine - clinopyroxene - amphibole - liquid - vapour peritectic curve. However, this composition appears rather unusual in containing 18% total iron; and may not represent the true parental magma.

Crystallisation of anorthosites

The depth of intrusion of anorthositic bodies has been discussed by several workers, on consideration of mineral assemblages. Estimates suggest total pressures of 0.5 - 3 kb with moderate water pressure (see review by Isachsen, 1968), although in some cases they are based on

TABLE 5.2

Compositions of possible parental magmas of some anorthosite intrusions

	1	2	3	4	5	6	7
SiO_2	47.01	47.6	47.1	48.3	53.1	53.2	51.0
Al_2O_3	13.26	15.3	15.7	16.1	15.4	17.3	17.3
Fe_2O_3	2.19	2.8	2.9	3.0	3.8	3.4	-
FeO	15.08	10.0	9.2	9.4	6.6	6.0	7.0
MgO	6.99	6.9	6.0	6.2	5.9	6.1	5.0
CaO	9.03	12.5	11.7	12.0	9.1	8.7	9.5
Na_2O	2.75	2.6	2.9	3.0	3.3	3.2	4.6
K_2O	0.80	0.2	0.2	0.2	1.2	0.8	1.0
TiO_2	1.15	1.4	1.5	1.5	1.3	1.0	2.7

1. Mineral Lake chill zone - Olmsted(1968)
2. Fine grained marginal olivine gabbro, Michikamau - Emslie (1968)
3. Fine grained marginal hornblende olivine gabbro, Michikamau - Emslie (1968)
4. Chill margin, Michikamau - Emslie (1968)
5. Postulated parental magma of the anorthosite-mangerite series, Southern Quebec - Philpotts (1968)
6. Postulated parental magma of Morin anorthosite - Philpotts (1966)
7. Average norite, Thirteenth Lake dome - Letteney (1968)

FIG. 5.7.

Anorthosite parental magma compositions.

Projection from olivine, alkalis and vapour into the plane CS - MS - A (weight percent) of parental magmas of some anorthosite complexes. Phase relationships at 3% and 5% soda for synthetic material under 5 kb water pressure are taken from Figs. 3.12d and 3.12f, and the amphibole solid solution limit from Fig. 3.19.

Compositions and sources of data are given in Table 5.2.

Abbreviations as for Fig. 3.12.

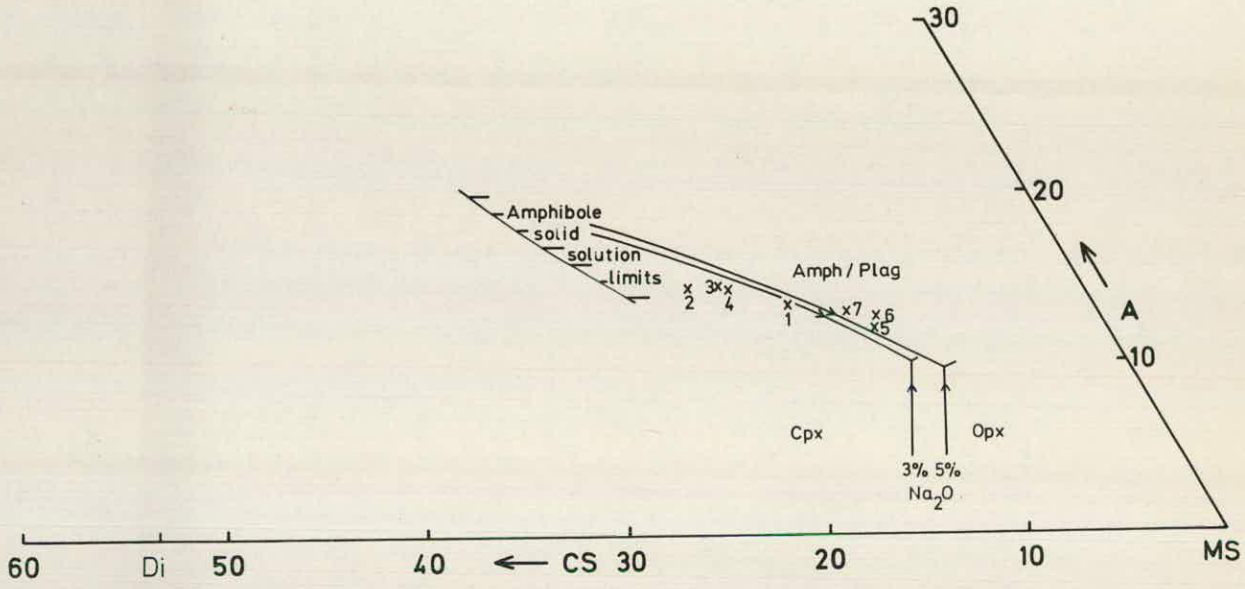
30
20
10
A
Amphibole
solid
solution
limits
Amph / Plag
x 2
3x
4
x 1
x7
x6
x5
Cpx
Opx
3% 5%
Na2O
60
Di
50
40
CS
30
20
10
MS

FIG. 5.8.

Anorthosite parental magma compositions.

Projection from clinopyroxene, alkalis and vapour into the plane CA - M - S (weight percent) of parental magmas of some anorthosite complexes. Phase relationships at 3% and 6% soda for synthetic material under 5 kb water pressure are taken from Figs. 3.14c and 3.14e, and the amphibole solid solution limits from Fig. 3.20.

Compositions and sources of data are given in Table 5.2.

Abbreviations as for Fig. 3.12.

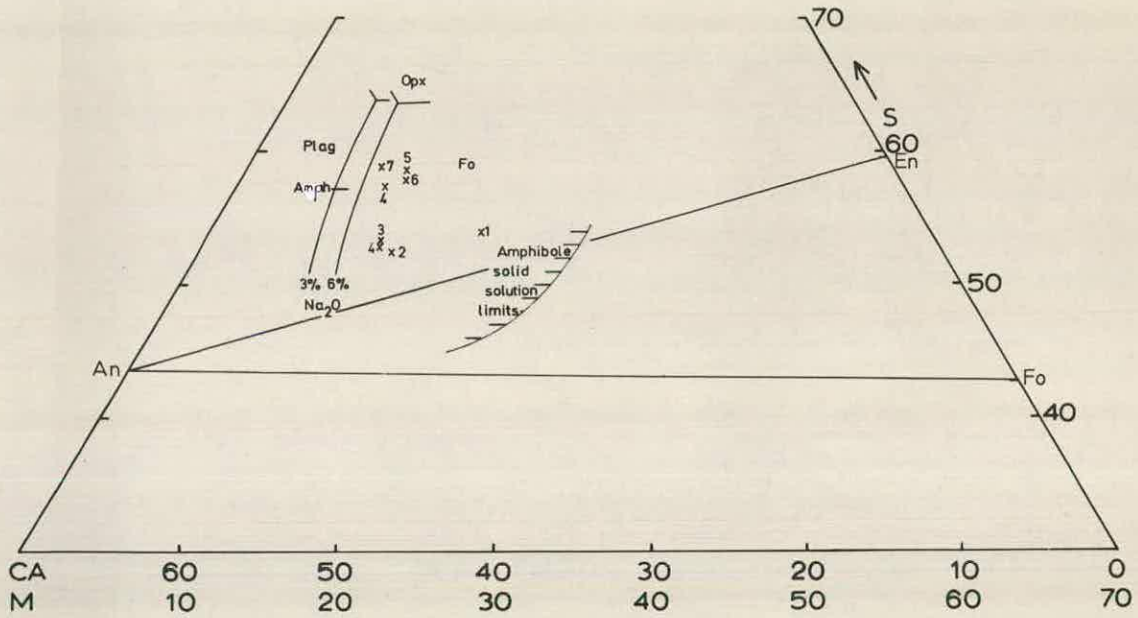
70
S
60
En
50
40
Fo
An
Opx
Plag
Amph
Fo
x7
5
x
x6
x
4
3
x
4x
x2
x1
Amphibole
solid
solution
limits
3% 6%
Na2O
CA
M
60 10
50 20
40 30
30 40
20 50
10 60
0 70

metamorphic mineral assemblages.

The data of Brown & Schairer (1971) at atmospheric pressure suggest that for andesitic compositions plagioclase crystallises alone over a considerable temperature interval. The effect of increasing water content at elevated pressure is to decrease the thermal stability of plagioclase relative to olivine and pyroxene.

Under hydrous pressure in excess of 2 kb amphiboles crystallise from basic compositions as the first aluminous phase, while at lower pressures plagioclase appears as the main aluminous phase (Yoder & Tilley, 1962; Holloway & Burnham, 1972). For such feldspar-rich compositions as some of the anorthosite magmas this transition may occur at higher pressure, but there are no relevant experimental data.

It is probable that plagioclase may be the liquidus mineral for anorthosite parental magmas up to the hydrous pressures likely to correspond to the conditions of their formation. This is supported by data from Fig. 3.7, in which an andesite-type composition containing up to 1.5% soda crystallises plagioclase first even under 5 kb water pressure. In compositions containing up to 3% soda plagioclase occurs very early in the crystallisation sequence, together with forsterite. Hence, crystallisation under these conditions could produce anorthositic and troctolitic cumulates typical of many massif anorthosite complexes.

Comparison with other models

Physical separation of plagioclase from other phases crystallising from a basaltic liquid was first proposed by Bowen (1917) to explain the monomineralic anorthosites. However, Emslie (1968) has shown that the various ratios of olivine to plagioclase in troctolites and anorthositic troctolites may be explained in terms of co-precipitation of these minerals from phase diagram considerations. Hence, although feldspar floatation may operate in some instances (Bridgewater & Harry, 1968) it is not thought a plausible general mechanism.

Anatectic melting of crustal material may explain some of the characteristics of anorthosites (Michot & Michot, 1968). However, Sr^{87}/Sr^{86} isotope ratios (Heath & Fairbairn, 1968) suggest a source for most anorthosites in the upper mantle.

Arguments against the presence of water in the anorthosite parental magmas include: the absence of hydrous minerals in the earliest rocks of the suite, and the frequent iron-enrichment of the more evolved rocks (Philpotts, 1966). The absence of hydrous minerals may be explained by the fairly low pressure of crystallisation of anorthosites, analogous to the situation with calc-alkaline rocks. Iron-enrichment within the suite is fairly common (Philpotts, 1966; Olmsted, 1968). However, there are other suites which show no iron-enrichment (Letteney, 1968) analogous to the calc-alkaline compositions. The arguments developed by Osborn (1959 and 1962) concerning iron-enrichment refer to

evolving liquids. Because many rocks of anorthosite complexes are cumulates or contain some cumulus material this reasoning must be applied with caution. Indeed, iron-enrichment in the cumulates is to be expected if there is to be iron-depletion in the residual liquids.

T.H. Green (1968) advocates crystallisation of a quartz diorite composition under moderate pressure to produce the anorthosites. To crystallise the appropriate plagioclase composition for massif anorthosites pressures over 9 kb are required. However, Kushiro & Yoder (1966) demonstrated that troctolites may not precipitate above 8 kb, and hence these set an upper limit to the pressure at which anorthosites could be formed.

Hydrous melting data from Luth & Simmons (1968) on an anorthosite sample are in accord with crystallisation conditions deduced from isotope ratios (Isachsen, 1968), and support the hypothesis that water pressure is fundamental to the origin of anorthosite complexes.

Conclusions

Detailed discussions on the general properties of calc-alkaline and anorthositic provinces and petrogenetic models for their origins may be found in McBirney (1969) and Isachsen (1968).

From the equilibrium phase relationships deduced in this study an alternative petrogenetic model for the generation of feldspar-rich liquids from basaltic compositions is proposed. Crystallisation of amphibole, by itself, or together with olivine and clinopyroxene, under

2 - 10 kb water pressure can produce a liquid composition akin to andesite and some anorthosite magmas. This process allows for a continuum of compositions from basaltic to andesitic, an important observation not adequately explained by many of the alternative models. The predominance of andesite over all other compositions in many calc-alkaline volcanic provinces is attributable to its lying very close to the thermal minimum involving olivine - two pyroxenes - amphibole - plagioclase in the system C - M - A - S - N - H and in natural compositions under 5 kb water pressure.

CHAPTER 6

SUMMARY OF CONCLUSIONS

Results of synthetic study

The main conclusions which may be extracted from the previous chapters are that at 5 kb in the presence of excess water-rich vapour:-

1) Basalt-like liquids containing less than 3% soda will not crystallise amphibole. The effect of small amounts of soda is to lower the temperature of any equilibrium relative to the soda-free system and to produce a plagioclase containing a small percent of albite.

2) With increasing soda content amphibole first appears in equilibrium with liquid in the isobaric invariant equilibrium forsterite - two pyroxenes - plagioclase - amphibole - liquid - vapour. The liquid is quartz-normative. The temperature of this equilibrium is 960 $\pm$ 12°C. Amphibole does not become stable with silica-undersaturated liquids until slightly higher soda contents.

3) The liquid in equilibrium with forsterite - two pyroxenes - aluminous phase - vapour is quartz-normative up to at least 6% soda, and forsterite is in reaction relationship with this liquid. The degree of silica-oversaturation decreases with increasing soda content. The liquids are low in normative diopside.

4) The assemblage forsterite - clinopyroxene - amphibole - vapour is observed with liquid in a wide range of compositions. There is a thermal maximum for this assemblage for liquids containing at least 10% normative nepheline. The same crystalline assemblage is observed

with quartz-normative liquids and hence crystallisation in this equilibrium can produce a silica-oversaturated liquid from silica-undersaturated compositions. Crystallisation of highly undersaturated liquids in this equilibrium has not been studied in detail, but a nepheline stability field will eventually be encountered. The two thermal divides, the olivine gabbro or forsterite - clinopyroxene - plagioclase divide and the norite or two pyroxenes - plagioclase divide, are not found in this system. An amphibole stability field intersects these two tie-planes for soda contents greater than 5% and 3% respectively.

5) Forsterite and clinopyroxene are in reaction relationship with the liquid once amphibole becomes stable. Hence, in a fractional crystallisation sequence only amphibole will precipitate under these conditions. There is some evidence to suggest that amphibole and clinopyroxene may coprecipitate from certain compositions. The exact conditions have not been elucidated but are encountered at high soda concentrations in the liquids.

6) Because of these reaction relationships most basic and intermediate magma compositions will crystallise amphibole and plagioclase only over a large temperature range after a short period of crystallisation of forsterite and/or clinopyroxene.

7) In the equilibrium forsterite - two pyroxenes - amphibole - plagioclase - liquid - vapour the pyroxenes contain about 3% Al_2O_3 and the plagioclase is more calcic than An_{87}.

8) In a soda-free system it is not possible to produce a corundum-normative liquid from a diopside-normative parent except by crystallisation of an orthopyroxene with a CaO/Al_2O_3 ratio higher than in the initial liquid. In soda-bearing systems the position of the normative basalt tetrahedron is difficult to define, but the fractional crystallisation of amphibole-bearing assemblages from diopside-normative parent liquids may produce corundum-normative residual liquids.

9) There is a thermal maximum at about 975 $\pm$ 10°C in the equilibrium forsterite - two pyroxenes - amphibole - liquid - vapour for liquids containing slightly less than 4% soda.

10) Electron microprobe analyses of quenched glasses are not consistent with the predicted phase relationships. It is suggested that crystallisation from the liquid during the quench produces glasses with little resemblance to the equilibrium liquid compositions.

Comparison with studies on natural material

There are few data available on the hydrous melting of natural material under 5 kb pressure. However, most of the data show good correlation with the situation predicted from the phase relationships determined in the synthetic study. It is likely that amphibole becomes stable at slightly lower soda contents in liquids in natural material than it does in the synthetic system.

Crystallisation from water-undersaturated and water-saturated magmas can be predicted from these phase diagrams,

and there do not appear to be any significant differences.

Geological Applications

Partial melts from a water-saturated mantle composition under 5 kb pressure are likely to be quartz-normative.

Any basic magma containing significant water pressure undergoing fractional crystallisation within the pressure range 2 - 10 kb will tend to produce a residual liquid of andesitic composition. Orogenic volcanism which is characterised by explosive andesitic eruption, but also includes a wide range of basaltic compositions, may be explained by such a process. Cores of feldspars in calc-alkaline volcanics and associated blocks of cumulus material are extremely calcic. This is in accordance with the compositions calculated in this study, and may be attributable to crystallisation under moderate water pressure. These provinces frequently contain nodules and xenocrysts of pargasitic amphibole, supporting the suggestion that the liquids have evolved by amphibole fractionation under water pressure.

Parental magmas of anorthositic and related complexes range from basaltic to andesitic in composition. The aluminous residual liquids produced during fractional crystallisation of varying amounts of amphibole from any of these parents, will crystallise abundant plagioclase on reduction of total and/or water pressure.

Future studies

Data from natural material under intermediate hydrous pressures are scarce. The stability of amphibole in the presence of various vapour phases and oxygen fugacities in basic compositions requires detailed examination.

Although the 6-component system studied here approximates sufficiently closely to the available data for natural material to produce a working model, a study of the effect of other oxides, mainly FeO, TiO_2, K_2O and CO_2 would be informative. Calculations involving iron/magnesium ratios and K_2O contents of various fractionating liquid compositions can then be attempted.

A detailed investigation of the reciprocal stability relationships between plagioclase and amphibole under 1 - 3 kb pressure may assist in the interpretation of conditions of crystallisation of anorthosites.

ACKNOWLEDGEMENTS

Professors F.H. Stewart and G.Y. Craig kindly placed the facilities of the Grant Institute at my disposal.

I wish to thank my supervisor, Professor M.J.O'Hara, for suggesting the research subject and for his guidance and assistance throughout.

I am especially grateful to Mr. C.E. Ford for his instruction and assistance in the operation and maintenance of the experimental equipment, and to Dr. G.M. Biggar for his advice in many problems of experimental petrology.

Mr. D.J. Humphries wrote the C.I.P.W. norm and projection computer programs and Dr. R.F. Cheeney advised in the manipulation of multi-dimensional phase equilibria.

Drs. K.R. Gill and W.C. Storey offered helpful suggestions during the preparation of the script.

Mr. C. Chaplin and technical staff provided excellent support at all stages of the work.

Mrs. Williams very kindly and expertly typed the thesis.

Thanks are also due to Miss P. Burnett who preserved my sanity during the final stages of the work.

The work was carried out during the tenure of a N.E.R.C. Research Studentship, which is gratefully acknowledged.

APPENDIX A

THE PROJECTION OF MULTICOMPONENT PHASE EQUILIBRIA

Diagrammatic representation of geologically relevant phase relationships

Data on binary and ternary systems may be easily shown diagrammatically on simple 2 dimensional models. To simulate geological problems more closely greater numbers of components are required, and these increase the complexity of diagrammatic representation. Once 3 dimensional models are required (for systems of 4 or more variables) reading and interpretation becomes difficult. It is, therefore, desirable to have a technique which will reduce such information into a series of 2 dimensional diagrams. One technique is to use a projection method.

Projection Concept

The simplest projections of phase relationships involve the reduction of a multidimensional model by one dimension, producing a figure which is easier to interpret. In the case of a 3 dimensional model this is effected by viewing the model from a particular point and visualising all the information and data in relation to a predetermined plane. Perspective and relief are lost as everything is transposed into this plane.

The particular point from which the system is viewed is called the projection point, and the plane into which all the data are transposed is called the plane of projection. The projection point and plane will usually

lie inside or on the surface of the model.

The projection point is conveniently chosen to be the mineral which crystallises first from the compositions under investigation. The plane chosen to act as the projection diagram may be any shape, but is usually triangular so that the diagram takes the form of a pseudoternary system, with which it has certain similarities.

The calculation by which any composition within the model is represented by a point within the projection plane is carried out by adding or subtracting an amount of the projection point composition to the specified composition such that the bulk composition may be calculated in terms of the end-members of the projection plane.

The important features of the projection procedure are best explained with reference to diagrams.

The system forsterite - anorthite - silica (Andersen, 1915) is chosen to illustrate how a forsterite-saturated projection diagram may be constructed from these data. The pseudoternary system is presented in Fig. A.1a. It is intended to project these data from forsterite into the plane which contains the join anorthite - silica, Fig. A.1b.

In Fig. A.1a, composition A will crystallise forsterite first and will be joined by anorthite when the residual liquid reaches point Z. Composition B also crystallises forsterite first, but is joined by clino-enstatite when the liquid reaches point Y, while composition C begins to crystallise anorthite and pyroxene simultaneously after forsterite when the residual liquid reaches point X.

FIG. A.1.

a. The pseudoternary system forsterite - anorthite - silica at 1 atmosphere pressure after Andersen (1915) showing the principle features of a projection diagram.

b. Projection from forsterite into the join $CaAl_2Si_2O_8$ - SiO_2, showing the information which may be transferred from Fig. A.1a.

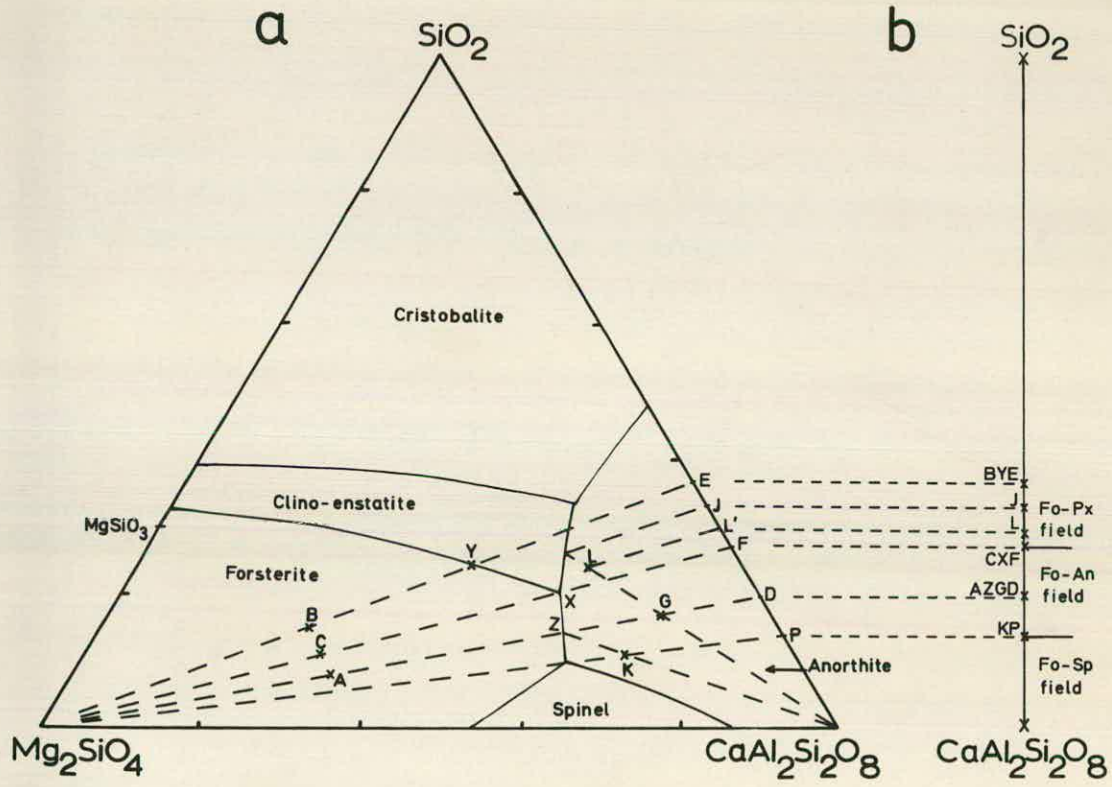
a
SiO2
Cristobalite
Clino-enstatite
MgSiO3
Forsterite
Spinel
Mg2SiO4
CaAl2Si2O8
E
J
L'
F
Y
L
X
G
D
B
C
Z
P
A
K
Anorthite
b
SiO2
BYE
J
L
CXF
AZGD
KP
Fo-Px field
Fo-An field
Fo-Sp field
CaAl2Si2O8

It is possible to project the compositions A, B and C from forsterite onto the projection plane (which is shown in this diagram as the section anorthite - silica) as points D, E and F. Hence, in a forsterite-saturated projection diagram any forsterite-saturated composition projecting between P and F will crystallise anorthite second and be followed by pyroxene when the projected residual liquid composition reaches F. The section P - F represents the projection of the forsterite - anorthite - liquid cotectic in the projection diagram.

However, if the composition is not saturated with respect to forsterite, e.g. composition G, then the projected liquid composition when pyroxene begins to crystallise will not be F but J. Hence, unless forsterite (the projection phase) is present in the equilibrium it is incorrect to say that in the projection diagram a liquid which projects at F will begin to crystallise both anorthite and pyroxene together.

Composition K does not crystallise forsterite first. However, shortly after beginning to crystallise anorthite the liquid composition will reach the forsterite - anorthite - liquid cotectic and hence reach the invariant point involving forsterite - anorthite - pyroxene - liquid with a residual liquid composition which projects at F. Hence, provided the projection phase is the second mineral to crystallise the subsequent crystallisation history may be treated by reference to the projection diagram.

Compositions plotting between forsterite and Z will have different liquidus temperatures. However, the

temperature at which anorthite appears for these compositions is always the same and is given by the temperature at Z. Hence, for the projection point D, the temperature of anorthite appearance is fixed, even though the liquidus temperature is not known. However, this does not apply if forsterite is not the liquidus mineral. Composition G will begin to crystallise anorthite at a higher temperature than suggested by its projection point D, which refers to the equilibrium involving forsterite - anorthite and the residual liquid Z.

Although a liquid of anorthite composition will crystallise directly to a mineral of the same composition, a composition which projects at the anorthite point, but crystallises forsterite first will crystallise spinel before anorthite. Hence, the section of the projection diagram from P to the anorthite point will represent the forsterite - spinel - liquid cotectic surface.

Fig. A.1b indicates how all this information appears in a projection diagram. Compositions A, Z, G and D all plot at the same point on the projection diagram, as do B, Y and E, and C, X and F. Point F represents the projection of the invariant point involving forsterite - pyroxene - anorthite - liquid. Hence, the boundary between the forsterite - anorthite and forsterite - pyroxene stability fields in the projection diagram passes through F.

From the projection diagram, composition L appears to have a crystallisation sequence of forsterite, followed by pyroxene and then anorthite, whereas in the pseudo-

ternary phase diagram, Fig. A.1a, it is seen to crystallise anorthite followed by pyroxene. This emphasises the importance of only considering equilibria which are saturated with respect to the projection phase.

Forsterite is in reaction relationship with the liquid at point X, and once the liquid begins to migrate along the pyroxene - anorthite - liquid cotectic curve the equilibria are not saturated with forsterite and so it is incorrect to use this projection diagram to consider the crystallisation history of the liquid beyond X, or its projected point, F.

The projection diagram shows the two dimensional system forsterite - anorthite - silica as a one dimensional join, reducing the complexity of the resultant diagram, but also being incapable of showing as much detail about liquid compositions.

Projection within the system C - M - A - S - N - H

For 4-component systems it is possible to represent pseudoternary phase relationships by a single projection process, see O'Hara (1968) and Jamieson (1969). However, in the 6-component system studied here there are too many variables for a rigorous examination of the system using a single projection technique. It is therefore necessary to consider other methods of reducing the system such that simple diagrams may be presented.

In the previous section it was demonstrated that for a projection scheme to be valid the projection phase must

be present in all the equilibria included in the diagram. In this study, water-saturated conditions have been created in all runs and so vapour is a ubiquitous phase. Consequently, it is possible to project all the data from vapour (assumed to be pure water), thus reducing the variance of the system, and reducing the number of phases which require representation. The vapour is not pure water (as explained in Appendix C), but this introduces a very small error and is ignored here.

The remaining 5-component system requires 2 projection phases if pseudoternary relationships are to adequately indicate the phase equilibria. The use of forsterite and orthopyroxene as such a pair of projection phases has been considered in Chapter 2.

Projections within the system XO - YO - R_2O_3 - ZO_2, with components recalculated according to the scheme of Jamieson (1969), treats soda as an ancillary component which does not cause the introduction of any new minerals in the crystallisation sequence, but slightly modifies existing relationships by entering the feldspar and possibly pyroxene. Hence, recalculation of soda in terms of albite and combination with anorthite appears justifiable. The addition of soda to the system C - M - A - S - H allows a hornblendic amphibole to crystallise and it is essential to correlate the stability of this mineral with soda content. In this study, soda does not enter plagioclase to any appreciable extent (see Appendix F), hence it is invalid to recalculate soda content as if it did. It must be

treated as a separate component. This system cannot be reduced to less than 6 essential components.

Reduction of the vapour-saturated data to produce simplified diagrams is effected by projection from a suitable mineral to produce a pseudoquaternary system having soda as one apex of the tetrahedron. By cutting sections through this tetrahedron at various soda contents a series of pseudoternary diagrams may be presented.

One of the projection models used in Chapter 3 is explained here as an example. Starting with the quinary system C - M - A - S - N, a projection is made from or towards forsterite into the tetrahedral volume CS - MS - A - N. This is shown diagrammatically by a series of sections cut at different soda levels in the liquid showing the phase relationships at fixed soda content projected from forsterite and soda into the plane CS - MS - A. However, there is a difference between the nature of the forsterite projection and the soda projection. The addition of more forsterite to the bulk composition does not affect the projected phase relationships (compare compositions A and Z in Fig. A.1a). If more soda is added the projected phase relationships will change.

Only 4 solid phases, liquid and vapour coexist at an isobaric invariant point in these diagrams which is one phase less than demanded by the phase rule. However, consideration of a fixed soda content in each diagram provides the additional constraint (loss of one degree of freedom) which makes such diagrams comply with the requirements of the phase rule.

It is not sufficient merely to take the experimental data for a bulk composition with a particular soda content and present all the phase relationships of that composition in the pseudoternary section containing that specific soda content. This is because the residual liquid composition ought to be projected into the plane containing the same soda content as itself, which will not, in general, be the same as the bulk composition. This is most easily explained by considering a hypothetical example.

Suppose that for a liquid with a particular C - M - A - S ratio, the minimum soda content at which amphibole crystallises before plagioclase is 3%. Now suppose there are 2 gels, which both contain 2% soda. One gel lies close to the specified composition in terms of C - M - A - S, while the other is significantly different, but both may approach it by a crystallisation sequence involving soda-free phases. The first gel reaches the specified composition in terms of C - M - A - S after 20% crystallisation producing a residual liquid containing 2.5% soda. However, the other gel requires 50% crystallisation prior to reaching the desires C - M - A - S proportions and this remaining liquid will contain 4% soda. Consequently, while the latter gel has produced a liquid containing enough soda for amphibole crystallisation, the former gel will continue its crystallisation sequence with plagioclase appearing. Hence, simply presenting sections containing the phase relationships of bulk compositions with a fixed soda content will not give consistent diagrams. It is therefore necessary

to be able to predict the soda content of the liquid in any equilibrium and to be able to present the data concerning that equilibrium in the section containing the same soda level.

Calculation of soda contents in liquid

There are several ways in which the soda content of liquids may be obtained.

1) Electron microprobe analysis.

Provided there is sufficient liquid present in the charge, electron microprobe analysis ought to provide an estimate of the soda content. However, it has been found that alkali elements in hydrous glasses show a rapidly decreasing count rate when exposed to the electron beam (Holloway & Burnham, 1972; Modreski, 1972; Cawthorn et al., 1973). Hence, reliable analyses cannot be obtained in this way.

2) Optical estimation of percent crystallinity.

If the percent crystallinity of the charge can be found by optical inspection, and if the proportion and composition of soda-bearing phases is known, simple calculation could produce an estimate of the soda content in the liquid. However, estimation of crystallinity of charges is extremely difficult and is not thought to be a reliable method.

3) Estimation and iteration of results.

This process cannot be used on one charge in isolation, but requires the examination of a large amount of data, construction of models using approximate estimates, and

then rechecking this estimated value against a calculated level.

This complex procedure is best explained with the aid of an example. Sufficient data are available to construct preliminary projection diagrams. A composition, G, containing 1% soda is found to have a crystallisation sequence forsterite, clinopyroxene, plagioclase. What is the soda content of the liquid when plagioclase first appears?

The approximate positions of the forsterite - clinopyroxene - plagioclase - liquid - vapour cotectic curves are known at different soda levels in the projections forsterite into the plane CS - MS - A and diopside into the plane CA - M - S from the near-liquidus phase relationships of various other gels. These are presented in Figs. A.2a and A.2b, together with the projection of the composition, G.

It is optically estimated that immediately prior to the appearance of plagioclase the charge is 50% crystalline, producing a liquid containing 2% soda. Hence, the cotectic curves for this soda level are used in the first calculation. The composition of the residual liquid in this equilibrium in the two projection diagrams, Figs. A.2a and A.2b, is shown by the points A and B, being the intersection of the cotectic curve with the extension of the tie-line from forsterite or clinopyroxene through G.

The actual composition of the liquid is given by the composition of the projected liquid point <u>in the plane</u> plus or minus an unknown weight of the projection mineral; i.e.

FIG. A.2.

a. Projection from forsterite, soda and vapour into the plane CS - MS - A (weight percent). The approximate positions of the phase boundaries at different soda contents are shown (at 1%, 2% and 3%). G is the bulk composition of the starting material, A is the liquid composition when plagioclase begins to crystallise and Cpx is the composition of the crystallising clinopyroxene.

b. Projection from diopside, soda and vapour into the plane CA - M - S (weight percent). The approximate positions of the phase boundaries at different soda contents are shown (at 1%, 2% and 3%). G is the bulk composition of the starting material and B is the liquid composition when plagioclase begins to crystallise.

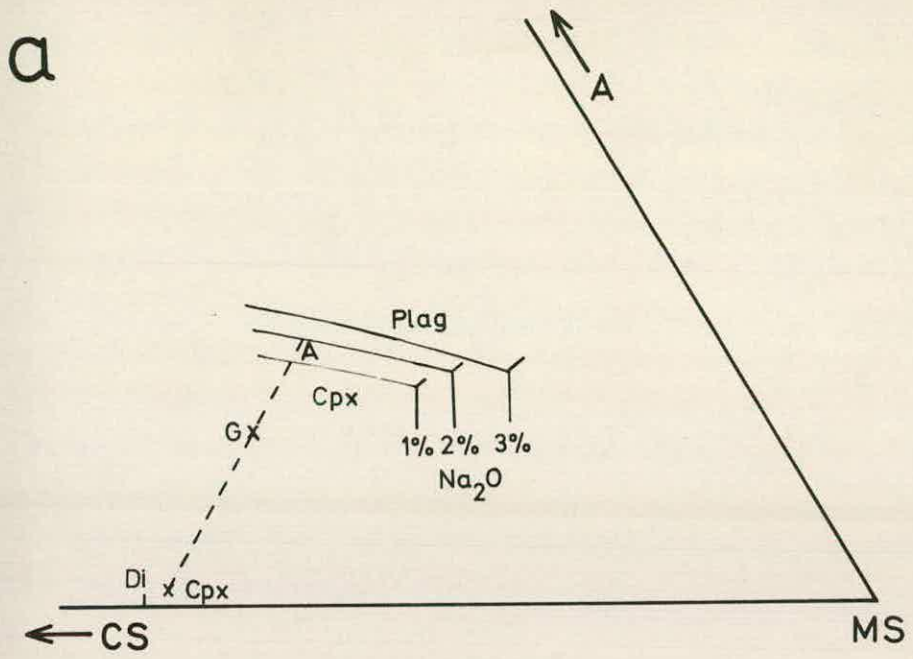
a
A
Plag
A
Cpx
G
1% 2% 3%
Na2O
Di
Cpx
CS
MS

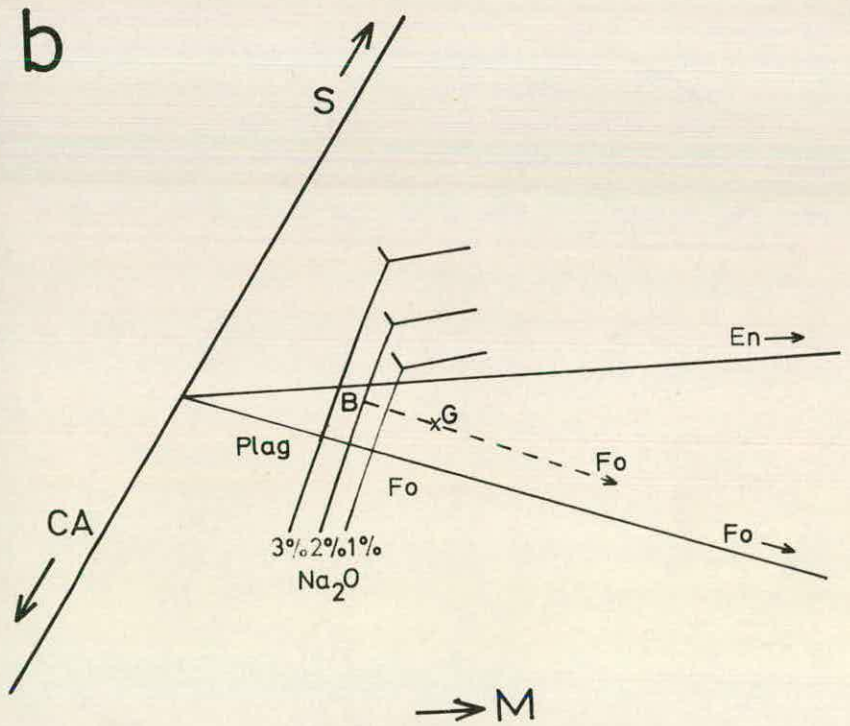
b
S
En
B
G
Plag
Fo
Fo
Fo
CA
3% 2% 1%
Na2O
M

actual liquid composition = a x (composition in plane CS - MS - A) + b x forsterite composition

also = c x (composition in plane CA - M - S) + d x diopside composition

Hence,

a x (composition in CS - MS - A) + b x forsterite composition = c x (composition in CA - M - S) + d x diopside composition

(designated equation 1).

This equation may be solved for C, M, A and S in turn producing 4 equations containing the 4 unknowns a, b, c, d. Because of the uncertainties in the construction of the projection diagrams, these equations may not be perfectly soluble. They are solved to produce the smallest possible residual errors in each equation, by using a modified version of a computer program written by Wright & Docherty (1970). The solutions may then be incorporated into equation 1 to produce the actual C - M - A - S proportions in the residual liquid.

The next stage is to calculate the proportion of forsterite and clinopyroxene which must crystallise from the bulk composition to produce this residual liquid. A second equation may be written; 100 units of starting material - x units of forsterite - y units of clinopyroxene = 100 - x - y units of residual liquid

(designated equation 2).

Again equations may be written for each oxide in turn, and 4 linear equations with 2 unknowns obtained. This over-

determined system may similarly be solved by the modified version of the computer program of Wright & Docherty (1970). The percent crystallinity is derived from these results. Knowing the soda content of the bulk composition it is simple to calculate the soda concentration in the residual liquid by using the equation;

$$\text{percent soda in liquid} = \frac{\text{percent soda in bulk composition} \times 100}{100 - \text{percent crystallinity}}$$

(designated equation 3).

With this more reliable estimate of the soda content in the liquid of a particular equilibrium, combined with the results of many similar calculations, it is possible to redraw the phase relationships at the various soda levels more accurately. By repeating the entire operation an internally consistent model can eventually be constructed.

There are several points to note in this calculation.

a) Because the phase relationships are presented in a projection from soda and water it is only the C - M - A - S ratios which are involved in both parts of this calculation. The composition of the starting material in equation 2 is therefore the C - M - A - S proportions of the gel normalised to 100%.

b) The projections are carried out from forsterite and diopside ideal compositions. However, in equation 2, it is the composition of the actual crystallising minerals which are required. These are not always available, and so an estimate of their compositions is made from the results of the electron microprobe analysis of minerals in various equilibria. Changing composition slightly has little effect

on the solution of the equation. This only applies for clinopyroxene. The stoichiometry of forsterite makes its ideal composition suitable for use in equation 2.

c) If there were any significant amount of soda in the clinopyroxene this would affect the soda content of the liquid as calculated above. However, if the concentration of soda in the pyroxene is known this may easily be allowed for.

d) Only 2 phases are involved in the crystallinity calculation using equation 2. However, it is possible to have up to 4 crystallising phases and still obtain a meaningful solution. If soda-bearing phases are included an estimated composition must be used which is first re-calculated to include only its C - M - A - S components and normalised to 100%. For feldspars this can be done most conveniently by including both anorthite and albite (less its soda content) as separate phases in equation 2. A rough estimate of feldspar composition may subsequently be obtained by recombining these in the proportions indicated by the solution to the equation.

e) The calculation of the liquid composition depends upon a knowledge of its position in 2 projection diagrams. It is only possible therefore to do these calculations for forsterite- and clinopyroxene-saturated equilibria, as these are the only two minerals from which projection diagrams have been drawn. For other equilibria optical estimation has to be relied upon.

Accuracy of the calculations

The accuracy of the preceding calculations depends upon how precisely the location of the crucial equilibria may be established in the projection diagrams during the iteration process. As a guide to the precision of this calculation technique the chosen point in the diagrams for one calculation was deliberately displaced from its supposed true location. The deliberately displaced loci exceed the range of uncertainty in the construction of the diagrams, and so this is thought to indicate the maximum error likely.

Gel 3 initially crystallises forsterite and clinopyroxene over a considerable range of soda values. However, it is desired to determine the soda content in the liquid at which amphibole and plagioclase appear simultaneously, (see Fig. 3.6a). The projection diagrams, Figs. 3.12 and 3.14, suggest that this occurs at about 3.5% soda. The preferred phase relationships for this soda level in the 2 projection diagrams are shown in Figs. A.3a and A.3b, together with the deliberately displaced alternative models (referred to as 1 - 4). The calculations concerning residual liquid composition and percent crystallinity are shown in Table A.1 for the various possible phase relationship orientations. For the calculation of displacement 1 and 2 the true location of the point in Fig. A.3b is used, and for displacement 3 and 4, the true location in Fig. A.3a is used.

The results suggest that the maximum error in the composition of the residual liquid is $\pm$ 1.5% absolute for C - M - A - S, and is $\pm$ 0.4% absolute for the soda value.

FIG. A.3.

a. Projection from forsterite, soda and vapour into the plane CS - MS - A (weight percent). The supposed true location of the phase boundaries at a soda content of 3.5% are shown. They are also deliberately displaced to positions 1 and 2 to investigate the error introduced in the calculation procedure by such an uncertainty, (see Table A.1, for calculation). Gel 3 is the projection of the composition of gel series 3 for which this calculation is performed.

b. Projection from diopside, soda and vapour into the plane CA - M - S (weight percent). The supposed true locations of the phase boundaries at a soda content of 3.5% are shown. They are also deliberately displaced to positions 3 and 4 to investigate the error introduced in the calculation procedure by such an uncertainty, (see Table A.1, for calculation). Gel 3 is the projection of the composition of gel series 3 for which this calculation is performed.

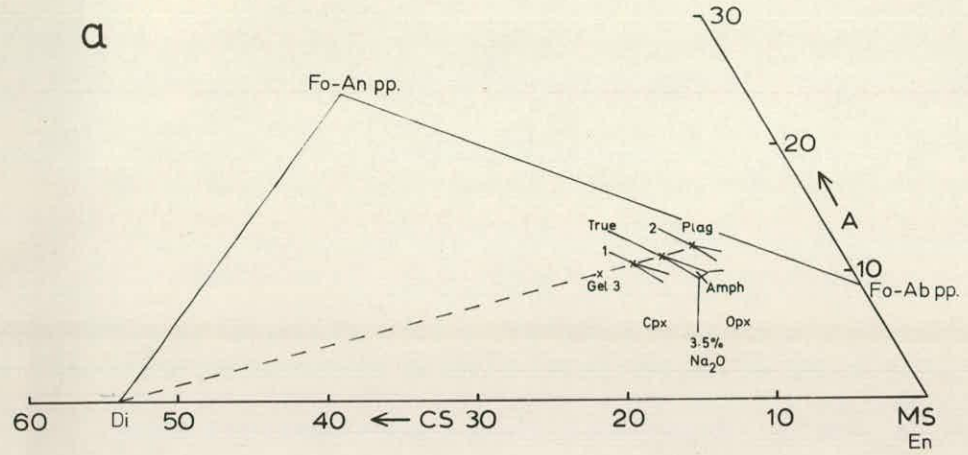
a
Fo-An pp.
30
20
A
10
Fo-Ab pp.
True
2
Plag
1
Gel 3
Amph
Cpx
Opx
3.5%
Na2O
60
Di
50
40
← CS
30
20
10
MS
En

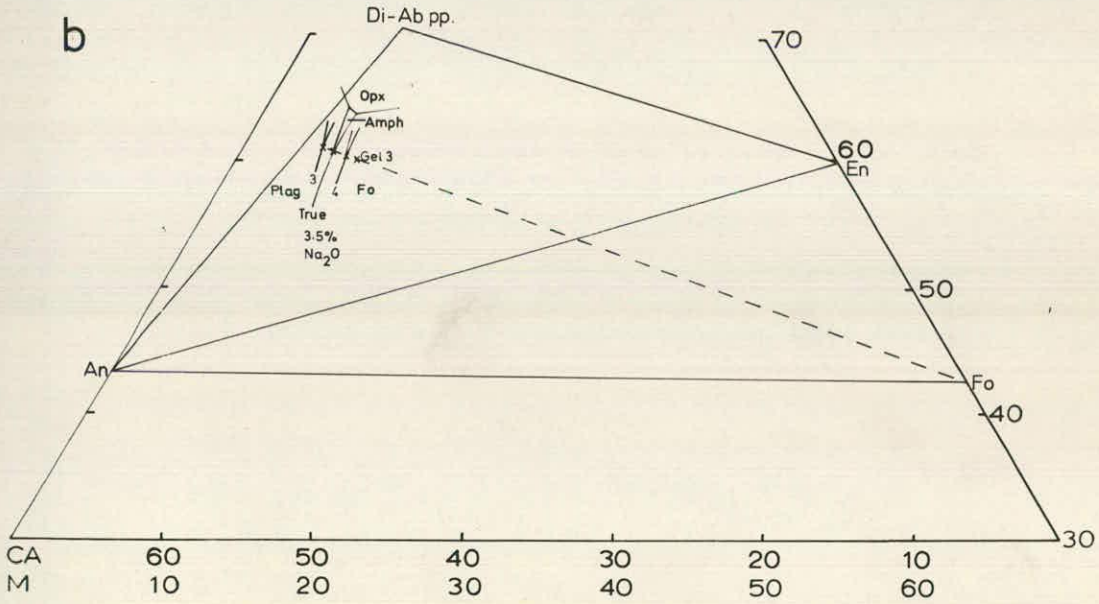
b
Di-Ab pp.
70
Opx
Amph
60
En
Gel 3
3
Plag
4
Fo
True
3.5%
Na2O
50
An
Fo
40
30
CA
M
60
10
50
20
40
30
30
40
20
50
10
60

TABLE A.1

Percent crystallinity and soda content of liquid calculation for gel 3, with deliberately induced errors

		"True" location		Displacement 1		Displacement 2		Displacement 3		Displacement 4	
		1	2	1	2	1	2	1	2	1	2
Location of liquid composition in planes CA - M - S and CS - MS - A, Figs. A.3a and A.3b. Column 1 refers to CA, M and S proportions respectively, column 2 to CS, MS and A.		32.5	12.5	32.5	14.4	32.5	10.9	33.3	12.5	32.3	12.5
		6.4	76.0	6.4	75.8	6.4	77.0	5.3	76.0	7.2	76.0
		61.1	11.5	61.1	10.8	61.6	12.1	61.4	11.5	60.5	11.5
Result of least squares calculation using equation 1.	a	102.8		92.9		111.0		102.9		102.4	
	b	- 2.8		7.1		- 11.0		- 2.9		- 2.4	
	c	192.0		186.9		198.2		196.3		188.8	
	d	- 92.0		- 86.9		- 98.2		- 96.3		- 88.8	
Composition of liquid obtained from above ratios, ignoring soda, and recalculated to 100%	SiO_2	60.4		59.5		60.6		60.7		60.1	
	Al_2O_3	22.1		20.2		23.8		22.6		21.7	
	MgO	6.0		7.2		5.1		4.9		6.9	
	CaO	11.5		13.1		10.4		11.8		11.3	
Percent crystallinity, using equation 2	x	2.0		2.4		1.7		3.6		0.7	
	y	23.6		14.1		29.8		23.5		23.5	
	100-x-y	74.4		83.5		68.5		72.9		75.8	
Soda content in liquid, using equation 3	Na_2O	3.5		3.1		3.8		3.6		3.4	

"True" location is best position of primary phase volumes of minerals
Displacements 1-4 are discussed in text.
Percent soda in the bulk composition which begins to crystallise amphibole and plagioclase simultaneously in 2.6% (Fig. 3.6a).

Soda in liquid isopleths

The soda in liquid isopleths shown in Figs. 3.2 - 3.10 are constructed by this calculation process. Some of these suggest that the soda content in the liquid decreases with increasing crystallisation. See, for example, the 4% soda isopleth in Fig. 3.6a. The only precipitating phase in this region is amphibole. This does not imply that the amphibole contains more than 4% soda. Not all the components required to form the amphibole are coming from the liquid. All the soda, and most of the alumina, will be obtained from the liquid. However, some of the lime, magnesia and silica required by the amphibole will be derived from the resorbing forsterite and clinopyroxene. Hence, the soda content of the material removed from the liquid will be greater than that of the amphibole produced. The soda removed from the liquid is calculated to be approximately 5%, and hence the isopleths indicate a reverse trend in this equilibrium.

APPENDIX B

EXPERIMENTAL PROCEDURE

Preparation of gels

The method for preparing gels, described by O'Hara & Biggar (1969), was adopted here. Comparisons of analysed material with intended compositions are presented by them, and suggest errors of ± 0.2% for the major oxides.

Encapsulation of charges

Platinum capsules were used for containing the sample, 10 mg usually being used. Platinum tubes were cut to appropriate length (usually 1 cm), cleaned in HF, and annealed by heating in a blow torch flame for several minutes. One end was crimped and welded by a 100 volt D.C. arc with a graphite electrode.

1 mg of distilled water was introduced into the capsule by a syringe and a further 9 mg of gel added by spatula. (In some of the early runs up to 25% by weight water was added to the charge). The weights of empty capsule, capsule with water, and capsule with water and gel were recorded to 0.1 mg, or 0.01 mg if the water content of the liquid was to be determined (see Appendix C). The lip of the capsule was cleaned and welded, the capsule being partly submerged in water to avoid evaporation. If the capsule lost more than 0.1 mg on welding it was rejected as water may have been lost. The capsule was dried on a hot-plate at about 100°C for at least 15 minutes, and reweighed to test the seal. Again, if a weight change of 0.1 mg was recorded it was rejected.

After each run the capsule was reweighed to ensure that water remained inside.

Operation of equipment

All the data were obtained from charges run in internally heated gas-pressurised bombs described by Ford (1972).

Up to 25 capsules have been run in one operation, but generally 10 - 15 charges were inserted. The gas pressure medium was usually argon. A few charges run together with natural samples required buffering, and for these a small pressure of hydrogen was introduced.

Temperatures were recorded by a platinum/platinum - rhodium$_{13}$ thermocouple, and the pressure by a manganin coil connected through a Wheatstone Bridge circuit. The errors in these measurements have been calculated by Ford (1972). Pressure-uncorrected temperatures are presented here.

Identification of charges

Small circular depressions were often observed on the surface of the capsule indicating quenched vapour bubbles inside the charge. On cutting open the capsule a hiss was often detected, thought to be residual vapour escaping. Subsequent heating usually resulted in a loss of weight, presumed to be water. Any of these observations was taken as evidence of vapour during the run (see Appendix E).

The charge was inspected to check for homogeneity and its state (glassy, powdery, transparent, etc.). The charge was crushed under acetone and dried. An optical

grain mount and an X-ray diffraction slide were prepared. Both methods of identification were employed, although because of quenching products or the possibility of small amounts of a mineral not showing on the diffraction pattern, optical identification was regarded as the more reliable.

Cu K_α radiation was used for the X-ray diffraction. X-ray generating power was 28 mA and 44 kV. A Ni filter was used. A scan speed of $2^\circ(2\theta)$. $min.^{-1}$ was employed and characteristic mineral peaks for identification are given in Table B.1.

TABLE B.1.

Mineral	$2\theta^\circ$	d(Å)	Mineral	$2\theta^\circ$	d(Å)
Forsterite	22.7	3.91	Clinopyroxene	27.5	3.24
	32.2	2.78		29.9	3.00
	35.7	2.51		30.4	2.94
	36.4	2.47		30.9	2.89
				35.0	2.56
Plagioclase	21.9	4.1		35.6	2.52
	23.5	3.8		35.9	2.50
	27.6-27.9	3.2	Amphibole	10.4	8.5
				26.4	3.37
Spinel	31.2	2.86		28.5	3.13
	36.8	2.44		31.8	2.81
	65.2	1.43		33.1	2.70
				35.2	2.55
Melilite	21.0	4.2		38.4	2.34
	29.2	3.1			
	31.3	2.9	Orthopyroxene	28.1	3.17
				31.1	2.87
				32.8	2.47

Criteria for optical identification of phases from the grain mount are given in Table B.2. A liquid of refractive index 1.657 was used for all slides.

TABLE B.2.

Mineral	Relief	Shape	Refractive Index	Birefringence	Extinction
Forsterite	moderate - low	rounded euhedral	+ive	high	usually parallel
Clino-pyroxene	moderate - high	stubby prisms	+ive	high	oblique, 12-40°
Ortho-pyroxene	low - very low	elongated prisms	+ive	very low	usually parallel
Amphibole	moderate - low	elongated prisms	-ive	moderate	oblique, 10-20°
Plagioclase	very high	irregular	-ive	very low	-
Spinel	very high	round - octahedral	+ive	isotropic	-
Nepheline	high	euhedral prismatic	-ive	very low	oblique
Mica	high - moderate	elongate - prismatic	-ive	low	usually parallel

APPENDIX C

WATER CONTENT OF GLASSES AND COMPOSITION OF THE VAPOUR PHASE

Water content of glasses

It is possible to estimate the percent of water in a liquid by weighing the sample at various stages of preparation and after running.

The weight of water introduced into the capsule, can be weighed to 0.01 mg. The weight of charge can be weighed equally accurately. Loss of weight during welding and running is usually less than 0.03 mg. On completion of the run the charge is weighed, cut open, reweighed, dried for at least one hour at greater than 100°C and reweighed. On opening there is often a small weight loss due to escaping water. After drying there may be a further loss as excess water is driven off. Repeated weighing and drying suggests that no significant weight loss occurs after about 30 minutes.

The total weight loss during these operations is taken to represent the water from the vapour present during the run. By difference, it is possible to estimate the weight of water dissolved in the glass or as hydrous minerals in the charge. For charges containing very little glass the percent of water remaining in the charge during drying is likely to be small. However, with increasing temperature the proportion of liquid increases as will the percent of trapped water. At the liquidus the percent of water trapped may be taken as an estimate of the water content of the liquid.

The results are presented in Fig. C.1. In general, the increasing percentage of trapped water correlates well with the proportion of liquid present. Hydrous phases are not likely to retain significant quantities of water.

A few spurious results are obtained. Low values of water content could be attributed to very small weights of capsule or charge being lost while cutting open, hence increasing the apparent weight loss. High values could be explained by incomplete drying of the charges.

Extrapolation to liquidus temperatures suggests that the liquids generally contain about 7 - 10% by weight water. This compares with data from Hamilton et al. (1964) on natural materials, who suggest that under comparable pressure basaltic and andesitic liquids may dissolve up to 5 and 8% water respectively.

At the completion of the study large samples of several gels were weighed into open crucibles and dried at 100°C for several hours. The average weight loss was 0.25%. They were then dried for a further 18 hours at over 800°C and cooled in a desiccator when weight losses amounted to up to 1%. It is suggested that the maximum weight of water dissolved in the original gels does not exceed 1.25%. This is not included in the calculations involving water solubility.

FIG. C.1.

Water content of liquids.

The percent of water retained by the charges on drying at > 100°C for 1 hour after the run for various compositions over a range of temperatures. At the liquidus this value will represent the water content of the liquid having the same composition as the starting material.

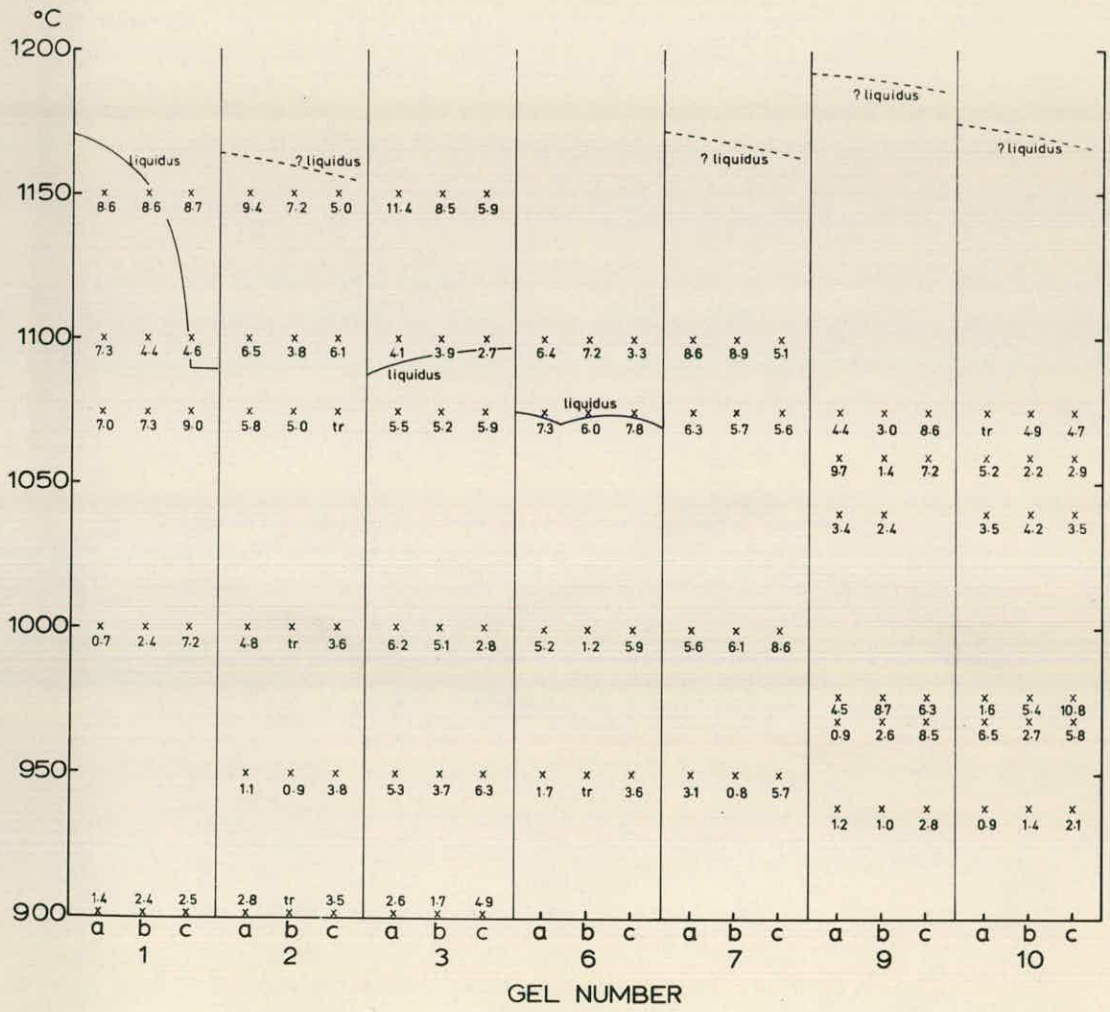
°C
1200
1150
1100
1050
1000
950
900
liquidus
? liquidus
? liquidus
liquidus
liquidus
? liquidus
? liquidus
a b c a b c a b c a b c a b c a b c a b c
1 2 3 6 7 9 10
GEL NUMBER

Composition of the vapour

All runs were thought to have been carried out with excess water. It was not always possible to ascertain whether water was present (see Appendix B), but the phase diagrams in Chapter 3 assume water-saturated conditions.

In the presentation of the data and of the projection diagrams it is assumed that the vapour is pure water. It will, in fact, contain some dissolved material from the gel. The composition of the liquid plus solid phases will not be the same as the initial composition. The error introduced by this effect will depend upon the composition and proportion of the vapour phase.

The proportion of the vapour phase can be calculated by subtracting from the weight of water added (Appendix E) the weight of water dissolved in the liquid plus solid phases. It is not possible to estimate the composition of the vapour accurately. Luth & Tuttle (1969) present data on the proportion of silicate material dissolved in vapour at various pressures in the alkali feldspar - quartz - water system. They suggest that the vapour contains 5% of dissolved silicate under 5 kb water pressure at 750°C. In the system quartz - water, Clark (1966) found about 10% silica dissolved in the vapour under similar conditions. Direct comparison of these results with this study is difficult because the composition of the vapour will depend upon the bulk composition. However, an estimate of 5% dissolved material is taken for the following calculation.

If there is 10% weight of vapour in the charge it will

dissolve 0.55% by weight of the gel. Because of the high concentration of C - M - A - S in the original bulk composition such small amounts of solution in the vapour will not significantly affect the composition of the remaining material in terms of these components. The data of Clark (1966) suggest that soda is less soluble than silica in vapour, up to 2.5 kb (the limit of the data). Soda dissolved in the vapour is not likely to exceed 0.5% by weight if there is 10% vapour. Reference to Fig. F.3 suggests that this is an extremely high estimate.

Fig. 3.10a suggests that a bulk composition containing about 0.65% soda (certainly considerably less than 1%) may crystallise in the isobaric invariant equilibrium forsterite - 2 pyroxenes - amphibole - plagioclase - liquid - vapour. If 0.5% soda were dissolved in the vapour the projected point of this bulk composition in Fig. F.3 should contain very little soda. This would demand a feldspar composition in this equilibrium which is almost pure anorthite. This is considered unlikely and so a smaller solubility of soda in the vapour is preferred.

All the calculations regarding percent crystallinity and soda content of liquids assume no soda dissolved in the vapour. The error introduced by this approximation is thought to be minimal.

APPENDIX D

COMPOSITIONS OF GELS USED IN QUENCHING EXPERIMENTS

Pargasite gel	SiO_2	44.08
	Al_2O_3	18.70
	MgO	19.72
	CaO	13.71
	Na_2O	3.79

Gel Identification	42	45	48	51	54	57
SiO_2	42.00	45.00	48.00	51.00	54.00	57.00
Al_2O_3	16.53	15.68	14.82	13.97	13.11	12.26
MgO	19.72	18.70	17.68	16.66	15.64	14.62
CaO	18.12	17.18	16.24	15.31	14.37	13.43
Na_2O	3.63	3.44	3.26	3.07	2.88	2.69

Gel Identification	42EN	45EN	48EN	51EN	54EN	57EN
SiO_2	50.97	52.40	53.97	55.48	56.99	58.48
Al_2O_3	8.27	7.84	7.42	6.99	6.53	6.13
MgO	29.89	29.45	28.86	28.35	27.84	27.32
CaO	9.06	8.59	8.12	7.65	7.18	6.72
Na_2O	1.81	1.72	1.63	1.53	1.44	1.35

Gel Identification	1a	1b	1c	2a	2b	2c
SiO_2	48.68	47.70	46.22	51.69	50.64	49.08
Al_2O_3	27.54	26.98	26.15	21.93	21.49	20.82
MgO	9.53	9.33	9.05	17.34	16.99	16.46
CaO	13.25	12.99	12.58	8.04	7.88	7.64
Na_2O	1.00	3.00	6.00	1.00	3.00	6.00

APPENDIX D (Contd.)

Gel Identification	3a	3b	3c	6a	6b	6c
SiO_2	58.79	57.61	55.82	54.23	53.14	51.49
Al_2O_3	16.23	16.29	15.79	23.01	22.55	21.85
MgO	9.86	9.66	9.36	9.10	8.91	8.64
CaO	13.72	13.44	13.03	12.66	12.40	12.02
Na_2O	1.00	3.00	6.00	1.00	3.00	6.00

Gel Identification	7a	7b	7c	9a	9b	9c
SiO_2	49.48	48.49	46.98	53.34	52.26	50.64
Al_2O_3	27.99	27.42	26.58	7.54	7.39	7.16
MgO	13.83	13.55	13.13	29.82	29.22	28.32
CaO	7.70	7.54	7.31	8.30	8.13	7.88
Na_2O	1.00	3.00	6.00	1.00	3.00	6.00

Gel Identification	10a	10b	10c
SiO_2	56.20	55.07	53.36
Al_2O_3	7.95	7.78	7.55
MgO	28.29	27.72	26.86
CaO	6.56	6.43	6.23
Na_2O	1.00	3.00	6.00

APPENDIX E.1.

EXPERIMENTAL RUN CONDITIONS

Run No.	Duration hrs.	Final Temp. °C	Maximum Recorded Fluctuations, °C		Final Pressure, kb	Maximum Recorded Fluctuations, kb	
13	5	1073.8	+0.7	-0.0	5.13	+0.00	-0.13
14	30	901.3	+1.4	-0.0	4.80	+0.20	-0.00
15	26	1026.7	+0.4	-0.5	4.91	+0.08	-0.00
17[I]	96	801.2	+1.1	-0.3	4.99	+0.06	-0.01
18	75	953.3	+0.9	-0.0	5.02		
19[I]	3	928.4	+0.0	-0.0	5.00	+0.00	-0.00
20	15	978.0	+0.0	-3.5	4.66	+0.34	-0.00
21	18	1005.6	+0.0	-2.1	4.98	+0.03	-0.19
23	72	960.5	+0.0	-0.8	4.95	+0.05	-0.00
24	43	999.8	+0.0	-0.9	5.00	+0.00	-0.19
25	24	1199.3	+0.0	-1.0	5.00	+0.00	-0.00
26	29	1148.2	+0.1	-0.3	5.00	+0.00	-0.00
27	70	851.0	+0.0	-1.6	4.76	+0.24	-0.00
31	17	1044.0	+0.0	-0.3	4.90	+0.10	-0.10
33	95	901.0	+0.4	-2.2	4.88	+0.14	-0.27
34	38	1150.3	+0.0	-0.4	4.89	+0.21	-0.14
37	146	1000.9	+0.1	-0.3	4.61	+0.55	-0.00
40	24	1105.3	+4.6	-0.0	4.82	+0.18	-0.00
42	3	1160.0	+0.1	-0.0	5.01	+0.00	-0.00
43	40	775.0	+0.0	-0.2	4.99	+0.04	-0.24
45	18	1170.1	+0.0	-0.2	4.87	+0.13	-0.00
46	96	1091.0	+0.0	-0.2	4.89	+0.11	-0.12
47	72	898.9	+0.5	-0.0	4.83	+0.19	-0.00
48	72	1089.6	+0.1	-0.4	4.96		
49	13	1052.0	+0.2	-0.0	5.07	+0.00	-0.07

(Contd.

Appendix E.1 (Contd.)

Run No.	Duration hrs.	Final Temp. °C	Maximum Recorded Fluctuations, °C		Final Pressure, kb	Maximum Recorded Fluctuations, kb	
50	110	984.5	+0.4	-0.0	4.98	+0.02	-0.15
51	24	1048.5	+0.3	-1.0	5.05	+0.00	-0.00
52	10	1151.4	+0.2	-0.0	5.01	+0.00	-0.00
53	72	1002.2	+0.0	-0.2	5.02	+0.10	-0.00
54	85	900.9	+0.4	-0.3	4.94	+0.06	-0.00
55	20	1101.9	+0.1	-0.5	4.98	+0.01	-0.00
56	120	953.9	+0.4	-0.7	4.99	+0.02	-0.00
57	72	1002.0	+0.0	-0.6	4.91	+0.10	-0.00
58	80	1075.1	+0.3	-0.1	4.97	+0.04	-0.02
58a	65	1076.1	+0.0	-0.2	5.04	+0.00	-0.04
59	108	976.6	+0.2	-0.0	4.93	+0.07	-0.08
60	264	833.5	+0.1	-0.1	4.99	+0.05	-0.20
61[I]	27	1059.7	+0.1	-0.3	5.06	+0.00	-0.00
62	26	1040.4	+0.0	-0.4	5.10	+0.00	-0.00
63	118	968.6	+0.1	-0.9	4.96	+0.14	-0.00
64	120	940.6	+0.3	-0.1	5.06	+0.00	-0.00
65[I]	2	1132.2	+0.0	-0.1	5.03	+0.00	-0.02
66	11	1101.6	+0.0	-0.4	5.03	+0.06	-0.00
67[2]	132	947.1	+0.3	-0.1	4.91	+0.15	-0.00

[I] Run quenched by fuse blowing - final conditions uncertain, last recorded conditions given.

[2] Held at 1049°C for 48 hours.

Fluctuations are the maximum recorded, for temperatures these are not necessarily the maximum during the run.

Thermal gradients within the sample holder are less than 5°C.

Accuracy of measurement of conditions are ±0.1°C, ±4 bars.

Comparison of melting temperatures of standards is discussed by Ford (1972).

APPENDIX E.2

EXPERIMENTAL RUN DATA

All run data are under approximately 5 kb water pressure.

Results of quenching experiments on pargasite gel.

Run No.	Temp. °C.	% H_2O in charge	Optical	X-ray	Evidence of vapour
52	1151	11.6	Fo,qu-p,L	Fo,(Cpx)	✓
55	1102	9.3	Fo,(Sp),qu-p,L	Fo,(Cpx)	x
58a	1076	8.3	Fo,(Sp),(Cpx),qu-p,L	Fo,Cpx,(Sp)	✓
51	1048	9.5	Fo,Cpx,(Sp),(Amph),qu-p,L	Fo,Cpx,Amph	✓
53	1002	9.8	Amph,(Fo),(L)	Amph	✓
59	977	9.0	Amph,(Sp),(L)	Amph	✓
56	954	9.7	Amph,(L)	Amph	✓
67	947	10.1	Amph,(Fo),(Sp)	Amph,Fo	✓
54	901	10.3	Amph,(Sp),(L)	Amph	✓

Legend given at end of Appendix E.2.

Results of quenching experiments on gel '42'

Run No.	Temp. °C	% H_2O in charge	Optical	X-ray	Evidence of vapour
25	1199	23.6	Fo, qu-p, L	Fo, Cpx	✓
42	1160	16.6	Fo, qu-p, L	Fo, Cpx, (Mel)	x
26	1148	23.3	Fo, qu-p, L	Fo, Cpx	x
65	1132	12.8	Fo, Cpx, qu-p, L	Fo, Cpx	✓
40	1108	19.7	Fo, Cpx, qu-p, L	Fo, Cpx	x
48	1090	23.2	Fo, Cpx, qu-p, L		✓
61	1060	10.2	Fo, Cpx, qu-p, L	Fo, Cpx, Amph	✓
49	1052	33.0	Fo, Cpx, (Sp), qu-p, L	Fo, Cpx, Amph	✓
15	1027	17.0	Fo, Cpx(Amph), qu-p, L	Fo, Cpx, Amph	x
21	1006	20.1	Fo, Cpx, Amph, qu-p, L	Fo, Cpx, Amph	✓
24	1000	25.2	(Fo), Cpx, Amph, qu-p, L	Fo, Cpx, Amph, (Mel)	✓
50	985	16.3	(Fo), Cpx, Amph, qu-p, L	Fo, Cpx, Amph, (Mel)	✓
20	978	25.2	Cpx, Amph, qu-p, (L)	Cpx, Amph, (Mel)	✓
59	977	9.6	(Fo), Cpx, Amph, (Neph), (L)	(Fo), Cpx, Amph, Mel	x
63	968	9.6	(Fo), Cpx, Amph, (Neph), (L)	(Fo), Cpx, Amph, Mel	✓
67	947	6.8	Amph, Neph, (L)	(Fo), Cpx, Amph, Mel	x
64	941	7.8	Amph, Neph, (L)	(Cpx), Amph, Mel	✓
19	928	25.0	Amph, Neph, (L)	(Cpx), Amph, Mel	✓
47	899	17.6	Amph, Neph, (L)	(Cpx), Amph, Mel	✓
27	851	25.4	Amph, Neph, (L)	(Cpx), Amph, Mel	✓
17	801	19.5	Amph, Neph, (L)	(Cpx), Amph, Mel	x
43	775	17.9	Amph, Neph, (L)	(Cpx), Amph, Mel	✓

Results of quenching experiments on gel '45'

Run No.	Temp. °C	% H_2O in charge	Optical	X-ray	Evidence of vapour
25	1199	26.3	Fo,qu-p,L	Fo,Cpx	✓
42	1160	21.6	Fo,qu-p,L	Fo,Cpx,(Mel)	✓
65	1132	9.3	Fo,Cpx,qu-p,L	Fo,Cpx	
40	1108	24.5	Fo,Cpx,qu-p,L	Fo,Cpx	x
48	1090	31.0	Fo,Cpx,qu-p,L		✓
13	1074	27.0	Fo,Cpx,qu-p,L	Fo,Cpx,Amph	x
61	1060	10.8	Fo,Cpx,qu-p,L	Fo,Cpx,Amph	✓
15	1027	20.0	Fo,Cpx,Amph,qu-p,L	Fo,Cpx,Amph	✓
24	1000	25.8	(Fo),Cpx,Amph,qu-p,L	Cpx,Amph	✓
50	985	16.1	(Fo),Cpx,Amph,(Neph),(L)	(Fo),Cpx,Amph,Mel	x
20	978	20.0	Cpx,Amph,Neph,(L)	(Fo),Cpx,Amph,Mel	✓
59	977	10.8	Cpx,Amph,(L)	Cpx,Amph,Mel	✓
63	968	12.6	Cpx,Amph,Neph,(L)	(Fo),Cpx,Amph,Mel	✓
18	953	25.7	Cpx,Amph,Neph,(L)	(Fo),Cpx,Amph,Mel	✓
67	947	14.3	Fo,Cpx,Amph,(Neph),(L)	Cpx,Amph	✓
64	941	17.6	Cpx,Amph,Neph,(L)	(Fo),Cpx,Amph,Mel	✓
19	928	23.7	Cpx,Amph,Neph,(L)	Cpx,Amph,Mel	x
14	901	20.0	(Cpx),Amph,Neph,(L)	(Fo),Cpx,Amph,Mel	x
47	899	26.7	(Cpx),Amph,Neph,(L)	(Fo),Cpx,Amph,Mel	✓
27	851	26.4	(Cpx),Amph,Neph,(L)	Cpx,Amph,Mel	✓
60	833	10.1	(Cpx),Amph,Neph,(L)	Cpx,Amph,Mel	✓
17	801	20.0	(Cpx),Amph,Neph,(L)	Cpx,Amph,Mel	✓
43	775	22.4	Cpx?,Amph,Neph,L?	Cpx,Amph,Mel	✓

Results of quenching experiments on gel '48'

Run No.	Temp. °C	% H_2O in charge	Optical	X-ray	Evidence of vapour
25	1199	30.5	Fo,qu-p,L	Fo,Cpx	√
42	1160	25.2	Fo,qu-p,L	Fo,Cpx	√
26	1148	24.6	Fo,qu-p,L	Fo,Cpx	√
65	1132	9.5	Fo,Cpx,qu-p,L	Fo,Cpx	√
40	1108	20.2	Fo,Cpx,qu-p,L	Fo,Cpx,Amph	√
48	1090	21.3	Fo,Cpx,qu-p,L		x
13	1074	28.0	Fo,Cpx,qu-p,L	Fo,Cpx,Amph	x
61	1060	14.2	Fo,Cpx,Amph,qu-p,L	Fo,Cpx,Amph	√
15	1027	23.0	Fo,Cpx,Amph,qu-p,L	(Fo),Cpx,Amph	√
24	1000	25.6	Fo,Cpx,Amph,qu-p,L	(Fo),Cpx,Amph	√
50	985	15.4	(Fo),Cpx,Amph,qu-p,(L)	(Fo),Cpx,Amph	x
20	978	23.1	Cpx,Amph,qu-p,(L)	(Fo),Cpx,Amph	x
59	977	11.5	Cpx,Amph,qu-p,(L)	(Fo),Cpx,Amph	√
63	968	11.4	Cpx,Amph,qu-p,(L)		√
18	953	21.6	Cpx,Amph,(L)	Cpx,Amph	x
67	947	13.2	(Fo),Cpx,Amph,(L)	Cpx,Amph	√
64	941	12.3	Cpx,Amph,(L)	(Fo),Cpx,Amph	√
19	928	24.7	Cpx,Amph,Plag,(L)	Cpx,Amph,Plag	x
14	901	23.0	Cpx,Amph,Plag,(L)	Cpx,Amph,Plag	√
27	851	23.7	Cpx,Amph,Plag,(L)	Cpx,Amph,Plag	√
60	833	8.0	Cpx,Amph,Plag,(L)	Cpx,Amph	√
17	801	24.3	Cpx,Amph,Plag,(L)	Cpx,Amph,Plag	x
43	775	24.4	Cpx,Amph,Plag,Mica?, L?	Cpx,Amph,Plag	√

Results of quenching experiments on gel '51'

Run No.	Temp. °C	% H_2O in charge	Optical	X-ray	Evidence of vapour
25	1199	25.6	(Fo),qu-p,L	Cpx	✓
45	1170	16.5	(Fo),qu-p,L	(Fo),Cpx	✓
42	1160	23.0	Fo,(Cpx),qu-p,L	Fo,Cpx	x
26	1148	24.8	Fo,(Cpx),qu-p,L	Fo,Cpx	✓
40	1108	22.4	Fo,Cpx,qu-p,L	Fo,Cpx,Amph	✓
48	1090	18.5	Fo,Cpx,qu-p,L	Fo,Cpx,Amph	✓
13	1074	23.0	Fo,Cpx,Amph,qu-p,L	Fo,Cpx,Amph	x
61	1060	14.2	Fo,Cpx,Amph,qu-p,L	Fo,Cpx,Amph	✓
15	1027	19.0	Fo,Cpx,Amph,qu-p,L	Fo,Cpx,Amph	✓
24	1000	25.6	(Fo),Cpx,Amph,qu-p,L	Cpx,Amph	x
50	985	15.2	(Fo),Cpx,Amph,qu-p,(L)	Cpx,Amph	✓
59	977	13.8	(Fo),Cpx,Amph,qu-p,(L)	(Fo),Cpx,Amph	✓
63	968	11.4	Cpx,Amph,(L)		✓
18	953	25.4	Cpx,Amph,Plag,(L)	Cpx,Amph,Plag?	x
67	947	12.5	(Fo),Cpx,Amph,Plag,(L)	Cpx,Amph	✓
64	941	19.4	Cpx,Amph,Plag,(L)	Fo?,Cpx,Amph	✓
19	928	25.2	(Cpx),Amph,Plag,(L)	Fo?,Cpx,Amph,Plag	✓
47	899	20.8	(Cpx),Amph,Plag,(L)	Cpx,Amph	✓
27	851	25.0	(Cpx),Amph,Plag,Mica?,(L)	Cpx,Amph,Plag	✓
60	833	10.5	(Cpx),Amph,Plag,(L)	Cpx,Amph,Plag	✓
17	801	25.2	(Cpx),Amph,Plag,(L)	Cpx,Amph,Plag	x
43	775	22.1	(Cpx),Amph,Plag,Mica?,L?	Cpx,Amph	✓

Results of quenching experiments on gel '54'

Run No.	Temp. °C	% H_2O in charge	Optical	X-ray	Evidence of vapour
25	1199	24.1	qu-p,L	Cpx	√
45	1170	21.4	Fo?,qu-p,L	Cpx	√
42	1160	24.7	Fo,Cpx,qu-p,L	Fo,Cpx	√
26	1148	24.6	Fo,Cpx,qu-p,L	Fo,Cpx,(Amph)	√
40	1108	23.2	Fo,Cpx,qu-p,L	Fo,Cpx,Amph	√
48	1090	28.7	Fo,Cpx,qu-p,L		√
13	1074	31.0	Fo,Cpx,qu-p,L	Fo,Cpx,Amph	√
61	1060	15.3	Fo,Cpx,qu-p,L	Fo,Cpx,Amph	x
24	1000	24.2	Fo,Cpx,(Amph),qu-p,L	Fo,Cpx,Amph	√
50	985	25.3	Fo,Cpx,Amph,qu-p,L	Fo,Cpx,Amph	√
20	978	28.8	Fo,Cpx,Amph,qu-p,L	(Fo),Cpx, Amph,Plag?	x
59	977	13.1	Fo,Cpx,Amph,qu-p,L	(Fo),Cpx,Amph	√
63	968	12.7	Cpx,Amph,qu-p,L		√
18	953	23.9	Cpx,Amph,qu-p,L	Cpx,Amph	x
67	947	14.1	(Fo),Cpx,Amph,L	Fo?,Cpx,Amph	√
64	941	14.5	Cpx,Amph,Plag,qu-p,L	(Fo),Cpx,Amph, Plag	√
19	928	23.9	Cpx,Amph,(Plag),qu-p, L	Cpx,Amph, (Plag)	√
14	901	25.0	(Cpx),Amph,Plag, qu-p,(L)	Cpx,Amph,Plag	x
47	899	26.8	(Cpx),Amph,Plag, qu-p,(L)	Cpx,Amph,Plag	√
27	851	26.7	(Cpx),Amph,Plag, Mica,L?	Cpx,Amph,Plag	√
43	775	25.6	Cpx?,Amph,Plag, Mica,L?	(Cpx),Amph,Plag	√

Results of quenching experiments on gel '57'

Run No.	Temp. °C	% H_2O in charge	Optical	X-ray	Evidence of vapour
25	1199	25.9	qu-p,L	Cpx	✓
45	1170	27.8	qu-p,L	Cpx,Amph	✓
42	1160	23.0	qu-p,L	Fo,Cpx	✓
65	1132	9.9	Fo,Cpx,qu-p,L	Fo,Cpx	✓
40	1108	29.9	Fo,Cpx,qu-p,L	Fo,Cpx,Amph	✓
48	1090	30.5	Fo,Cpx,qu-p,L		✓
13	1074	29.0	Fo,Cpx,qu-p,L	Fo,Cpx,Amph	✓
61	1060	10.6	Fo,Cpx,qu-p,L	Fo,Cpx,Amph	✓
49	1052	25.5	Fo,Cpx,qu-p,L	Fo,Cpx,Amph	✓
62	1040	11.5	Fo,Cpx,qu-p,L	Fo,Cpx,Amph	✓
15	1027	18.0	Fo,Cpx,qu-p,L	Fo,Cpx,Amph	x
24	1000	32.3	Fo,Cpx,Amph,qu-p,L	Fo,Cpx,Amph	✓
50	985	18.2	Fo,Cpx,Amph,qu-p,L	Cpx,Amph	✓
20	978	23.9	Fo,Cpx,Amph,qu-p,L	Fo,Cpx,Amph	✓
59	977	17.0		Cpx,Amph	✓
63	968	12.4	Fo,Cpx,Amph,qu-p,L	Cpx	✓
23	960	24.6	Cpx,Amph,qu-p,L	Cpx,Amph	x
18	953	24.0	Cpx,Amph,Plag?, qu-p,L	Cpx,Amph,Plag?	x
67	947	18.1	Fo,Cpx,Amph,L	Cpx,Amph	✓
64	941	13.9	Cpx,Amph,qu-p,(L)	(Fo),Cpx,Amph	✓
19	928	24.3	Cpx,Amph,qu-p,L	Cpx,Amph,Plag	✓
14	901	28.0	Cpx,Amph,Plag?, Mica,L?	Cpx,Amph,Plag	✓
47	899	27.4	Cpx,Amph,Plag,Mica,L?	Cpx,Amph,Plag	✓
17	801	24.7	(Cpx),Amph,Plag, Mica,L?	Cpx,Amph,Plag	✓
43	775	26.2	(Cpx),Amph,Plag, Mica,L?	Cpx,Amph,Plag	x

Results of quenching experiments on gel "42EN"

Run No.	Temp. °C	% H_2O in charge	Optical	X-ray	Evidence of vapour
45	1170	31.6	Fo,qu-p,L	Fo,Cpx	√
42	1160	22.8	Fo,qu-p,L	Fo,Cpx	√
34	1150	19.4	Fo,(Cpx),qu-p,L	Fo,Cpx	x
65	1132	9.1	Fo,Cpx,qu-p,L	Fo,Cpx	√
40	1108	20.3	Fo,Cpx,qu-p,L	Fo,Cpx	√
58	1075	12.6	Fo,Cpx,qu-p,L	Fo,Cpx	√
49	1052	26.8	Fo,Cpx,qu-p,L	Fo,Cpx	√
31	1044		Fo,Cpx,qu-p,L	Fo,Cpx	x
37	1001	19.6	Fo,Cpx,(Amph),qu-p,L	Fo,Cpx	√
63	968	11.1	Fo,Cpx,Amph,Opx, qu-p,L	Fo,Cpx,Amph	√
67	947	12.1	(Fo),(Cpx),Amph,Opx, qu-p,L	Fo,Cpx,Amph,Opx	x
64	941	12.1	Fo,Amph,Opx	Fo,Amph,Opx	√
60	833	10.4	Fo,(Cpx),Amph,Opx	Fo,Amph,Opx	√
43	775	27.2	Fo,(Cpx),Amph,Opx	Fo,Amph,Opx	√

Results of quenching experiments on gel "45EN"

Run No.	Temp. °C	% H_2O in charge	Optical	X-ray	Evidence of vapour
45	1170	36.9	Fo,qu-p,L	Fo	√
42	1160	20.8	Fo,qu-p,L	Fo,Cpx	√
34	1150	24.5	Fo,qu-p,L	Fo,Cpx	√
65	1132	13.4	Fo,Cpx,qu-p,L	Fo,Cpx	√
40	1108	16.7	Fo,Cpx,qu-p,L	Fo,Cpx,Amph	√
46	1091	25.0	Fo,Cpx,qu-p,L	Fo,Cpx	√
31	1044	29.4	Fo,Cpx,qu-p,L	Fo,Cpx,Amph	x
63	968	12.1	Fo,Cpx,Amph,Opx,L	Fo,Cpx,Amph,Opx	√
67	947	13.8	Fo,(Cpx),Amph,Opx, (L)	Fo,Cpx,Amph,Opx	√
64	941	11.9	Fo,(Cpx),Amph,Opx	Fo,Amph,Opx	√
33	902	24.0	Fo,Cpx,Amph,Opx	Fo,Amph,Opx	√
43	775	27.2	Fo,Cpx?,Amph,Opx	Fo,Cpx,Amph,Opx	√

Results of quenching experiments on gel "48EN"

Run No.	Temp. °C	% H_2O in charge	Optical	X-ray	Evidence of vapour
45	1170	34.1	Fo, qu-p, L	Fo, Cpx	√
42	1160	20.5	Fo, qu-p, L	Fo, Cpx	√
34	1150	18.4	Fo, qu-p, L	Fo, Cpx	√
65	1132	10.0	Fo, Cpx, qu-p, L	Fo, Cpx, (Opx)	√
40	1108	22.5	Fo, Cpx, qu-p, L	Fo, Cpx, Opx	x
46	1091		Fo, Cpx, Opx, qu-p, L	Fo, Cpx, Opx	√
31	1044	23.0	Fo, Cpx, Opx, qu-p, L	Fo, Cpx	√
37	1001	20.6	Fo, Cpx, Opx, qu-p, L	Fo, Cpx, Opx	√
63	968	11.5	Fo, Cpx, Opx, (L)	Fo, Cpx, Opx, Amph	x
67	947	14.5	Fo, Cpx, Opx, Amph, (L)	(Fo), Cpx, Opx, Amph	√
64	941	10.9	Fo, (Cpx), Opx, Amph, (L)	(Fo), Opx, Amph	√
33	902	19.1	Opx, Amph	(Fo), Opx, Amph	√
43	775	21.1	(Fo), (Cpx), Opx, Amph	(Fo), (Cpx), Opx, Amph	√

Results of quenching experiments on gel "51EN"

Run No.	Temp. °C	% H_2O in charge	Optical	X-ray	Evidence of vapour
42	1160	20.0	Fo, Cpx?, qu-p, L	Fo, Cpx	√
34	1150	22.5	Fo, qu-p, L	Fo, Cpx	√
65	1132	11.8	Fo, Opx, qu-p, L	Fo, Cpx	√
40	1108	21.1	Fo, Cpx, Opx, qu-p, L	Fo, Cpx, Opx	x
58	1075	14.2	Fo, Cpx, Opx, qu-p, L	Fo, Cpx, Opx	√
31	1044	22.0	Fo, Cpx, Opx, qu-p, L	Fo, Cpx, Opx	√
63	968	11.5	Fo, Cpx, Opx, Amph, L	Fo, Cpx, Opx, Amph	√
67	947	14.5	(Fo), Cpx, Opx, Amph, (L)	(Fo), Cpx, Opx, Amph	√
64	941	10.8	Cpx, Opx, Amph, Plag, (L)	(Fo,) Opx, Amph	√
33	902	21.2	(Cpx), Opx, Amph, Plag, (L)	(Fo), (Cpx), Opx, amph, (Plag)	√
60	833	10.5	Cpx, Opx, Amph, Plag, L?	(Fo), Cpx, Opx Amph	√
43	775	38.1	Cpx, Opx, Amph, Plag?	(Fo), Cpx, Opx, Amph, (Sp)	√

Results of quenching experiments on gel "54EN"

Run No.	Temp. °C	% H_2O in charge	Optical	X-ray	Evidence of vapour
45	1170	26.3	Fo, qu-p, L	Fo, Cpx, Opx	x
34	1150	23.9	Fo, Opx, qu-p, L	Fo, Cpx, Opx	√
65	1132	13.6	Fo, Opx, qu-p, L	Fo, Cpx, Opx	√
40	1108	29.5	Fo, Opx, (Cpx), qu-p, L	Fo, Cpx, Opx	√
58	1075	11.9	Fo, Opx, qu-p, L	Fo, Cpx, Opx	√
31	1044	24.8	Fo, Opx, Cpx, qu-p, L	Fo, Cpx, Opx	√
63	968	10.9	Fo, Opx, Cpx, qu-p, L	Fo, Cpx, Opx, Amph	x
67	947	13.2	Fo, Opx, Cpx, Amph, (L)	(Fo), Cpx, Opx, Amph	√
64	941	13.2	Opx, Cpx, Amph, Plag, (L)	(Fo), Cpx, Opx, Amph, Plag	√
33	902	24.3	Opx, (Cpx), Amph, (Plag), (L)	Fo, (Cpx), Opx, Amph	√
43	775	26.2	Opx, (Cpx), Amph, (Plag), L?	(Cpx), Opx, Amph	√

Results of quenching experiments on gel "57EN"

Run No.	Temp. °C	% H_2O in charge	Optical	X-ray	Evidence of vapour
45	1170	28.3	Fo, Opx, qu-p, L	Fo, Cpx, Opx	√
42	1160	22.1	Fo, Opx, qu-p, L	Fo, Cpx, Opx	√
34	1150	23.8	Fo, Opx, qu-p, L	Fo, Cpx, Opx	√
65	1132	13.4	Fo, Cpx, Cpx, qu-p, L	Fo, Cpx, Opx	√
40	1108	23.0	Fo, Opx, Cpx, qu-p, L	Fo, Cpx, Opx	√
58	1075	11.6	Fo, Opx, Cpx, qu-p, L	Fo, Cpx, Opx	√
31	1044	29.8	Fo, Opx, Cpx, qu-p, L	Fo, Cpx, Opx	√
63	968	11.6	Fo, Opx, Cpx, (Amph), (L)	Fo, Cpx, Opx, Amph	√
67	947	14.5	Fo, Opx, Cpx, Amph, (L)	Cpx, Opx, Amph	√
64	941	6.1	Opx, Cpx, Amph, (Plag), (L)	(Fo), Cpx, Opx, Amph, Plag	√
33	902	27.7	Opx, Cpx, Amph, Plag, L?	(Fo), Opx, Amph, (Plag)	√
43	775	26.2	Opx, Amph, Plag?, L?	(Fo), (Cpx), Opx, Amph, (Plag)	√

Results of quenching experiments on gel "1a"

Run No.	Temp. °C	% H_2O in charge	Optical	X-ray	Evidence of vapour
52	1151	9.3	Sp,qu-p,L	-	√
55	1102	11.5	Sp,qu-p,L	Cpx	√
58a	1076	11.0	Sp,qu-p,L	Cpx,Sp	√
61	1059	7.5	Sp,Fo,Plag,qu-p,L	Sp,Fo,Plag	√
51	1048	9.2	Sp,Fo,Plag,qu-p,L	Fo,Plag	√
53	1002	6.7	Sp,Fo,Plag,Opx,L	Sp,Fo,Plag	√
56	954	11.3	Sp,(Fo),Plag, Opx,L	Fo,Plag,Opx	√
67	947	6.7	(Fo),Plag,Opx,(L)	Plag,(Opx)	√
64	941	11.3	Sp,Plag,Opx,Amph,(L)	Plag,Opx,Cpx	√
54	901	10.5	Sp,Plag,Opx,Amph,(L)	Sp,Plag,Opx	√

Results of quenching experiments on gel '1b'

Run No.	Temp. °C	% H_2O in charge	Optical	X-ray	Evidence of vapour
52	1151	8.6	Sp,qu-p,L	Amph	x
55	1102	10.2	Sp,qu-p,L	Amph	√
58a	1076	11.0	Sp,qu-p,L	Amph,Sp,Cox	√
61	1059	8.5	Sp,Fo,Plag?,qu-p,L	Sp,Plag	√
51	1048	12.2	Sp,Fo	Sp,Amph	√
53	1002	9.5	Sp,Fo,Amph,Plag,qu-p L	Sp,Amph,Fo,Plag	√
56	954	9.3	Sp,Fo,Amph,Plag,L	Sp,Amph,(Fo), Plag	x
67	947	11.7	Sp,Amph,Plag, Opx,(L)	Amph,(Fo),Plag	√
64	941	10.1	Sp,Amph,Plag,Opx,(L)	Amph,Plag	√
54	901	9.8	Sp,Amph,Opx,L?	Amph,Plag	√

Results of quenching experiments on gel '1c'

Run No.	Temp. °C	% H_2O in charge	Optical	X-ray	Evidence of vapour
52	1151	9.4	qu-p,L	Cpx	√
55	1102	8.0	qu-p,L	Cpx,Amph	x
58a	1076	9.0	Fo,qu-p,L	Fo,Cpx	√
61	1059	7.9	Fo,Amph,Sp,qu-p,L	(Fo),Amph	√
51	1048	6.3	Fo,Amph,Sp,qu-p,L	Fo,Cpx,Amph	√
53	1002	11.0	Amph,Sp,Cpx,qu-p,L	(Fo),Cpx,Amph	x
56	954	8.5	Amph,Sp,Cpx,Plag, qu-p,L	Cpx,Amph,Plag	√
67	947	8.4	Amph,Cpx,Plag,qu-p,(L)	Cpx,Amph,Plag	√
64	941	9.8	Amph,Cpx,Plag,(L)	Cpx,Amph,Plag	√
54	901	8.2	Amph,Cpx,Plag,(L)	Cpx,Amph,Plag	√

Results of quenching experiments on gel '2a'

Run No.	Temp. °C	% H_2O in charge	Optical	X-ray	Evidence of vapour
52	1151	10.8	Fo,(Sp),qu-p,L	Fo	√
65	1132		Fo,Sp,qu-p,L	Fo	√
55	1102	10.3	Fo,Sp,qu-p,L	Fo,Sp,Cpx	√
58a	1076	9.9	Fo,Sp,qu-p,L	Fo,Sp	√
61	1059	8.0	Fo,Sp,qu-p,L	Fo,Sp	√
51	1048	9.1	Fo,Sp,(Plag),qu-p,L	Fo,Sp	√
53	1002	13.0	Fo,Sp,Plag,Opx,qu-p,L	Fo,Sp,Plag	√
56	954	10.8	Sp,Plag,Opx,qu-p,L	Sp,Plag,Opx	√
54	901	11.0	Sp,Plag,Opx,Amph, Mica,L?	Plag,Opx,Amph	√

Results of quenching experiments on gel '2b'

Run No.	Temp. °C	% H_2O in charge	Optical	X-ray	Evidence of vapour
52	1151	8.6	Fo,qu-p,L	Fo,Cpx	√
65	1132	10.2	Fo,qu-p,L	Fo	√
55	1102	5.9	Fo,Sp,qu-p,L	Fo,Cpx	√
58a	1076	9.2	Fo,Sp,qu-p,L	Fo	√
61	1059	12.3	Fo,Sp,qu-p,L	Fo,Sp	√
51	1048	7.6	Fo,Sp,Plag,qu-p,L	Fo,Plag	√
53	1002	11.0	Fo,Sp,Plag,Amph, qu-p,L	Fo,Plag,Amph	√
56	954	8.5	Fo,Sp,Plag,Amph, qu-p,L	Fo,Plag,(Amph)	√
54	901	11.8	Sp,Plag,Amph,Opx, Mica,(L)	Plag,Amph,Opx, (Cpx)	√

Results of quenching experiments on gel '2c'

Run No.	Temp. °C	% H_2O in charge	Optical	X-ray	Evidence of vapour
52	1151	7.9	Fo,qu-p,L	Fo,Cpx	√
55	1102	11.4	Fo,qu-p,L	Fo	√
58a	1076	5.6	Fo,qu-p,L	Fo	√
61	1059	7.9	Fo,qu-p,L	Fo	√
51	1048	9.2	Fo,qu-p,L	Fo	x
53	1002	9.8	Fo,Amph,Plag,qu-p,L	Fo,Amph	√
56	954	8.5	Amph,Plag,Mica,L	Amph	√
54	901	9.4	Amph,Plag,Mica,L?	Amph	√

Results of quenching experiments on gel '3a'

Run No.	Temp. °C	% H_2O in charge	Optical	X-ray	Evidence of vapour
52	1151	11.4	qu-p,L	-	x
55	1102	6.6	qu-p,L	Cpx	√
58a	1076	10.2	(Fo),Cpx,qu-p,L	Cpx,Amph	√
51	1048	9.7	(Fo),Cpx,qu-p,L	Fo,Cpx,Amph	√
53	1002	10.3	Fo,Cpx,Opx,qu-p,L	Cpx,Amph	√
63	968	9.8	Cpx,Opx,Plag,qu-p,L	Cpx,Opx,Plag	√
56	954	11.5	Cpx,Opx,Plag,qu-p,L	Cpx,Plag	√
67	947	11.2	(Fo),Cpx,Opx,Plag, qu-p,L	Cpx,Plag	√
54	901	8.6	Cpx,(Opx),Amph,Plag,L	Cpx,Plag,Amph	√

Results of quenching experiments on gel '3b'

Run No.	Temp. °C	% H_2O in charge	Optical	X-ray	Evidence of vapour
52	1151	10.0	qu-p,L	-	√
55	1102	7.8	qu-p,L	Cpx,Amph	√
58a	1076	9.3	(Fo),Cpx,qu-p,L	Fo,Cpx,Amph	√
51	1048	10.0	Fo,Cpx,qu-p,L	Cpx,Amph	x
53	1002	9.6	Fo,Cpx,Amph,qu-p,L	Cpx,Amph,Plag	√
63	968	9.3	Cpx,Amph,Plag,L	Cpx,Amph	√
56	954	7.5	Cpx,Amph,Plag,L	Cpx,Amph,Plag	√
67	947	14.3	Fo?,Cpx,Amph,Plag, (Opx),L	Cpx,Amph,Plag	√
54	901	9.8	Cpx,Amph,Plag,Opx,(L)	Cpx,Amph,Plag	√

Results of quenching experiments on gel '3c'

Run No.	Temp. °C	% H_2O in charge	Optical	X-ray	Evidence of vapour
52	1151	10.9	qu-p,L	Cpx	√
55	1102	7.0	qu-p,L	Cpx	√
58a	1076	7.9	Fo,Cpx,qu-p,L	Fo,Cpx,Amph	√
61	1059	9.0	Fo,Cpx,qu-p,L	Cpx,Amph	√
51	1048	8.5	Fo,Cpx,(Amph),qu-p,L	Fo,Cpx,Amph	x
53	1002	9.2	Fo,Cpx,Amph,qu-p,L	Cpx,Amph	√
63	968	11.2	Cpx,Amph,Plag,qu-p,L	Cpx,Amph	√
56	954	8.1	Cpx,Amph,Plag,qu-p,L	Fo,Cpx,Amph	√
67	947	8.9	Cpx,Amph,Plag,qu-p,L	Cpx,Amph	√
54	901	9.9	Cpx,Amph,Plag,qu-p,L	Cpx,Amph	√

Results of quenching experiments on gel '6a'

Run No.	Temp. °C	% H_2O in charge	Optical	X-ray	Evidence of vapour
55	1102	8.6	qu-p,L	Cpx,Plag	x
58a	1076	11.3	qu-p,L	-	√
61	1059	6.2	qu-p,L	Opx,Plag	√
62	1040	7.5	Opx,Plag,qu-p,L	Opx,Plag	√
57	1002	5.2	Opx,Plag,qu-p,L	Opx,Plag	√
59	977	12.1	Opx,Plag,Cpx,qu-p,L	Opx,Plag,(Sp)	√
56	954	9.7	Opx,Plag,Cpx,(Sp), qu-p,L	Opx,Plag	√

Results of quenching experiments on gel '6b'

Run No.	Temp. °C	% H_2O in charge	Optical	X-ray	Evidence of vapour
55	1102	9.6	qu-p,L	-	√
58a	1076	13.0	qu-p,L	-	√
61	1059	6.8	Fo,qu-p,L	Cpx,Plag	√
62	1040	9.4	Fo,Cpx,qu-p,L	Cpx,Plag	√
57	1002	7.1	Fo,Cpx,Plag,qu-p,L	Cpx,Plag	√
59	977	8.1	Fo,Plag,Amph,qu-p,L	Plag,Amph	√
56	954	8.8	Fo,Plag,Amph,Opx, qu-p,L	Plag,Amph	√

Results of quenching experiments on gel '6c'

Run No.	Temp. °C	% H_2O in charge	Optical	X-ray	Evidence of vapour
55	1102	11.4	qu-p,L	-	√
58a	1076	9.4	Fo,qu-p,L	-	√
61	1059	10.5	Fo,qu-p,L	Fo	√
62	1040	11.4	Fo,Amph,Cpx,qu-p,L	Fo,Amph	√
57	1002	10.9	Amph,Cpx,Plag, qu-p,L	Amph,Plag	√
59	977	9.2	Amph,Plag,qu-p,L	Amph,Plag	√
56	954	9.5	Amph,Plag,qu-p,L	Amph,Plag	√

Results of quenching experiments on gel '7a'

Run No.	Temp. °C	% H_2O in charge	Optical	X-ray	Evidence of vapour
65	1132	7.0	Sp, qu-p, L	Sp, Opx	√
55	1102	10.3	Sp, qu-p, L	Sp	√
58	1075	9.4	Sp, Opx, qu-p, L	Sp, Opx	√
62	1040	6.8	Sp, Opx, qu-p, L	Sp, Opx, Amph	√
57	1002	7.4	Sp, Opx, Plag, qu-p, L	Sp, Opx, Plag	√
59	977	13.5	Sp, Opx, Plag, qu-p, L	Sp, Opx, Plag	√
56	954	8.1	Sp, Opx, Plag, qu-p, L	Sp, Plag	√
64	941	5.0	Sp, Opx, Plag, Amph, qu-p, L	(Sp), Opx, Plag, Amph, Cpx	√

Results of quenching experiments on gel '7b'

Run No.	Temp. °C	% H_2O in charge	Optical	X-ray	Evidence of vapour
65	1132	6.1	Sp, qu-p, L	Sp	√
55	1102	7.9	Sp, Fo, qu-p, L	Sp, Fo	√
58	1075	8.2	Sp, Fo, qu-p, L	Sp, Fo	√
62	1040	10.0	Sp, Fo, Opx, qu-p, L	Sp, Fo, Amph	√
57	1002	9.7	Sp, Opx, Plag, qu-p, L	Sp, Opx, Plag	√
59	977	12.6	Sp, Opx, Plag, qu-p, L	Sp, Fo, Opx, Plag	√
56	954	6.4	Sp, (Fo), Opx, Plag, qu-p, L	Sp, Fo, Opx, Plag	√
64	941	5.6	Sp, Opx, Plag, Amph, (L)	Sp, Opx, Plag	√

Results of quenching experiments on gel '7c'

Run No.	Temp. °C	% H_2O in charge	Optical	X-ray	Evidence of vapour
65	1132	6.5	Fo, Sp, qu-p, L	Fo, Sp	x
55	1102	7.1	Fo, Sp, qu-p, L	Fo, Sp	√
58	1075	13.1	Fo, Sp, qu-p, L	Fo, Sp	√
62	1040	11.0	Fo, Sp, qu-p, L	Fo, Sp, Cpx	√
57	1002	8.6	Fo, Sp, Amph, qu-p, L	Sp, Amph	√
59	977	10.7	Sp, Amph, qu-p, L	Sp, Amph	√
56	954	9.7	Sp, Amph, qu-p, L	(Fo), Sp, Amph	√
64	941	7.5	Sp, Amph, Opx, Plag, qu-p, L	Sp, Amph, Opx	x

Results of quenching experiments on gel '9a'

Run No.	Temp. °C	% H_2O in charge	Optical	X-ray	Evidence of vapour
65	1132	9.8	Fo, qu-p, L	Fo, Cpx	√
66	1101	10.1	Fo, (Cpx), qu-p, L	Fo, Cpx	√
58	1075	8.8	Fo, Cpx, (Opx), qu-p, L	Fo, Cpx, Opx	√
61	1059	10.2	Fo, Cpx, Opx, qu-p, L	Fo, Cpx, Opx	√
62	1040	10.1	Fo, Cpx, Opx, qu-p, L	Fo, Cpx, Opx	√
59	977	10.2	Fo, Cpx, Opx, qu-p, L	Fo, Cpx, Opx	√
63	968	12.9	Fo, Cpx, Opx, qu-p, L	Fo, Cpx, Opx	√
67	947	8.2	(Fo), Cpx, Opx, Amph, Plag, (L)	Fo, Cpx, Opx, Amph	√
64	941	11.2	Cpx, Opx, Amph, Plag, (L)	(Fo), Cpx, Opx, Amph	√

Results of quenching experiments on gel '9b'

Run No.	Temp. °C	% H_2O in charge	Optical	X-ray	Evidence of vapour
65	1132	7.7	Fo,qu-p,L	Fo,Cpx	√
66	1101	8.5	Fo,Cpx,qu-p,L	Fo,Cpx	√
58	1075	8.1	Fo,Cpx,qu-p,L	Fo,Cpx	√
61	1059	8.6	Fo,Cpx,qu-p,L	Fo,Cpx	√
62	1040	8.7	Fo,Cpx,Opx,qu-p,L	Fo,Cpx	√
59	977	13.1	Fo,Cpx,Opx,qu-p,L	Fo,Cpx	√
63	968	9.9	Fo,Cpx,Opx,Amph, qu-p,L	Fo,Cpx,Opx, Amph	√
67	947	11.9	Fo,Cpx,Opx,Amph,(L)	Fo,Cpx,Amph	√
64	941	11.0	Fo,Cpx,Opx,Amph,(L)	Fo,Cpx,Opx,Amph	√

Results of quenching experiments on gel '9c'

Run No.	Temp. °C	% H_2O in charge	Optical	X-ray	Evidence of vapour
65	1132	7.1	Fo,qu-p,L	Fo,Cpx	√
66	1101	7.9	Fo,Cpx,qu-p,L	Fo,Cpx	x
58	1075	13.2	Fo,Cpx,qu-p,L	Fo,Cpx	√
61	1059	9.9	Fo,Cpx,qu-p,L	Fo,Cpx	√
62	1040	9.1	Fo,Cpx,qu-p,L	Fo,Cpx,Amph	x
59	977	7.6	Fo,Cpx,(Opx),qu-p,L	Fo,Cpx	√
63	968	8.5	Fo,Cpx,Opx,(Amph), qu-p,L	Fo,Cpx,Opx	x
67	947	10.3	Fo,Cpx,(Opx),Amph, qu-p,L	Fo,Cpx,Amph	√
64	941	7.3	Fo,Cpx,Opx,Amph,(L)	Fo,Cpx,Opx, Amph	√

Results of quenching experiments on gel '10a'

Run No.	Temp. °C	% H_2O in charge	Optical	X-ray	Evidence of vapour
65	1132	7.4	Fo, qu-p, L	Fo, Cpx, Opx	√
66	1101	8.6	Fo, Opx, qu-p, L	Fo, Cpx, Opx	√
58	1075	7.2	Fo, Opx, Cpx, qu-p, L	Fo, Cpx, Opx	√
61	1059	8.8	Fo, Opx, Cpx, qu-p, L	Fo, Cpx, Opx	√
62	1040	9.7	Fo, Opx, Cpx, qu-p, L	Fo, Cpx, Opx	√
59	977	9.7	Fo, Opx, Cpx, qu-p, L	Fo, Cpx, Opx	√
63	968	8.5	Fo, Opx, Cpx, Plag, qu-p, L	Fo, Cpx, Opx, Plag	√
67	947	19.4	Fo, Opx, Cpx, Amph, Plag, (L)	Cpx, Opx, Amph	√
64	941	7.2	Opx, Cpx, Amph, Plag, (L)	Cpx, Opx, Amph	√

Results of quenching experiments on gel '10b'

Run No.	Temp. °C	% H_2O in charge	Optical	X-ray	Evidence of vapour
66	1101	8.4	Fo, (Cpx), qu-p, L	Fo, Cpx	√
58	1075	9.8	Fo, Cpx, qu-p, L	Fo, Cpx	√
61	1059	8.1	Fo, Cpx, Opx, qu-p, L	Fo, Cpx	√
62	1040	9.2	Fo, Cpx, Opx, qu-p, L	Fo, Cpx	√
59	977	9.0	Fo, Cpx, Opx, qu-p, L	Fo, Cpx, Opx	√
63	968	8.8	Fo, Cpx, Opx, Amph, qu-p, L	Fo, Cpx, Opx	√
67	947	7.4	Fo, Cpx, Opx, Amph, qu-p, L	Fo, Cpx, Opx	√
64	941	9.7	Fo, Cpx, Opx, Amph, (L)	Fo, Cpx, Opx, Amph	√

Results of quenching experiments on gel '10c'

Run No.	Temp. °C	% H_2O in charge	Optical	X-ray	Evidence of vapour
66	1101	8.3	Fo,(Cpx),qu-p,L	Fo,Cpx	√
58	1075	8.6	Fo,Cpx,qu-p,L	Fo,Cpx	√
61	1059	9.5	Fo,Cpx,qu-p,L	Fo,Cpx	√
62	1040	10.4	Fo,Cpx,(Opx),qu-p,L	Fo,Cpx,Opx	√
59	977	12.1	Fo,Cpx,Opx,qu-p,L	Fo,Cpx	√
63	968	10.9	Fo,Cpx,Opx,qu-p,L	Fo,Cpx,Opx	√
67	947	10.1	Fo,Cpx,Opx,qu-p,L	Fo,Cpx,Opx	√
64	941	6.7	Fo,Cpx,Opx,Amph, qu-p,(L)	Fo,Cpx,Opx, Amph	√

Legend: detailed experimental conditions for each run are presented in Appendix E.1.

? identification questionable

( ) small amount only

Fo - forsterite; Cpx - clinopyroxene;

Opx - orthopyroxene; Amph - amphibole;

Plag - plagioclase; Sp - spinel; Mel - melilite;

Neph - nepheline; qu-p - quenching products;

L - liquid.

√ indicates at least 1 criterion for the existence of vapour was established (see Appendix B)

APPENDIX F

PROJECTION AND CALCULATION OF PLAGIOCLASE COMPOSITIONS

Projection of plagioclase compositions

The projection method developed by O'Hara (1968) and Jamieson (1969) recalculates plagioclase compositions such that they all project at the same point in all the projection diagrams. Consequently, the position of the projection of the basalt tetrahedron in the system $XO - YO - R_2O_3 - ZO_2$ is fixed regardless of the plagioclase composition.

However, in the projection scheme adopted here, soda is not recalculated in this way, with the result that all the plagioclase compositions do not project at the same point. The projections of the join anorthite - albite are shown in Figs. 3.11 and 3.13. The position of the basalt tetrahedron (which includes plagioclase rather than albite and anorthite as separate components) in these projection diagrams cannot be defined unless the plagioclase composition is known. As this is not always the same for bulk compositions containing the same soda content, it is not possible to indicate a unique location of the basalt tetrahedron in the projection diagrams, Figs. 3.12b-g and 3.14b-e.

A rigorous treatment of this problem is not attempted here. As a guide, a plagioclase composition which contains the same weight percent of soda as the liquid is projected into all the diagrams. In general, the soda content of the normative feldspar will be greater than that of the bulk

composition (except for highly nepheline-normative compositions, see for example Figs. 3.3b and 3.4b). The composition of the crystallising feldspar is not simply related to either bulk composition or to the normative feldspar and hence cannot be predicted.

Calculation of plagioclase compositions

It is possible to make some limiting calculations concerning plagioclase compositions in various equilibria from the phase diagrams presented in Chapter 3.

The crystallisation sequence of gel series 1 at the 3% soda-in-liquid level is considered in detail in Fig. F.1. The phase relationships for liquids containing 3% soda are taken from Fig. 3.12d, as is the feldspar composition with the same soda content (Fo - Plag piercing point). The normative feldspar for gel series 1 containing 3% soda in the bulk composition is given by point N. The crystallisation sequence of gel series 1 for liquids containing 3% soda is spinel, forsterite, plagioclase, orthopyroxene (Fig. 3.4a). The change in residual liquid composition as spinel and forsterite coprecipitate is given by the line 1 - A (Fig. F.1). When the liquid reaches A, plagioclase begins to crystallise, with spinel in reaction relationship with the liquid (a reaction displayed in the phase diagrams of Yoder (1966) and Yoder & Dickey (1971) for soda-free compositions). If the composition of the crystallising feldspar were given by the piercing point Fo - Plag, when the residual liquid reached B (the intersection of the extension of the tie-line from Fo - Plag piercing point

FIG. F.1.

Plagioclase compositions.

Projection from forsterite, soda and vapour into the plane CS - MS - A (weight percent). The phase relationships for vapour- and forsterite-saturated liquids containing 3% soda are taken from Fig. 3.12d. l is the projection of the composition of gel series 1, N is the normative composition of the plagioclase in gel 1b (which contains 3% soda), Fo-Plag pp. is the forsterite — plagioclase piercing point for a plagioclase composition containing 3% soda.

A - B - C is a possible crystallisation path discussed in the text. P is the composition of the most sodic feldspar which may crystallise in the equilibrium forsterite - orthopyroxene - spinel - plagioclase - liquid - vapour (see Fig. 3.3a) and has a composition An_{83}.

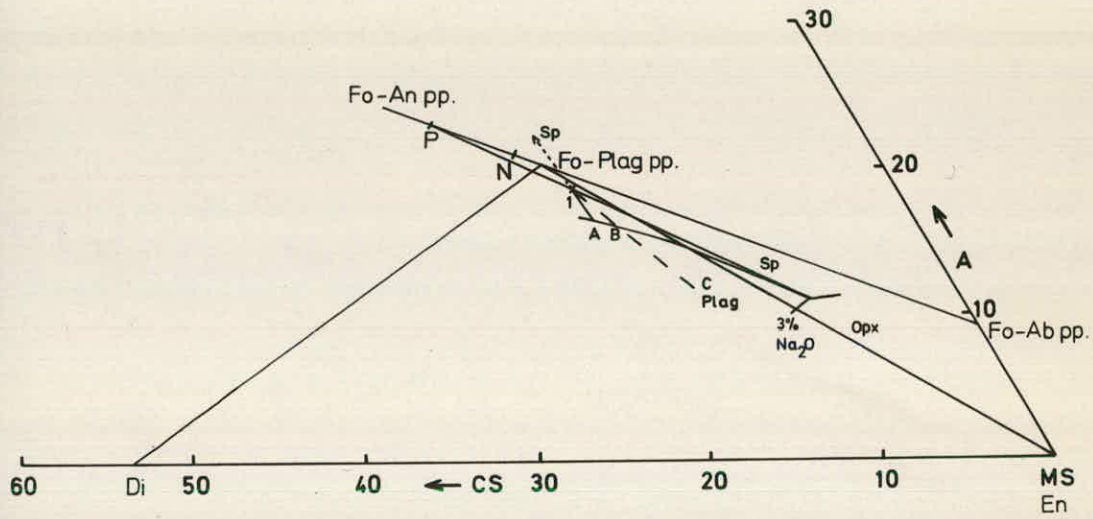
30
Fo-An pp.
P
Sp
N
Fo-Plag pp.
20
1
A B
A
Sp
C
Plag
10
3%
Na2O
Opx
Fo-Ab pp.
60
Di
50
40
CS
30
20
10
MS
En

through gel series 1 projection point with the peritectic curve) all the spinel should have disappeared and the liquid should subsequently migrate through the forsterite - plagioclase field along BC. In fact, spinel does not react out before orthopyroxene begins to crystallise (Fig. 3.4a). Hence, the extension of the tie-line joining the forsterite plus feldspar actually crystallising through gel series 1 projection point cannot intersect the forsterite - spinel - plagioclase - liquid - vapour peritectic curve. For this to occur, the plagioclase composition can be no more albitic than point P. The feldspar composition at point P is An_{83}, and hence an extremely anorthitic plagioclase must be involved in this equilibrium with a liquid containing 3% soda.

It is also possible to estimate the composition of the feldspars in some of the equilibria from other projection diagrams. This is demonstrated in Fig. F.2, which shows the phase relationships in the forsterite - orthopyroxene - vapour-saturated equilibria in the plane C - A - N. The anorthite - albite join is shown in this projection. The projection points for gel series 1 at varying soda levels are of importance and are projected onto Fig. F.2.

Gel series 1 at 0% soda (designated 1(0) in Fig. F.2) crystallises forsterite - orthopyroxene - anorthite - spinel leaving a residual liquid L. The liquid composition will remain at this point until forsterite has reacted out. (This composition is quartz-normative, see Fig. 3.4b, and so cannot crystallise completely to forsterite - orthopyroxene - spinel - anorthite.) However, as soda is added to the gel

FIG. F.2.

Plagioclase compositions.

Projection from forsterite, enstatite and vapour of equilibria saturated with these phases into the plane C - A - N (weight percent). Phase boundaries are taken from Fig. 3.15. Compositions are designated by the gel series number, and the soda content in parentheses, e.g. 1(2) refers to the gel from series 1 containing 2% soda. F1 - F5 refer to compositions of feldspars discussed in the text. P is the composition of the liquid in the equilibrium forsterite - orthopyroxene - amphibole - plagioclase - spinel - liquid - vapour under 5 kb water pressure.

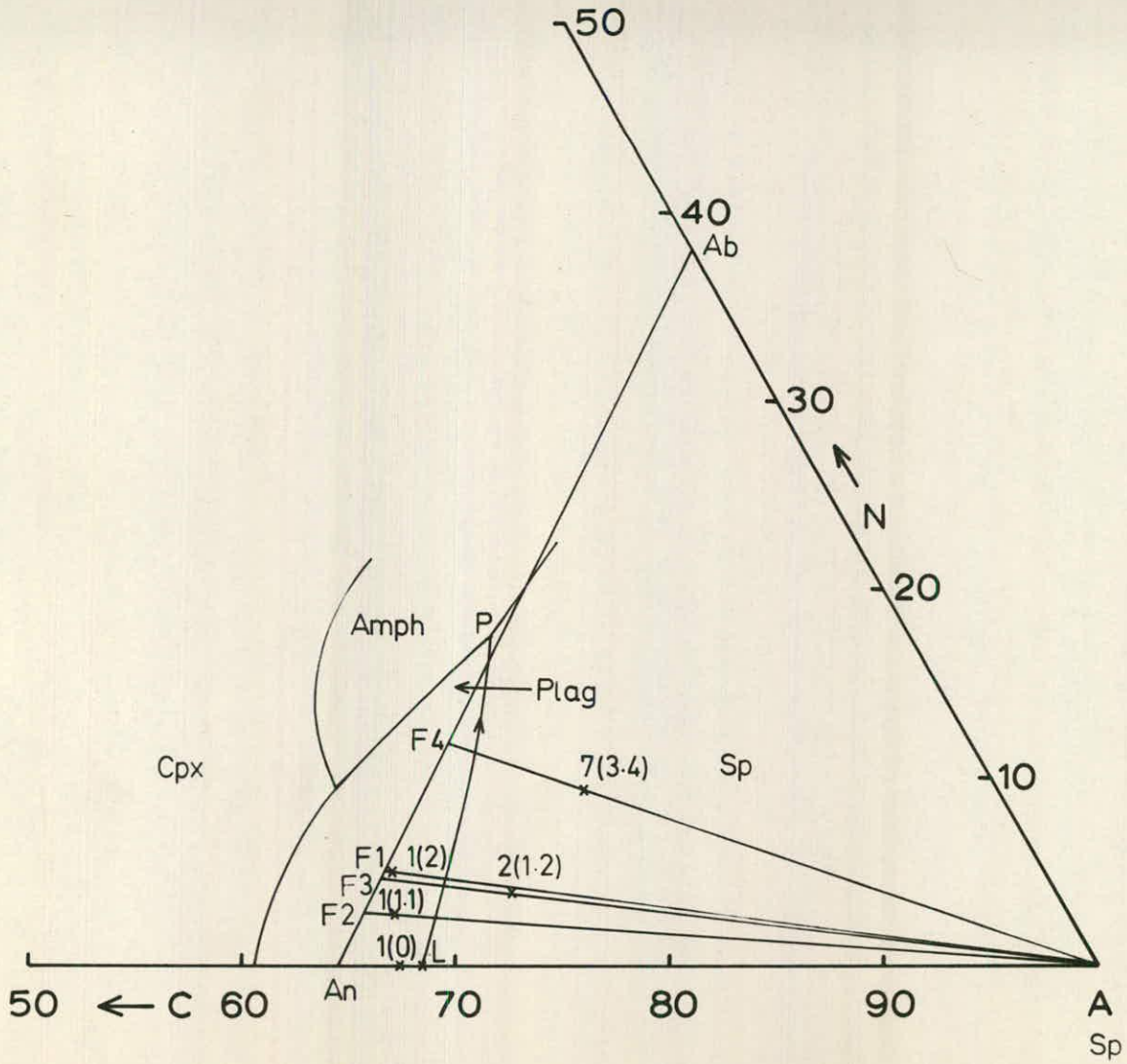
50
40
Ab
30
N
20
10
Amph
P
Plag
F4
Cpx
7(3.4)
Sp
F1
1(2)
2(1.2)
F3
1(1.1)
F2
1(0)
L
50
C
60
An
70
80
90
A
Sp

(e.g. 1(1.1) and 1(2), Fig. F.2) the composition of the crystallising feldspar becomes more albitic and the residual liquid will migrate along the forsterite - orthopyroxene - plagioclase - spinel - liquid - vapour cotectic curve from L towards point P. If during the crystallisation sequence the projection point of the gel composition intersects the tie-line joining spinel and the projection point representing the crystallising feldspar, the liquid cannot change composition further until forsterite has been completely resorbed (invalidating further use of this projection technique). Gel series 1 with 2% soda in the bulk composition (1(2)) encounters the equilibrium forsterite - orthopyroxene - plagioclase - amphibole - spinel - liquid - vapour (Fig. 3.4a). Hence the liquid composition has reached point P, and the crystallising feldspar cannot be more sodic than the point F1 (Fig. F.2).

From diagram Fig. 3.4a it is suggested that compositions in gel series 1 may reach this isobaric invariant equilibrium for bulk compositions containing greater than 1.1% soda. Hence, the composition of the feldspar must be more anorthitic than F2 (Fig. F.2.). Likewise, the data from gel series 2 suggest a slightly higher minimum soda content for bulk compositions capable of encountering this equilibrium, of 1.2% soda (Fig. 3.5a). This suggests that the feldspar must be more anorthitic than F3. The crucial point involving the intersection of the phase boundaries between spinel - plagioclase - orthopyroxene; spinel - plagioclase - orthopyroxene - forsterite and spinel - plagioclase - orthopyroxene - amphibole is less precisely located for gel

series 2 than for gel series 1 (Figs. 3.4a and 3.5a).

Because of the early disappearance of forsterite in gel series 7 (Fig. 3.8a) from bulk compositions low in soda, this gel series is less restrictive of the plagioclase composition in the equilibrium forsterite - orthopyroxene - spinel - plagioclase - amphibole - liquid - vapour. This equilibrium is observed only at soda contents in the bulk composition greater than 3.4% and hence suggests that the feldspar must be more anorthitic than composition F4 in Fig. F.2.

F2 has a composition An_{87}, and this is thought to represent the most sodic plagioclase possible in the above equilibrium. The accuracy of this calculation depends upon a precise knowledge of the lowest soda content for a particular gel series which may crystallise this assemblage. From geometrical considerations the run data for gel series 1 are thought to locate this minimum value with reasonable accuracy. However, even if this minimum value were as high as 2% soda for gel series 1, which is extremely improbable according to Fig. 3.4a, the feldspar would still have to be more anorthitic than composition F1, which is An_{78}. It can be confidently stated that the feldspar in the equilibrium forsterite - orthopyroxene - amphibole - plagioclase - spinel - liquid - vapour must be extremely anorthitic.

Similar arguments may be used with Fig. F.3 to estimate the composition of the feldspar in the equilibrium forsterite - clinopyroxene - orthopyroxene - plagioclase - amphibole - liquid - vapour. The data from gel series 3, 9 and 10 are

FIG. F.3.

Plagioclase compositions.

Projection from forsterite, enstatite and vapour of equilibria saturated with these phases into the plane C - A - N (weight percent). Phase boundaries are taken from Fig. 3.15. Compositions are designated by the gel series number, and the soda content in parentheses, e.g. 3(1.5) refers to the gel from series 3 containing 1.5% soda. A1-A3 are compositions of feldspars referred to in the text. Q is the composition of the liquid in the equilibrium forsterite - clinopyroxene - orthopyroxene - amphibole - plagioclase - liquid - vapour under 5 kb water pressure. Cpx (10a) is the projection of the composition of the clinopyroxene analysed from gel 10a at 939°C (Table 3.3B).

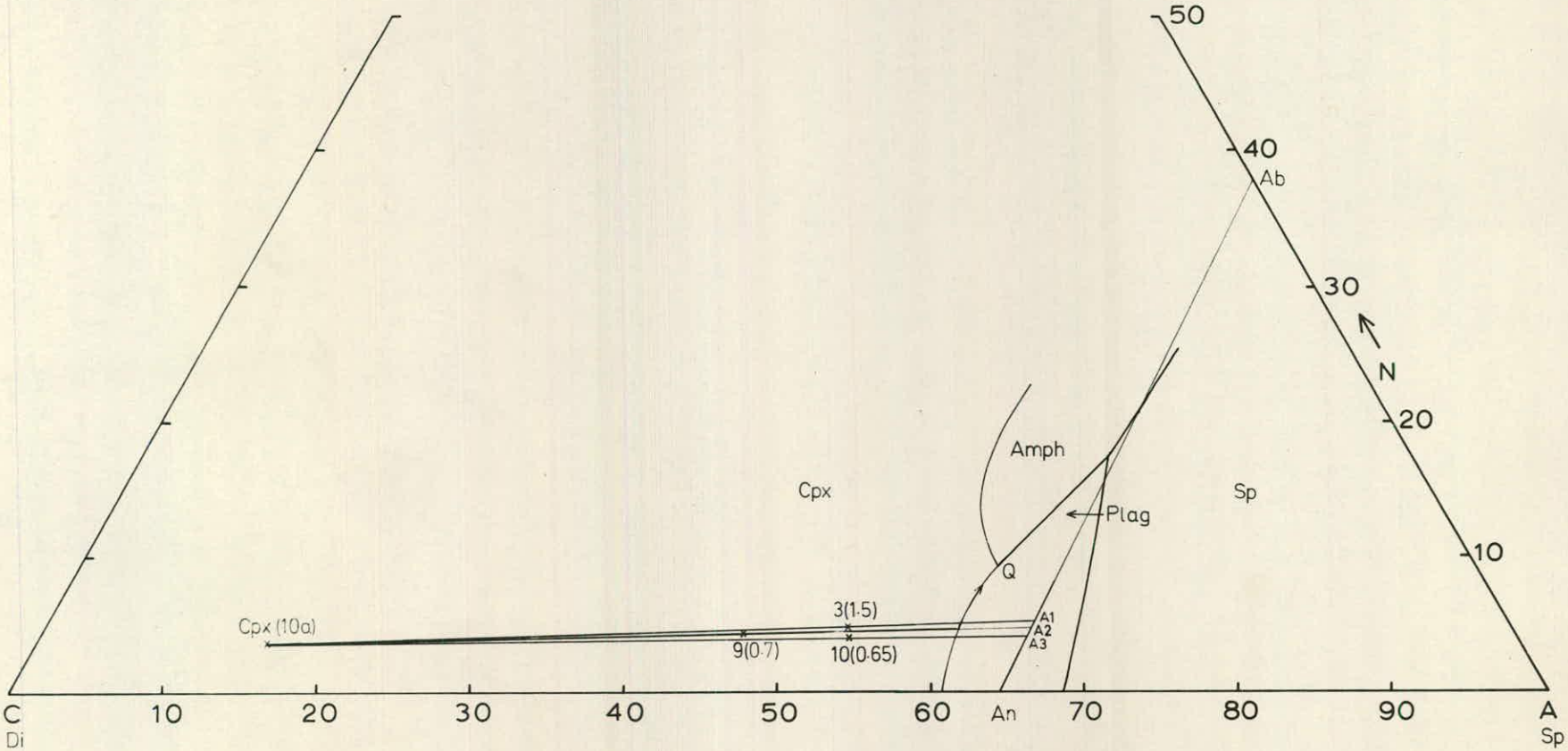
50
40
Ab
30
N
20
10
Amph
Cpx
Sp
Plag
Q
3(1·5)
A1
A2
A3
Cpx (10a)
9(0·7)
10(0·65)
C
Di
10
20
30
40
50
60
An
70
80
90
A
Sp

used for this geometrical construction. The minimum soda levels of these gel series for which the required equilibrium is encountered are 1.5, 0.7 and 0.65% respectively (Figs. 3.6a, 3.9a and 3.10a), and these compositions are shown in Fig. F.3 (3(1.5), 9(0.7) and 10(0.65)). The crucial tie-lines in this equilibrium are those joining clinopyroxene and plagioclase. The composition of the clinopyroxene will change slightly as the equilibrium liquid migrates towards Q, but the analysed clinopyroxene from gel 10a at 939°C (Table 3.3) is used in this diagram as it occurs in an equilibrium close to that desired.

The limiting feldspar compositions for which these three gel series may crystallise the required assemblage and produce a liquid Q are shown on Fig. F.3 as A1, A2 and A3. These are the most sodic compositions possible, and do not necessarily define the actual feldspar composition. The most anorthitic of these is A3, which has a composition An_{82}.

However, reference to Fig. 3.20 demonstrates that the feldspar in the equilibrium forsterite - two pyroxenes - amphibole - plagioclase - liquid - vapour must be more anorthitic than that in the equilibrium forsterite - orthopyroxene - plagioclase - amphibole - spinel - liquid - vapour. If this were not so there would be intersecting tie-planes for equilibria stable under the same conditions, which is not permissible. Hence, the composition of the feldspar in equilibrium with the former assemblage must be more anorthitic than An_{87}. The reason gel series 3, 9 and 10 do not indicate such a composition is partly because of

the lack of diagnostic data in the appropriate region of the diagrams, and because in compositions with very low soda levels forsterite disappears before the isobaric invariant equilibrium is encountered.

REFERENCES

ANDERSEN, O. 1915. The system anorthite-forsterite-silica. Am. J. Sci., 39, 407-454.

AOKI, K. 1963. The kaersutites and oxykaersutites from alkalic rocks of Japan and surrounding areas. J. Petrology, 4, 198-210.

AOKI, K. 1968. Petrogenesis of ultrabasic and basic inclusions in alkali basalts, Iki Island, Japan. Am. Miner., 53, pp.241-256.

AOKI, K. 1970. Petrology of kaersutite-bearing ultramafic and mafic inclusions in Iki Island, Japan. Contr. Mineral. Petrol., 25, 270-283.

AOKI, K. 1971. Petrology of mafic inclusions from Itinome-gata, Japan. Contr. Mineral. Petrol., 30, 314-331.

BAKER, P.E. 1968. Petrology of Mt. Misery volcano, St. Kitts, West Indies. Lithos, 1, 124-148.

BEST, M.G. 1969. Differentiation of calc-alkaline magmas, 65-73. in A.R. McBirney, ed., Proceedings of the Andesite Conference, State of Oregon, Bull. Dept. Geol. Mineral. Ind., 65, 193pp.

BEST, M.G. 1970. Kaersutite-peridotite inclusions and kindred megacrysts in basanitic lavas, Grand Canyon, Arizona. Contr. Mineral. Petrol., 27, 25-44.

BEST, M.G. & MERCY, E.L.P. 1967. Composition and crystallisation of mafic minerals in the Guadalupe igneous complex, California. Am. Miner., 52, 436-474.

BINNS, R.A., DUGGAN, M.B. & WILKINSON, J.F.G. 1970. High pressure megacrysts in alkaline lavas from northwestern New South Wales. Am. J. Sci., 269, 132-168.

BORISENKO, L.F. 1967. Trace elements in pyroxenes and amphiboles from ultramafic rocks in the Urals. Mineralog. Mag., 36, 403-410.

BORLEY, G.D., SUDDABY, P. & SCOTT, P. 1971. Some xenoliths from alkalic rocks of Teneriffe, Canary Islands, Contr. Mineral. Petrol., 31, 102-114.

BOWEN, N.L. 1917. The problem of the anorthosites. J. Geol., 25, 209-243.

BOYD, F.R. 1959. Hydrothermal investigations of amphiboles, 377-396. In P.H. Abelson, ed., Researches in Geochemistry, John Wiley & Sons, New York, Vol. 1, 511pp.

BRIDGEWATER, D. & HARRY, W.T. 1968. Anorthosite xenoliths and plagioclase megacrysts in precambrian intrusions of South Greenland. Medd. Grøn., 185, 1-237.

BROWN, G.M. 1967. Mineralogy of basaltic rocks. In Basalts, ed. H.H. Hess & A. Poldervaart, Interscience Publishers, 1, 103-153.

BROWN, G.M. & SCHAIRER, J.F. 1968. Melting relations of some calc-alkaline volcanic rocks. Carnegie Instn. Wash. Yb., 66, 460-467.

BROWN, G.M. & SCHAIRER, J.F. 1971. Chemical and melting relations of some calc-alkaline volcanic rocks. Geol. Soc. Am. Mem., 130, 139-156.

BUDDINGTON, A.F. 1961. The origin of anorthosite re-evaluated. Geol. Surv. India Rep., 86, 421-432.

BULTITUDE, R.J. & GREEN, D.H. 1967. Experimental study at high pressures on the origin of olivine nephelinites and olivine melilite nephelinite magmas. Earth Planet. Sci. Lett., 3, 325-337.

CARMICHAEL, I.S.E. 1964. The petrology of Thingmuli, a Tertiary volcano in Eastern Iceland. J. Petrol., 5, 435-460.

CATTERMOLE, P. 1969. A preliminary geochemical study of the Myndd Penarfynydd intrusion, Rhiw igneous complex, south-west Lleyn, in The Precambrian and Lower Palaeozoic rocks of Wales, ed., A. Wood, University of Wales Press, 435-446.

CAWTHORN, R.G., CURRAN, E.B. & ARCULUS, R.J. 1973. A petrogenetic model for the origin of the calc-alkaline suite of Grenada, Lesser Antilles. J. Petrology, 14, 327-337.

CHAYES, F. 1969. The chemical composition of Cenozoic andesite, 1-12. in A.R. McBirney, ed., Proceedings of the Andesite Conference, State of Oregon, Bull. Dept. Geol. Mineral. Ind., 65, 193pp.

CHURCH, W.R. & STEVENS, R.K. 1971. Early Palaeozoic ophiolite complexes of the Newfoundland Appalachians as mantle-oceanic crust sequences. J. Geophys. Res., 76, 1460-1466.

CLARK, S.P., Jr. 1966. Handbook of physical constants. Geol. Soc. Am. Mem., 97, 415-436.

CLARKE, D.B. 1970. Tertiary basalts of Baffin Bay: possible primary magma from the mantle. Contr. Mineral. Petrol., 25, 203-224.

COE, K. 1966. Intrusive tuffs of West Cork, Ireland. Q. Jl. geol. Soc. Lond., 122, 1-28.

COLEMAN, R.G. 1971. Plate tectonic emplacement of upper mantle peridotites along continental edges. J. Geophys. Res., 76, 1212-1222.

COLLÉE, A.L.G. 1963. A fabric study of lherzolites with special reference to ultrabasic nodular inclusions in the lavas of Auvergne (France). Leidse. Geol. Med., 28, 1-102.

CONQUÉRÉ, F. 1971. La lherzolite à amphibole du gisement de Caussau (Ariège, France). Contr. Mineral. Petrol., 30, 296-313.

DAWSON, J.B., POWELL, D.G. & REID, A.M. 1970. Ultrabasic xenoliths and lava from the Lashaine volcano, Northern Tanzania. J. Petrology, 11, 519-548.

DAWSON, J.B. & SMITH, J.V. 1973. Alkalic pyroxenite xenoliths from the Lashaine volcano, Northern Tanzania. J. Petrology, 14, 113-131.

DEWEY, J.F. & BIRD, J.M. 1971. Origin and emplacement of the ophiolitic suite: Appalachian ophiolites in Newfoundland. J. Geophys. Res., 76, 3179-3206.

EGGLER, D.H. 1972a. Water-saturated and undersaturated melting relations in a Paracutin andesite and an estimate of water content in the natural magma. Contr. Mineral. Petrol., 34, 261-271.

EGGLER, D.H. 1972b. Amphibole stability in H_2O-undersaturated calc-alkaline melts. Earth Planet. Sci. Lett., 15, 28-34.

EMSLIE, R.F. 1968. Crystallisation and differentiation of the Michikamau intrusion, in Y.W. Isachsen, ed., Origin of anorthosite and related rocks, Univ. State New York, Albany, New York, Mem. 18, 163-174.

ERNST, W.G. 1966. Synthesis and stability relations of ferrotremolite. Am. J. Sci., 264, 37-65.

FITTON, J.G. 1971. The generation of magma in island arcs. Earth Planet. Sci. Letters, 11, 63-67.

FORD, C.E. 1972. Furnace design, temperature distribution, calibration and seal design in internally heated, pressure vessels. Prog. in Expt. Petrology, 2, N.E.R.C., London, 89-96.

FORD, C.E. & O'HARA, M.J. 1972. The system $MgSiO_3$ - $Ca_3Al_2Si_3O_{12}$ - H_2O. Prog. in Expt. Petrology, 2, N.E.R.C., London, 151-153.

FUDALI, R.F. & MELSON, W.G. 1972. Ejecta velocities, magma chamber pressure and kinetic energy associated with the 1968 eruption of Arenal volcano. Bull. Volcan., 35, 383-401.

GASS, I.G., MALLICK, D.I.J. & COX, K.G. 1965. Royal Society volcanological expedition to the South Arabian Federation and the Red Sea. Nature, 205, 952-955.

GILBERT, M.C. 1966. Synthesis and stability relations of the hornblende ferropargasite. Am. J. Sci., 264, 698-742.

GILBERT, M.C. 1968. Reconnaissance study of the stability of amphiboles at high pressure. Carnegie Instn. Wash. Yb., 67, 167-170.

GREEN, D.H. 1969. The origin of basaltic and nephelinitic magmas in the earth's mantle. Tectonophysics, 7, 409-422.

GREEN, D.H. 1971. Basaltic magmas as indicators of conditions of origin: application to oceanic volcanism. Phil. Trans. R. Soc., A., 268, 707-725.

GREEN, D.H. & RINGWOOD, A.E. 1963. Mineral assemblages in a model mantle composition. J. Geophys. Res., 68, 937-944.

GREEN, D.H. & RINGWOOD, A.E. 1967a. An experimental investigation of the gabbro to eclogite transformation and its petrological applications. Geochim. cosmochim. Acta, 31, 767-833.

GREEN, D.H. & RINGWOOD, A.E. 1967b. The genesis of basaltic magmas. Contr. Mineral. Petrol., 15, 103-190.

GREEN, D.H. & RINGWOOD, A.E. 1970. Mineralogy of peridotitic compositions under upper mantle conditions. Phys. Earth Planet. Interiors, 3, 359-371.

GREEN, T.H. 1968. Experimental fractional crystallisation of quartz diorite and its application to the problem of anorthosite origin, in Y.W. Isachsen, ed., Origin of anorthosite and related rocks, Univ. State New York, Albany, New York, Mem. 18, 23-30.

GREEN, T.H. & RINGWOOD, A.E. 1966. Origin of the calc-alkaline igneous rock suite. Earth Planet. Sci. Letters, 1, 307-316.

GREEN, T.H. & RINGWOOD, A.E. 1968. Genesis of the calc-alkaline igneous rock suite. Contr. Mineral. Petrol., 18, 105-162.

GREENWOOD, H.J. 1963. The synthesis and stability of anthophyllite. J. Petrology, 4, 317-351.

HALL, A. 1967. The chemistry of appinitic rocks associated with the Ardara pluton, Donegal, Ireland. Contr. Mineral. Petrol., 16, 156-171.

HAMILTON, D.L., BURNHAM, C.W. & OSBORN, E.F. 1964. The solubility of water and effects of oxygen fugacity and water content on crystallisation in mafic magmas. J. Petrology, 5, 21-39.

HAMILTON, W. 1964. Origin of high-alumina basalt, andesite and dacite magmas. Science, 146, 635-637.

HAWKINS, T.R.W. 1965. A note on the rhythmic layering in hornblende-rich picrite and dolerite intrusions, near Rhiw, Caernarvonshire. Geol. Mag., 102, 222-226.

HAWKINS, T.R.W. 1970. Hornblende gabbros and picrites at Rhiw, Caernarvonshire. J. Geol. 7, 1-24.

HEATH, S.A. & FAIRBAIRN, H.W. 1968. Sr^{87}/Sr^{86} ratios in anorthosites and some associated rocks, in Y.W. Isachsen, ed., Origin of anorthosite and related rocks, Univ. State New York, Albany, New York, Mem. 18, 99-110.

HOLLOWAY, J.R. & BURNHAM, C.W. 1972. Melting relations of basalt with equilibrium water pressure less than total pressure. J. Petrology, 13, 1-29.

ISACHSEN, Y.W. 1968. Origin of anorthosite and related rocks - a summarization, in Y.W. Isachsen, ed., Origin of anorthosite and related rocks, Univ. State New York, Albany, New York, Mem. 18, 435-446.

JAMIESON, B.G. 1969. Natural rock projection into a pseudo-quaternary system. Prog. in Expt. Petrology, 1, N.E.R.C., London, 152-155.

KUNO, H. 1967. Volcanological and petrological evidences regarding the nature of the upper mantle. in T.F. Gaskell, ed., The earth's mantle, Academic Press, London & New York, 89-109.

KUNO, H. 1968. Origin of andesite and its bearing on the island arc structure. Bull. volcan., 32, 141-173.

KUSHIRO, I. 1970. Systems bearing on melting of the upper mantle under hydrous conditions. Carnegie Instn. Wash. Yb., 68, 240-247.

KUSHIRO, I. 1972. Effect of water on the composition of magmas formed at high pressures. J. Petrology, 13, 311-334.

KUSHIRO, I. & ERLANK, A.J. 1970. Stability of potassic richterite, Carnegie Instn. Wash. Yb., 68, 231-233.

KUSHIRO, I. & YODER, H.S., Jr. 1966. Anorthite-forsterite and anorthite-enstatite reactions and their bearing on the basalt-eclogite transformation. J. Petrol., 7, 337-362.

KUSHIRO, I. & YODER, H.S., Jr. 1972. Origin of calc-alkalic peraluminous andesite and dacites. Carnegie Instn. Wash. Yb, 71, 411-413.

LAMBERT, I.B. & WYLLIE, P.J. 1968. Stability of hornblende and a model for the low velocity zone. Nature, 219, 1240-1241.

LAMBERT, I.B. & WYLLIE, P.J. 1972. Melting of gabbro (quartz eclogite) with excess water to 35 kb, with geological applications. J. Geol., 80, 693-706.

LEAKE, B.E. 1970. The fragmentation of the Connemara basic and ultrabasic intrusions. in G. Newall & N. Rast, eds. Mechanism of igneous intrusion, Gallery Press, 103-121.

LeMAITRE, R.W. 1969. Kaersutite-bearing plutonic xenoliths from Tristan da Cunha, South Atlantic, Mineralog. Mag., 37, 185-197.

LENSCH, G. 1968. Die ultramafitite der zone von Ivrea und ihre geologische interpretation. Schweiz. miner. petrogr. Mitt., 48, 91-102.

LETTENEY, C.D. 1968. The anorthosite-norite-charnockite series of the Thirteenth Lake Dome, south-central Adirondacks, in Y.W. Isachsen, ed., Origin of anorthosite and related rocks, Univ. State New York, Albany, New York, Mem. 18, 329-342.

LEWIS, J.F. 1969. Composition, physical properties and origin of the sodic anorthites from the ejected plutonic blocks of the Soufrière volcano, St. Vincent, West Indies. Contr. Mineral. Petrol., 21, 272-294.

LEWIS, J.F. 1973. Petrology of the ejected plutonic blocks of the Soufrière volcano, St. Vincent, West Indies. J. Petrology, 14, 81-112.

LUTH, W.C. & SIMMONS, G. 1968. Melting relations in natural anorthosite, in Y.W. Isachsen, ed., Origin of anorthosite and related rocks, Univ. State New York, Albany, New York, Mem. 18, 31-38.

LUTH, W.C. & TUTTLE, O.F. 1969. The hydrous vapour phase in equilibrium with granite and granite magmas. Geol. Soc. Am. Mem., 115, 513-548.

MASON, B. 1966. Pyrope, augite, and hornblende from Kakanui, New Zealand. N.Z. J. Geol. Geophys., 9, 474-480.

MASON, B. 1968. Kaersutite from San Carlos, Arizona, with comments on the paragenesis of this mineral. Mineralog. Mag., 36, 997-1002.

McBIRNEY, A.R. 1969. Compositional variations in Cenozoic calc-alkaline suites of Central America, 185-189. in A.R. McBirney, ed., Proceedings of the Andesite Conference, State of Oregon, Bull. Dept. Geol. Mineral. Ind., 65, 193pp.

MELSON, W.G. & JAROSEWICH, E. 1967. St. Peter and St. Paul rocks: a high temperature, mantle-derived intrusion. Science, 155, 1532-1535.

MICHOT, J. & MICHOT, P. 1968. The problem of anorthosites: The south-Rogaland igneous complex, southwestern Norway, in Y.W. Isachsen, ed., Univ. State New York, Albany, New York, Mem. 18, 399-410.

MODRESKI, P.J. 1972. The melting of phlogopite in the presence of enstatite, aluminous enstatite, diopside, spinel, corundum and pyrope. Carnegie Instn. Wash. Yb., 71, 392-396.

MOORES, E.M. 1969. Petrology and structure of the Vourinos ophiolite complex of northern Greece. Geol. Soc. Am. Spec. Pap., 118, 74pp.

MOORES, E. 1970. Ultramafics of orogeny with models of the U.S. Cordillera and the Tethys. Nature, 228, 837-842.

NAKAMURA, Y. 1971. Petrology of the Toba ultrabasic complex, Mie prefracture, central Japan. J. Fac. Sci. Univ. Tokyo, 18, 1-51.

NICHOLLS, G.D. 1967. Geochemical studies in the ocean as evidence for the composition of the mantle. in S.K. Runcorn, Mantles of the Earth and Terrestrial Planets, Interscience, J. Wiley and Sons, 285-303.

NISHIKAWA, M., KUSHIRO, I. & UYEDA, S. 1971. Stability of natural hornblende at high water pressures: preliminary experiments. Jap. J. Geol. Geogr., 41, 41-50.

NOCKOLDS, S.R. & ALLEN, R. 1953. The geochemistry of some igneous rock series. Geochim. Cosmochim. Acta, 4, 105-142.

O'HARA, M.J. 1965. Primary magmas and the origin of basalts. Scott. J. Geol., 1, 19-39.

O'HARA, M.J. 1967. Mineral facies in ultrabasic rocks. in P.J. Wyllie, ed., Ultramafic and Related Rocks, J. Wiley and Sons, 7-18.

O'HARA, M.J. 1968. The bearing of phase equilibria studies in synthetic and natural systems on the origin and evolution of basic and ultrabasic rocks. Earth Sci. Rev., 4, 69-133.

O'HARA, M.J. & BIGGAR, G.M. 1969. Diopside + spinel equilibria, anorthite and forsterite reaction relationships in silica-poor liquids in the system $CaO-MgO-Al_2O_3-SiO_2$ at atmospheric pressure, and their bearing on the genesis of melilites and nephelinites. Am. J. Sci., 267-A, 364-390.

OLMSTED, J.F. 1968. Petrology of the Mineral Lake intrusion, northwest Wisconsin, in Y.W. Isachsen, ed., Origin of anorthosite and related rocks, Univ. State New York, Albany, New York, Mem. 18, 149-162.

OSBORN, E.F. 1959. Role of oxygen pressure in the crystallisation and differentiation of basaltic magma. Am. J. Sci., 257, 607-647.

OSBORN, E.F. 1962. Reaction series for subalkaline igneous rocks based on different oxygen pressure conditions. Am. Miner., 47, 211-226.

OSBORN, E.F. 1969. The complementariness of orogenic andesite and alpine peridotite. Geochim. cosmochim. Acta, 33, 307-323.

OXBURGH, E.R. 1964. Petrological evidence for the presence of amphibole in the upper mantle and its petrogenetic and geophysical implications. Geol. Mag., 101, 1-19.

OXBURGH, E.R. & TURCOTTE, D.L. 1968. Problem of high heat flow and volcanism associated with zones of descending mantle convective flow. Nature, 218, 1041-1043.

PHILPOTTS, A.R. 1966. Origin of the anorthosite-mangerite rocks in southern Quebec. J. Petrology, 7, 1-64.

PHILPOTTS, A.R. 1968. Parental magma of the anorthosite-mangerite suite, in Y.W. Isachsen, ed., Origin or anorthosite and related rocks, Univ. State New York, Albany, New York, Mem. 18, 207-212.

PHINNEY, W.C. 1968. Anorthosite occurrences in Keweenawan rocks of northeastern Minnesota, in Y.W. Isachsen, ed., Origin of anorthosite and related rocks, Univ. State New York, Albany, New York, Mem. 18, 135-148.

RINGWOOD, A.E. 1966. The chemical composition and origin of the earth in P.M. Hurley, ed., Advances in Earth Sciences, M.I.T. Press, Cambridge, Mass., 287-399.

RUBEY, W.W. 1951. Geologic history of sea water. An attempt to state the problem. Bull. Geol. Soc. Am., 62, 1111-1148.

RUCKMICK, J.C. & NOBLE, J.A. 1959. Origin of the ultramafic complex at Union Bay, S.E. Alaska. Bull. Geol. Soc. Am., 70, 981-1018.

TAYLOR, S.R. 1969. Trace element chemistry of andesites and associated calc-alkaline rocks, 43-63. in A.R. McBirney, ed., Proceedings of the Andesite Conference, State of Oregon, Bull. Dept. Geol. Mineral. Ind., 65, 193pp.

TAYLOR, S.R., KAYE, M., WHITE, A.J.R., DUNCAN, A.R., EWART, A. 1969a. Genetic significance of Co, Cr, Ni, Sc. and V contents of andesites. Geochim. Cosmochim. Acta, 33, 275-284.

TAYLOR, S.R., KAYE, M., WHITE, A.J.R., DUNCAN, A.R. AND EWART, A. 1969b. Genetic significance of V and Ni contents of andesites: Reply to Prof, E.F. Osborn. Geochim. Cosmochim. Acta, 33, 1555-1556.

TILLEY, C.E. 1950. Some aspects of magmatic evolution. Q. Jl. geol. Soc. Lond. 106, 37-61.

TILLEY, C.E. & LONG, J.V.P. 1967. The porphyroclast minerals of the peridotite-mylonites of St. Paul's Rocks (Atlantic). Geol. Mag., 104, 46-48.

TRASK, N.J. 1969. Ultramafic xenoliths in basalt, Nye Country, Nevada. U.S. geol. Surv. Prof. Pap., 650-D, 43-48.

VARNE, R. 1970. Hornblende lherzolite in the upper mantle. Contr. Mineral. Petrol., 27, 45-51.

VOGT, P. 1962. Geologisch-petrographische untersuchungen im peridotitstock von Finero. Schweiz. miner. petrogr. Mitt., 42, 59-125.

WAGER, L.R. 1962. Igneous cumulates from the 1902 eruption of Soufrière, St. Vincent. Bull. volcan., 24, 93-99.

WESTOLL, N.D.S. 1968. The petrology of kentallenite. Ph.D. Thesis, Edinburgh Univ., 70pp.

WILKINSON, J.F.G. 1961. Some aspects of calciferous amphiboles, oxyhornblende, kaersutite and barkevikite. Am. Miner., 46, 340-354.

WILLIAMS, H. 1971. Mafic ultramafic complexes in Western Newfoundland Appalachians and the evidence for their transportation: A review and interim report. Geol. Assoc. Canada Proc., 24, 9-27.

WRIGHT, T.L. & DOCHERTY, P.C. 1970. A linear programming and least-squares computer method for solving petrologic mixing problems. Bull, Geol. Soc. Am., 81, 1995-2008.

WYLLIE, P.J. 1970. Ultramafic rocks and the upper mantle. Min. Soc. Am. Spec. Pap., 3, 3-32.

YAMAZAKI, T., ONUKI, H. & TIBA, T. 1966. Significance of hornblende gabbroic inclusions in calc-alkaline rocks. J. Jap. Ass. Miner. Petrol. Econ. Geol., 55, 87-103.

YODER, H.S., Jr. 1965. Diopside-anorthite-water at 5 and 10 kb and its bearing on explosive volcanism. Carnegie Instn. Wash. Yb., 64, 82-89.

YODER, H.S., Jr. 1966. Anorthite-forsterite-H_2O. Carnegie Instn. Wash. Yb., 65, 274-278.

YODER, H.S., Jr. 1969. Calc-alkaline andesites: Experimental data bearing on the origin of their assumed characteristics, 77-89. in A.R. McBirney, ed., Proceedings of the Andesite Conference, Bull. Dept. Geol. Mineral. Ind., 65, 193pp.

YODER, H.S., Jr. & CHINNER, G.A. 1960. Grossularite-pyrope-water system at 10,000 bars. Carnegie Instn. Wash. Yb., 59, 78-81.

YODER, H.S., Jr. & DICKEY, J.S., Jr. 1971. Diopside-pyrope at P_{H_2O} = 5 kb and its bearing on spinel problems. Carnegie Instn. Wash. Yb., 70, 122-125.

YODER, H.S., Jr. & TILLEY, C.E. 1962. Origin of basalt magmas: an experimental study of natural and synthetic rock systems. J. Petrology, 3, 342-532.

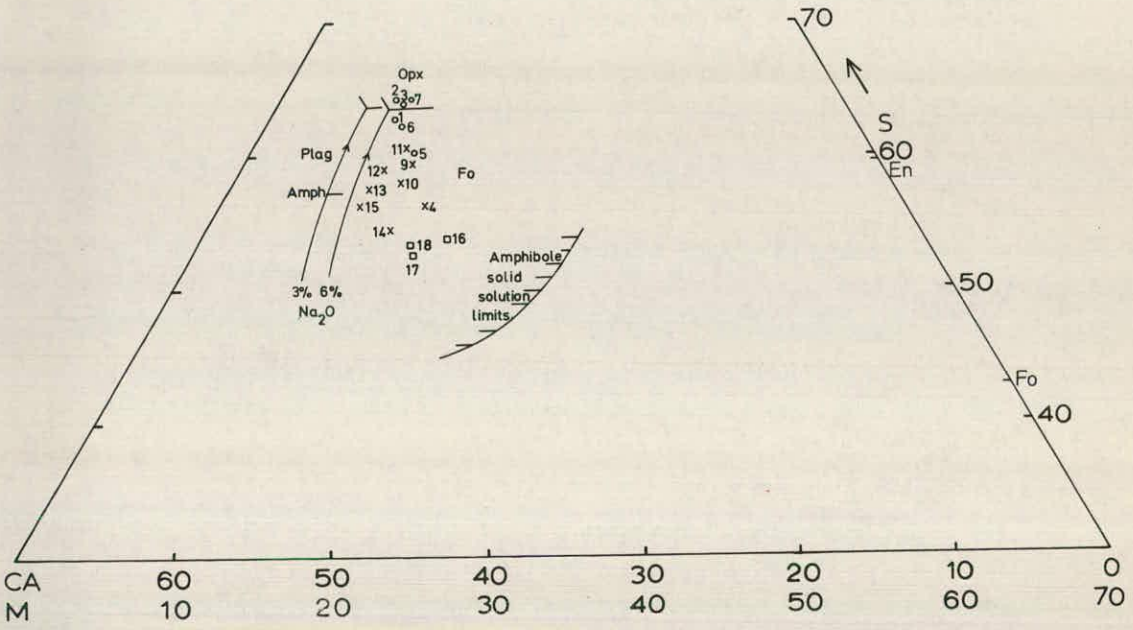
Opx
Plag
Amph
Fo
3% 6%
Na2O
Amphibole
solid
solution
limits
70
S
60
En
50
Fo
40
CA
M
60 10
50 20
40 30
30 40
20 50
10 60
0 70

FIG. 3.11

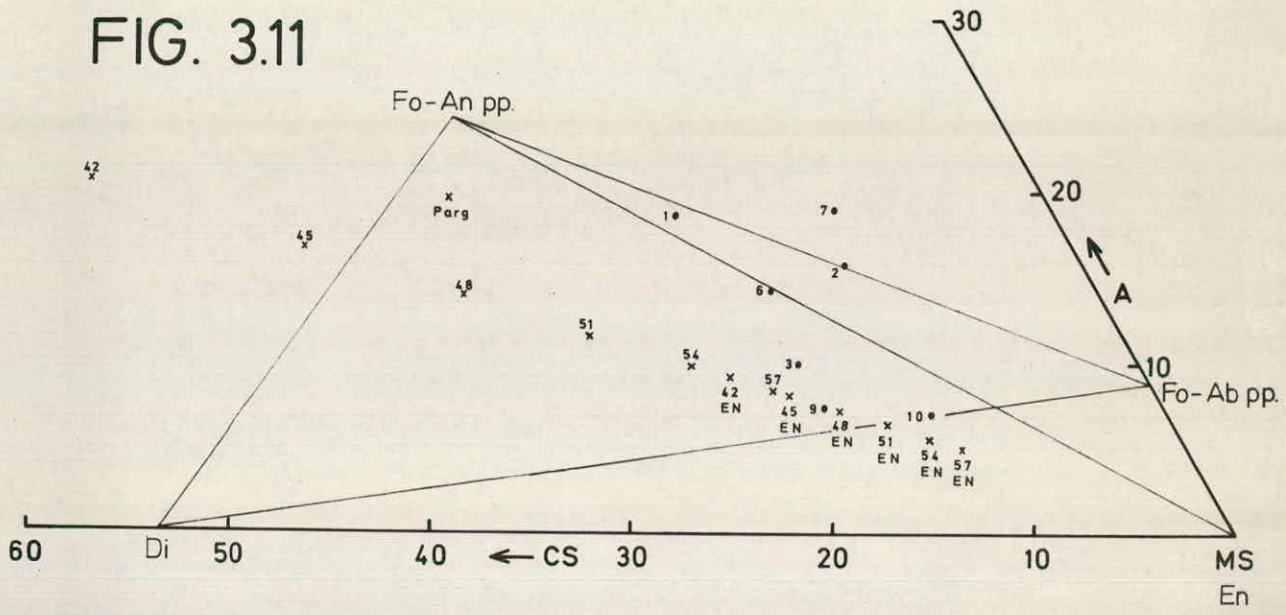
Fo-An pp.
30
20
10
A
Fo-Ab pp.
Parg
42
45
48
51
54
57
42
EN
45
EN
48
EN
51
EN
54
EN
57
EN
1
2
3
6
7
9
10
60
Di
50
40
CS
30
20
10
MS
En

FIG. 3.13

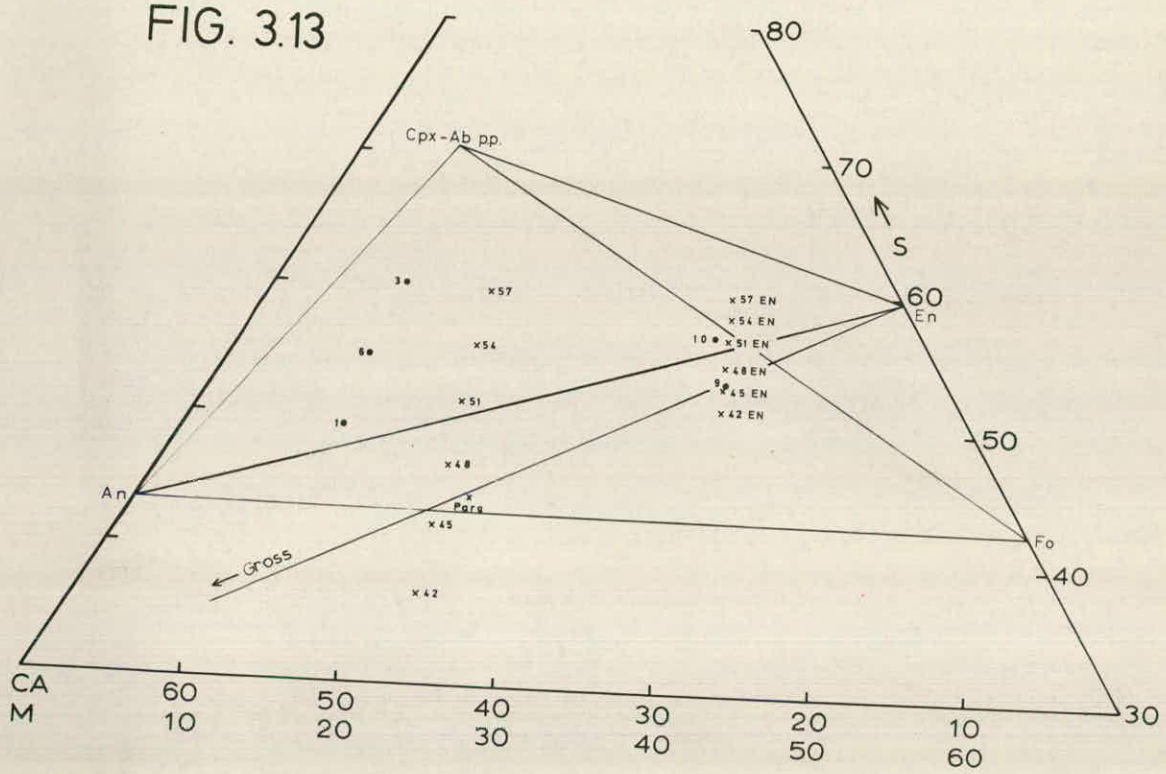
Cpx-Ab pp.
An
Fo
En
S
80
70
60
50
40
30
Gross
Pars
3●
6●
10●
8●
×57
×54
×51
×48
×45
×42
×57 EN
×54 EN
×51 EN
×48 EN
×45 EN
×42 EN
CA
M
60
10
50
20
40
30
30
40
20
50
10
60

A Petrogenetic Model for the Origin of the Calc-alkaline suite of Grenada, Lesser Antilles

by R. GRANT CAWTHORN,[1] E. B. CURRAN,[2] *and* R. J. ARCULUS[2]

[1] *Grant Institute of Geology, West Mains Road, Edinburgh EH9 3JW,* [2] *Department of Geology, University of Durham, South Road, Durham DH1 3LE*

(*Received 6 December 1972; in revised form 12 January 1973*)

ABSTRACT

Basanitoid, alkal basalt, andesite and dacite compositions from Grenada, Lesser Antilles, show a differentation trend from nepheline-normative, through hypersthene-normative to quartz-normative. This unusual sequence, in which the liquids migrate through the low-pressure thermal divide of olivine–clinopyroxene–plagioclase from critically undersaturated compositions, is interpreted from experimental and chemical data as the result of crystallization of amphibole under a hydrous pressure of several kilobars.

INTRODUCTION

THE volcanic sequence of Grenada, Lesser Antilles, includes a considerable development of basanitoid and alkali basalt lavas (Sigurdsson *et al.*, in press). These are part of a calc-alkaline series whose other members include basaltic andesites, andesites, and dacites. There is apparently a complete chemical and petrographic gradation between these various rock types. Cumulus rocks of ultramafic and basic composition, some of which are entirely or predominantly amphibole, occur as nodules in lavas and as blocks in reworked tuffs. The petrology and chemistry of similar blocks from St. Vincent, a major volcanic island to the north of Grenada, has been studied by Lewis (1964).

All the standard petrogenetic indicators such as decreasing $MgO/MgO+FeO+Fe_2O_3$ ratios, decreasing Ni and Cr contents, and increasing alkali and incompatible trace-element concentrations, suggest that the sequence from basanitoid to dacite is the result of fractional crystallization. This proposed liquid evolution path migrates through the low-pressure thermal divide of olivine–clinopyroxene–plagioclase (Yoder & Tilley, 1962, fig. 2) which is inexplicable by any anhydrous, low-pressure crystallization mechanism previously suggested. Furthermore, the direction of liquid migration from nepheline-normative to hypersthene-normative is the reverse of that suggested in any high-pressure crystallization mechanism (O'Hara, 1968, p. 71).

Current opinions on the origin of calc-alkaline magmas are diverse (Green & Ringwood, 1968; Hamilton, 1964; Osborn, 1969; Yoder, 1969; Kushiro, 1972; see McBirney, 1969, for general review), but there is general agreement that water content may be important in determining the characteristic evolution of

the suite. Brown & Schairer (1971) have demonstrated that inconsistencies in the experimentally determined phase relationships of the calc-alkaline suite at low pressure are to some extent resolved under the influence of water pressure.

The occurrence of amphibole-bearing nodules on Grenada strongly suggests that water is involved in the evolution of the suite. Therefore, a series of experiments was carried out to examine the stability range of amphibole in the various rock compositions and to determine the possible contribution of amphibole to the chemical variation observed. The oxygen fugacity of basaltic and andesitic magmas has been investigated by Fudali (1965). Comparable oxygen fugacity is generated by a Ni/NiO buffer at temperatures in the order of 1100 °C (Holloway & Burnham, 1972), and so this was used for controlling the experimental conditions. The experimental techniques and procedure are given in the Appendix.

EXPERIMENTAL RESULTS

The samples chosen for the experimental study are representative of the Grenada suite from basanitoid to basaltic andesite. Two basanitoids, one alkali basalt, and two basaltic andesites were used. Their major element chemistry and normative compositions are given in Table 1, together with brief petrographic descriptions.

A hydrous pressure of 5 kbs was chosen for this study because the stability of olivine, clinopyroxene, and amphibole have been shown to be fairly insensitive to small changes in pressure within the range 2–8 kb (Yoder & Tilley, 1962; Holloway & Burnham, 1972). Consequently small fluctuations in the pressure of individual runs will have little effect on the results.

The results of the experimental runs are given in Table 2 and shown diagrammatically on Fig. 1. The figure shows the order of crystallization for each composition and attempts to correlate this with the stage of evolution reached within the suite.

The liquidus temperature gradually decreases from the basanitoids to the basaltic andesites with olivine and clinopyroxene appearing almost simultaneously in all compositions except for the most siliceous basaltic andesite in which olivine is never observed. Amphibole appears at lower temperature and once it is present both olivine and clinopyroxene are in reaction relationship with the liquid. The proportion of clinopyroxene decreases with decreasing temperature while olivine is completely resorbed. The temperature range over which olivine is stable diminishes in the more silica-saturated liquid compositions, as might be expected of a mineral in reaction relationship with an evolving liquid. No attempt is made here to estimate the precise proportions of the minerals present, but the reaction relationship of both olivine and clinopyroxene after the appearance of amphibole was noted by Yoder & Tilley (1962, figs. 27–30) and by Holloway & Burnham (1972), for similar compositions and conditions. The latter give estimated modal contents.

Amphibole becomes extremely abundant only a few degrees below its upper stability limit. This is fairly constant for all the compositions examined with a very slight decrease being noted in the basaltic andesites. Comparison with the thermal stability of amphibole reported by Holloway & Burnham (op. cit.) shows that it does not change appreciably between the water saturated and

TABLE 1

Chemical compositions and norms of starting materials

	209	*184*	*286*	*201*	*198*
SiO_2	43·85	44·65	46·82	52·93	53·70
TiO_2	0·87	1·13	0·89	0·87	0·79
Al_2O_3	15·97	16·13	17·62	18·28	17·41
Fe_2O_3*	9·96	10·59	9·52	8·21	8·80
MgO	13·90	11·58	9·59	4·77	4·25
CaO	11·49	11·20	11·86	10·21	9·55
Na_2O	2·88	2·58	2·50	3·71	3·87
K_2O	0·67	1·46	0·71	0·59	1·10
TOTAL	99·59	99·32	99·51	99·57	99·47
Q	—	—	—	1·59	1·65
or	4·00	8·74	4·24	3·52	6·57
ab	4·61	5·91	16·99	31·69	33·10
an	28·97	28·50	35·14	31·78	27·18
ne	10·84	8·78	2·38	—	—
di	22·74	22·18	19·45	15·66	16·88
en	—	—	—	6·92	5·61
fs	—	—	—	3·41	3·46
fo	18·29	14·62	11·89	—	—
fa	4·32	4·22	3·84	—	—
mt	4·56	4·86	4·35	3·76	4·03
il	1·67	2·18	1·71	1·67	1·52

KEY

Figures in brackets are estimated modal percentages

209 *Basanitoid*—microphenocrysts of forsteritic olivine (20), clinopyroxene (5) and euhedral opaques (2) occur in a groundmass composed mainly of brown glass (50) with crystallites of plagioclase felspar (20).

184 *Basanitoid*—phenocrysts up to 2 mm in length of forsteritic olivine (20), zoned clinopyroxene (15) and euhedral opaques (2) occur in a vesicular, glassy groundmass (60) containing small plagioclase laths and crystallites of olivine, clinopyroxene and opaque minerals.

286 *Alkali basalt*—olivine phenocrysts (10) up to 2 mm in length, zoned clinopyroxenes (25) and opaques (5) occur in a glassy groundmass (60) containing crystallites of olivine, clinopyroxene, plagioclase felspar and opaque minerals.

201 *Basaltic andesite*—phenocrysts of concentric and oscillatory zoned plagioclase (40) with bytownite core compositions, zoned clinopyroxene (15), olivine (25), and opaque minerals (5) occur in a glassy crystalline groundmass containing small plagioclase laths.

198 *Basaltic andesite*—phenocrysts of concentric and oscillatory zoned plagioclase (50), up to 2½ mm in length, clinopyroxene (15) and iddingsitised olivines (25) together with euhedral opaques (5), occur in a coarsely crystalline plagioclase-rich groundmass.

* Total iron as Fe_2O_3. Norms calculated using ratio of FeO: Fe_2O_3 = 2.

water undersaturated conditions. Consequently, the increase in stability reported by them relative to the data of Yoder & Tilley (op. cit.) may be attributed more to the differing experimental oxygen fugacity than to the fugacity of water.

Primary magnetite has not been observed in any of the runs, despite the fairly high oxidizing conditions created by the Ni/NiO buffer (see Appendix).

However, very infrequent spinels, possibly picotite, were observed in the basanitoid compositions. These have a deep-red colour in plane polarized light.

Plagioclase was not observed until very much lower temperatures (< 950 °C), when very little liquid remained.

TABLE 2

Experimental results

Temp. °C*	*Pressure* kb*	*Time* hours	*209*	*184*	*286*	*201*	*198*
1132 ±5	5 ±0·05	2	(ol), (sp), qu, gl.	qu, gl.	qu, gl.		
1118 ±6	5 ±0·10	1	ol, cpx, (sp), qu, gl.	ol, cpx, (sp), qu, gl.	(ol), cpx, (sp), qu, gl.	qu, gl.	
1100 ±5	5 ±0·10	3	ol, cpx, qu, gl.	ol, cpx, qu, gl.	ol, cpx, qu, gl.	qu, gl.	qu, gl.
1071 ±5	5 ±0·05	6	ol, cpx, (sp), qu, gl.	buffer capsule leaked	ol, cpx, (sp), qu, gl.	(ol), cpx, qu, gl.	buffer capsule leaked
1051 ±7	5 ±0·10	7	ol, cpx, (sp), amph, qu, gl.	ol, cpx, (sp), qu, gl.	ol, cpx, qu, gl.	(ol), cpx, qu, gl.	qu, gl.
1031 ±6	5 ±0·05	5	ol, cpx, amph, qu, gl.	ol, cpx, amph, qu, gl.	ol, cpx, amph, (sp), qu, gl.	(ol), cpx, amph, qu, gl.	cpx, qu, gl.
1001 ±7	5 ±0·05	5	ol, cpx, amph, qu, gl.	ol, cpx, amph, qu, gl.	ol, cpx, amph, qu, gl.	(ol) cpx, amph, qu, gl.	cpx, amph, qu, gl.
961 ±7	5 ±0·10	20	(ol), cpx, amph, qu, gl.	(ol), cpx, amph, qu, gl.	cpx, amph, gl.	cpx, amph, qu, gl.	cpx, amph, qu, gl.
921 ±7	5 ±0·10	43	(cpx), amph, gl, plag?	cpx, amph, plag, gl.	cpx, amph, plag, gl.	cpx, amph, plag, gl.	cpx, amph, plag, gl.

Phases present: sp–spinel, ol–olivine, cpx–clinopyroxene, amph–amphibole, plag–plagioclase, qu–quenching products, gl–glass. Parentheses indicate small amount.

Vapour is assumed to be present in all runs if the outer Pt capsule remained sealed. It was not possible to identify a vapour phase in the charge.

All phases identified by optical examination and X-ray diffraction.

* 'Errors' quoted in temperature and pressure are a combination of: (1) actual measured fluctuations in conditions during the course of the run; (2) uncertainty between real conditions and apparent measured conditions; (3) limits of precision of equipment.

MINERAL COMPOSITIONS

Electron-microprobe analysis of the various minerals and glasses was undertaken to determine changes of composition with varying temperature and differing starting materials. The results are given in Table 3. Except for the expected change in the iron to magnesium ratio of the minerals, their compositions remain fairly constant.

Olivine

Olivine is never very abundant. Some are thought to be relic grains from the original charge. These have irregular outlines and sometimes contain minute opaques as if the olivine stable under the experimental conditions were more forsteritic than the natural phenocrysts in the erupted rock. Alternatively, differing oxygen fugacities between experimental and natural conditions could explain this phenomenon (Roedder & Emslie, 1970). Longer duration runs may permit complete recrystallization of such grains. However, this would

introduce larger errors as a result of iron loss to the capsule. The compromise adopted here is not thought to introduce any significant errors. The analysed olivines have compositions from Fo_{82}–Fo_{85}, the more iron-rich occurring surprisingly at higher temperature for the same starting material. However, this is a small compositional variation and may be due to analytical error, or to varying amounts of iron lost to the capsule during the run.

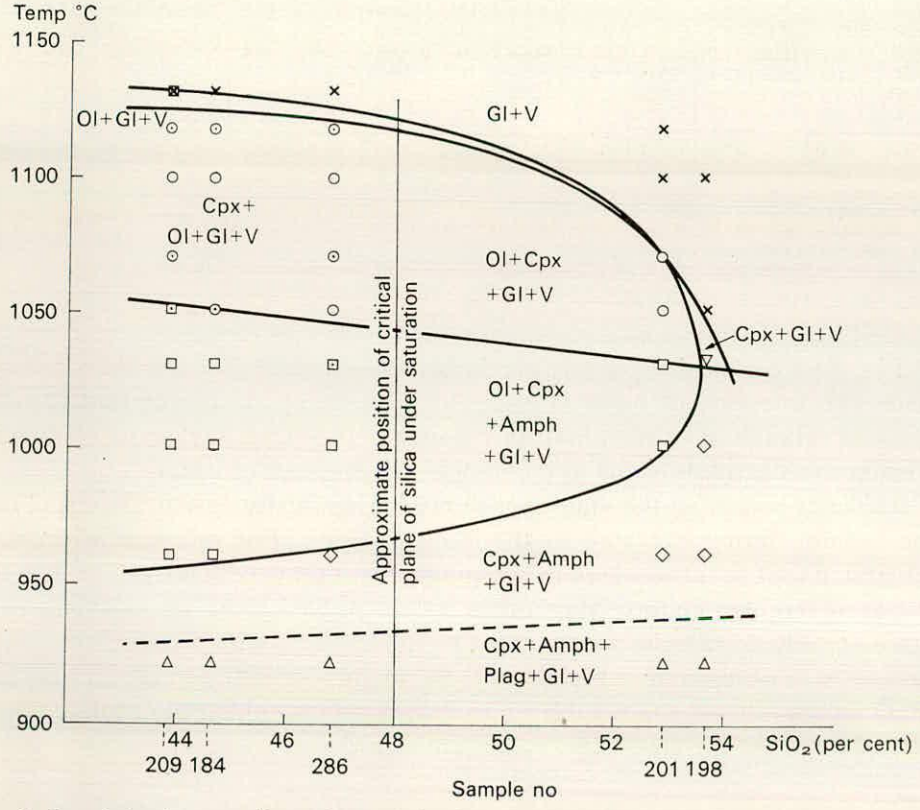

FIG. 1. Correlation between silicate phase relationships and stage of evolution in the suite, represented by SiO_2 concentrations. Experimental data from runs under 5 kb pressure with excess water and with a Ni/NiO buffer. X = assemblage Gl+V; O = Cpx+Ol+Gl+V; □ = Ol+Cpx+Amph+Gl+V; ◇ = Cpx+Amph+Gl+V; △ = Cpx+Amph+Plag+Gl+V; ▽ = Cpx+Gl+V. Symbols containing small dots represent charges with an extremely small amount of spinel, but no attempt is made to indicate its stability field. The stability field of Ol+Gl+V is the narrow, curved wedge-shaped field near the top of the diagram. Phase abbreviations as for Table 2.

Clinopyroxene

The clinopyroxenes are aluminous calcic augites, fairly low in TiO_2 and Na_2O, but extremely high in Al_2O_3 content. They have a remarkably uniform composition, regardless of assemblage or bulk composition of the charge.

Amphibole

The amphiboles are intermediate between the idealized pargasite–hastingsite end-members and common hornblende (Deer, Howie, & Zussman, 1963).

TABLE 3

Electron-microprobe analyses

	Clinopyroxenes				*Olivines*		*Glasses*				*Recalculated glasses*‡			
	*2**	*3*	*4*	*5*	*2*	*3*	*1*	*2*	*3*	*5*	*1*	*2*	*3*	*5*
SiO_2	50·7	n.a.	50·9	50·8	42·0	41·6	51·0	49·3	45·5	51·1	58·8	54·5	56·0	60·0
TiO_2	1·2	0·8	0·6	0·9	—	—	n.a.	0·5	0·5	0·5	n.a.	0·6	0·6	0·6
Al_2O_3	7·7	7·2	7·2	7·6	—	—	17·7	20·4	15·1	18·2	20·4	22·6	18·6	21·4
FeO†	5·3	5·9	5·5	8·5	16·2	13·4	6·9	4·0	5·1	2·8	7·9	4·4	6·3	3·3
MgO	12·6	10·4	11·0	10·4	42·6	42·8	0·6	2·3	3·6	0·4	0·7	2·6	4·4	0·5
CaO	21·3	20·8	22·1	21·0	0·2	—	8·3	10·5	8·6	6·7	9·6	11·6	10·6	7·9
Na_2O	0·2	—	—	0·8	—	—	2·2	2·9	2·0	4·0	2·5	3·2	2·5	4·7
K_2O	0·1	—	—	0·7	—	—	n.a.	0·4	0·8	1·4	n.a.	0·4	1·0	1·6
TOTAL	99·1	—	97·3	100·7	101·0	97·8	86·7	90·2	81·1	85·1	99·9	99·9	100·0	100·0

Amphibole analyses are presented in Table 4.

* Numbers ascribed to minerals refer to different charges; 1—basanitoid, 209; 1031 °C. 2—alkali basalt, 286; 1031 °C. 3—alkali basalt, 286; 1001 °C. 4—alkali basalt, 286; 961 °C. 5—Basaltic andesite, 198; 961 °C.

† Total iron as FeO. n.a. oxide not analysed.

‡ Recalculated glass compositions are glass analyses normalized to 100 per cent. for presentation on Fig. 2.

Glasses

The glass composition totals are invariably considerably less than 100 per cent. The solubility of water in andesites may be up to 10 per cent at 5 kb pressure (Hamilton *et al.*, 1964). It is possible, therefore, that most of the discrepancy in the totals is due to the undetected presence of water.

Replicate counts on the same spot showed a steady decrease in the count rate for sodium during exposure to the electron beam. For this reason the first integrated spot count was used in computing the sodium content, rather than the averaged repeated counts. Magnesium values proved to be unexpectedly low, but no steady decrease in counts could be observed, as with sodium, even using very short exposure times. Holloway & Burnham (op. cit.) also report very low MgO values (see especially table 9), as does Kushiro (1972). No explanation is offered here, but the glass MgO values are regarded as suspect.

THE LOW-PRESSURE THERMAL DIVIDE

Yoder & Tilley (1962) have demonstrated the importance of the low-pressure thermal divide (olivine–clinopyroxene–plagioclase) in the evolution of basaltic magmas. Lava suites are almost always confined to either the nepheline-normative or to the silica-saturated side of this divide which lies near to the critical plane of silica undersaturation within the basalt tetrahedron.

Under anhydrous conditions O'Hara (1968) has suggested that this thermal barrier may exist up to 8 kb. Mechanisms by which this divide may become inoperative demand higher pressures than this, but all the processes discussed by O'Hara (op. cit.) produce a trend towards silica-undersaturation. The reverse of these high-pressure fractionation processes could cause an increase in the degree of silica-saturation, but this would require the assimilation of large amounts of orthopyroxene, subcalcic clinopyroxene, or eclogite. A fractionation

process that produces such a trend has been considered by Westoll (1968), who suggested that the crystallization of amphiboles of suitable compositions could drive liquids in either direction through the divide.

Most of the undersaturated rocks of Grenada are less than 10 per cent nepheline-normative (Arculus, in prep.). Precipitation of material with an initially greater content of normative nepheline must have taken place to generate a trend towards silica-oversaturation. The compositions and normative values

TABLE 4

Compositions and normative values of amphiboles

	*1**	*1a*	*3†*	*3a*	*4*	*4a*	*5*	*5a*	*6*	*7*	*8*	*9*	*10*
SiO_2	42·5	42·5	43·3	43·3	43·7	43·7	43·7	43·7	42·2	41·2	40·9	41·0	41·0
TiO_2	n.a.	n.a.	1·2	1·2	1·1	1·1	0·9	0·9	2·1	2·1	2·5	2·3	1·9
Al_2O_3	15·2	15·2	13·4	13·4	13·5	13·5	15·9	15·9	13·7	14·0	14·2	13·9	13·9
Fe_2O_3	—	2·6	—	3·0	—	3·1	—	3·5	2·8	4·4	4·6	4·9	5·2
FeO	7·7	5·3	8·7	6·0	9·1	6·3	10·3	7·1	5·6	6·7	6·8	6·9	7·4
MgO	11·3	11·3	12·5	12·5	12·2	12·2	9·8	9·8	16·2	15·3	14·7	14·6	14·2
CaO	12·7	12·7	13·5	13·5	13·7	13·7	12·2	12·2	11·5	11·6	11·6	11·6	11·5
Na_2O	2·0	2·0	2·3	2·3	2·1	2·1	2·2	2·2	2·8	2·4	2·5	2·4	2·4
K_2O	n.a.	n.a.	0·7	0·7	0·6	0·6	0·9	0·9	0·4	0·3	0·3	0·3	0·3
TOTAL	—	—	95·6	95·9	96·0	96·3	95·9	96·2	97·3	98·0	98·1	97·9	97·8
or	—	—	1·2	4·3	3·7	3·7	5·5	5·5	2·4	1·6	1·7	1·7	1·8
ab	7·3	10·9	—	2·4	0·1	4·1	4·1	8·6	2·5	3·3	3·4	3·8	4·1
an	35·6	35·5	25·2	25·2	26·7	26·6	32·2	32·1	24·3	27·1	27·5	26·7	26·7
di	27·0	26·6	36·1	35·4	35·7	35·0	25·3	24·7	27·0	24·9	24·5	25·4	25·2
fo	15·5	14·5	14·4	13·0	14·4	12·6	12·8	11·6	21·1	20·0	19·0	18·7	18·3
fa	8·6	4·3	7·1	3·0	7·2	3·4	10·0	4·6	2·6	3·0	2·6	2·6	3·5
ne	6·1	4·1	11·0	9·7	10·0	7·8	8·3	5·8	11·8	9·6	9·6	9·3	9·1
mt	—	4·1	—	4·5	—	4·7	—	5·3	4·2	6·5	6·8	7·3	7·8
il	—	—	2·4	2·4	2·2	2·2	1·8	1·8	4·1	4·0	4·9	4·5	3·6

* Numbers 1–5 refer to different charges (see Table 3)—analyses with suffix *a* have recalculated FeO: Fe_2O_3 = 2. 6—xenocryst from basanitoid, G 40 (Arculus, Ph.D. thesis, in preparation). 7–10—phenocrysts in ejected blocks, St. Vincent (Lewis, 1964) T770, T896, T736, T774P.

† Contains 2·5 per cent normative leucite.

of possibly xenocrystic amphiboles from Grenada volcanics, of amphiboles from cumulus nodules (Lewis, 1964), and of the experimentally produced minerals are given in Table 4. These are all highly undersaturated and their withdrawal from the basanitoid liquids could produce the observed trend. The early appearance of amphibole after olivine and clinopyroxene, and the subsequent reaction relationship displayed by the latter minerals, is therefore, probably critical to the generation of this suite, and confirms the suggestion of Brown & Schairer (1971) that the removal of Ne-normative amphibole may be responsible for the derivation of the more evolved liquids.

DISCUSSION

Yoder & Tilley (1962) and Holloway & Burnham (1972) have shown that by increasing total and partial water pressure over the range 2–8 kb, the stability of

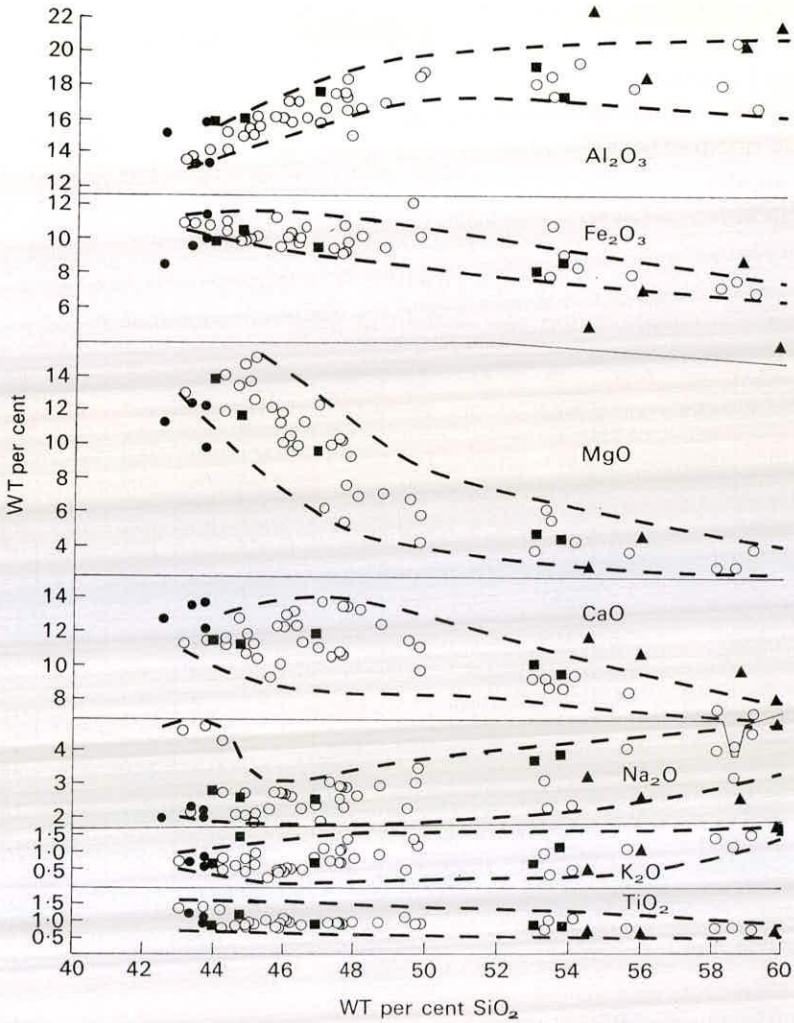

FIG. 2. Chemical variation diagram for the Grenada suite (see Arculus (in prep.) for individual analyses), plotted against SiO_2. Compositions of amphiboles and recalculated glasses are indicated for comparison with the trend. Open circles—compositions of lavas; solid squares—compositions used in this study; solid circles—experimental amphiboles; solid triangles—recalculated glass compositions; dashed lines—envelope of lava compositions enclosing liquid line of evolution, with possible modification by cumulus enrichment of lower-pressure phenocryst phases.

amphibole increases gradually by about 12 °C/kb. Over this same range of pressure, the stabilities of olivine and clinopyroxene may decrease slightly. In the present study amphibole is observed about 70 °C below the liquidus. If the pressure were increased to about 10 kb, it is likely that all three phases might begin to crystallize over a very short temperature interval.

In Fig. 2 the results of the amphibole analyses are superimposed on the chemical variation displayed by the suite, and are seen to lie on a backward

projected line for almost all the oxides (except iron, which may be attributable to iron loss to the capsule). The apparent glass compositions are also plotted. In view of the analytical problems discussed earlier the accuracy of these results is not high. In general, they show similarities to the more evolved compositions of the suite. However, as these are the result of equilibrium crystallization involving amphibole, olivine and clinopyroxene, and as it is postulated that predominantly amphibole crystallization alone may explain the evolution path of this suite perfect agreement is not expected.

Subsequent lower pressure crystallization has clouded the initial liquid trend; especially noticeable is the variable Al_2O_3 content in the more evolved rocks which may be due to varying degrees of plagioclase crystallization from an extremely aluminous liquid.

SUMMARY

Melting experiments completed at 5 kb in the presence of water on representatives of the Grenada volcanic suite, from basanitoid to basaltic andesite compositions, show that:

1. Olivine and clinopryoxene are the liquidus minerals for the suite, except for the most siliceous composition where olivine is not observed.
2. Amphibole becomes stable at lower temperature, and once present the proportion of olivine and clinopyroxene in the charges decreases. At a higher pressure, all three might appear simultaneously.
3. Plagioclase does not appear until very much lower temperatures when little liquid remains.
4. Infrequent picotite is observed in the more basic compositions.
5. The amphiboles are of a basaltic hornblende composition and are highly nepheline-normative.
6. The glasses are quartz-normative and have comparable compositions to the more evolved members of the suite.

The crucial observation of this study is that both olivine and clinopyroxene are in reaction relationship with the liquid once amphibole becomes stable. Although all three minerals co-exist over a considerable temperature range in the *equilibrium crystallization* situation recreated here, in the *fractional crystallization* case olivine and clinopyroxene will not precipitate from the liquid once amphibole appears.

Consequently, it is suggested that the unusual differentiation trend displayed by this suite, from nepheline-normative to silica-oversaturated compositions, is the result of amphibole fractionation under intermediate pressure in the presence of water.

ACKNOWLEDGEMENTS

The experimental work was carried out by one of us (R. G. C.) who gratefully acknowledges the assistance of Mr. C. E. Ford in the operation and maintenance of the equipment. Electron-probe and X-R.F. analytical work at Durham

University was aided by staff and technicians in the Geology Department. Professor M. J. O'Hara offered valuable guidance in the preparation of this manuscript.

Financial support from the Natural Environment Research Council and the Ministry of Education for Northern Ireland is acknowledged.

APPENDIX

Experimental procedure

Chemical analysis of the lavas was carried out by X-ray fluorescence on samples ground to < 100 mesh and bound with Mowiol in a compressed pellet. A small amount of this powder was crushed to < 5 mesh by hand grinding under acetone, for use in the experimental work.

10 mg of sample was loaded into $Ag_{70}Pd_{30}$ capsules together with about 1 mg water, and the tubes sealed by welding, placed on a hot plate, and reweighed to test the seal. These were loaded into larger Pt capsules containing a Ni/NiO buffer mixture and a small amount of water. They were sealed and weight-tested as before. For runs over 1100 °C, Pt inner capsules were used because of the low melting temperature of the AgPd alloy.

The charges were loaded into an internally heated gas pressure vessel of the type described by Ford (1972). A small pressure of hydrogen (1–2 bar) was introduced to prolong the life of the buffer and then argon pumped in to the required pressure.

The outer Pt capsule was reweighed after the run to ensure no loss of water, and the buffer inspected by X-ray and/or optically to ensure some Ni and NiO were preserved.

Mineral and glass analysis

Analyses were performed on a Cambridge Instruments Co. Mark II 'Geoscan' electron–microprobe, using pure metal, oxide, and simple silicate standards. The correction procedure used was that of Boyd *et al.* (1968).

REFERENCES

ARCULUS, R. J. (in preparation). The petrology of Grenada, Lesser Antilles island arc. Ph.D. thesis, University of Durham.

BOYD, F. R., FINGER, L. W., & CHAYES, F., 1968. Computer reduction of electron-probe data. *Carnegie Instn. Wash. Yearbook*, **67**, 210–15.

BROWN, G. M., & SCHAIRER, J. F., 1971. Chemical and melting relations of some calc-alkaline volcanic rocks. *Geol. Soc. Am., Memoir* **130**, 139–56.

DEER, W. A., HOWIE, R. A. & ZUSSMAN, J., 1963. *Rock forming minerals*; vol. 2, *Chain silicates*. London, Longmans.

FORD, C. E., 1972. Furnace design, temperature distribution, calibration and seal design in internally heated pressure vessels. *Progr. in Exp. Petrol.* **2**, 89–96, *N.E.R.C., London.*

FUDALI, R. F., 1965. Oxygen fugacities of basaltic and andesitic magma. *Geochim. Cosmochim. Acta*, **29**, 1063–75.

GREEN, T. H., & RINGWOOD, A. E., 1968. Genesis of the calc-alkaline igneous rock suite. *Contr. Mineral. Petrol.* **18**, 105–62.

HAMILTON, D. L., 1964. Origin of high-alumina basalt, andesite, and dacite magmas. *Science*, **146**, 635–7.

——, BURNHAM, C. W., & OSBORN, E. F., 1964. The solubility of water and effects of oxygen fugacity and water content on crystallisation of mafic magmas. *J. Petrology*, **5**, 21–39.

HOLLOWAY, J. R., & BURNHAM, C. W., 1972. Melting relations of basalt with equilibrium water pressure less than total pressure. *J. Petrology*, **13**, 1–29.

KUSHIRO, I., 1972. Effect of water on the composition of magmas formed at high pressures. *J. Petrology*, **13**, 311–34.

LEWIS, J. F., 1964. Mineralogical and petrological studies of plutonic blocks from the Soufrière volcano, St. Vincent, British West Indies. D.Phil. thesis, Oxford University, 270 pp.

MCBIRNEY, A. R. (ed.), 1969. *Proceedings of the Andesite Conference*, State of Oregon, Bull. Dept. Geol. Mineral Ind. **65**, 193 pp.

O'HARA, M. J., 1968. The bearing of phase equilibria studies in synthetic and natural systems on the origin and evolution of basic and ultrabasic rocks. *Earth Science Reviews*, **4**, 69–133.

OSBORN, E. F., 1969. The complementariness of orogenic andesite and alpine peridodite. *Geochim. Cosmochim. Acta*, **33**, 307–23.

ROEDDER, P. L., & EMSLIE, R. F., 1970. Olivine–liquid equilibria. *Contr. Miner. Petrol.* **29**, 275–89.

SIGURDSSON, H., TOMBLIN, J. F., BROWN, G. M., HOLLAND, J. G., & ARCULUS, R. J., (in press). Strongly undersaturated magmas in the Lesser Antilles island arc.

WESTOLL, N. D. S., 1968. The petrology of kentallenite. Unpubl. Ph.D. thesis, Edinburgh University, 80 pp.

YODER, H. S., 1969. Calc-alkaline andesites: experimental data bearing on the origin of their assumed characteristics. In McBirney, A. R. (ed.) *Proceedings of the Andesite Conference*, State of Oregon, Bull. Dept. Geol. Mineral Ind. **65**, 77–89.

—— & TILLEY, C. E., 1962. Origin of basaltic magmas: an experimental study of natural and synthetic rock systems. *J. Petrology*, **3**, 342–532.

FIG. 3.11

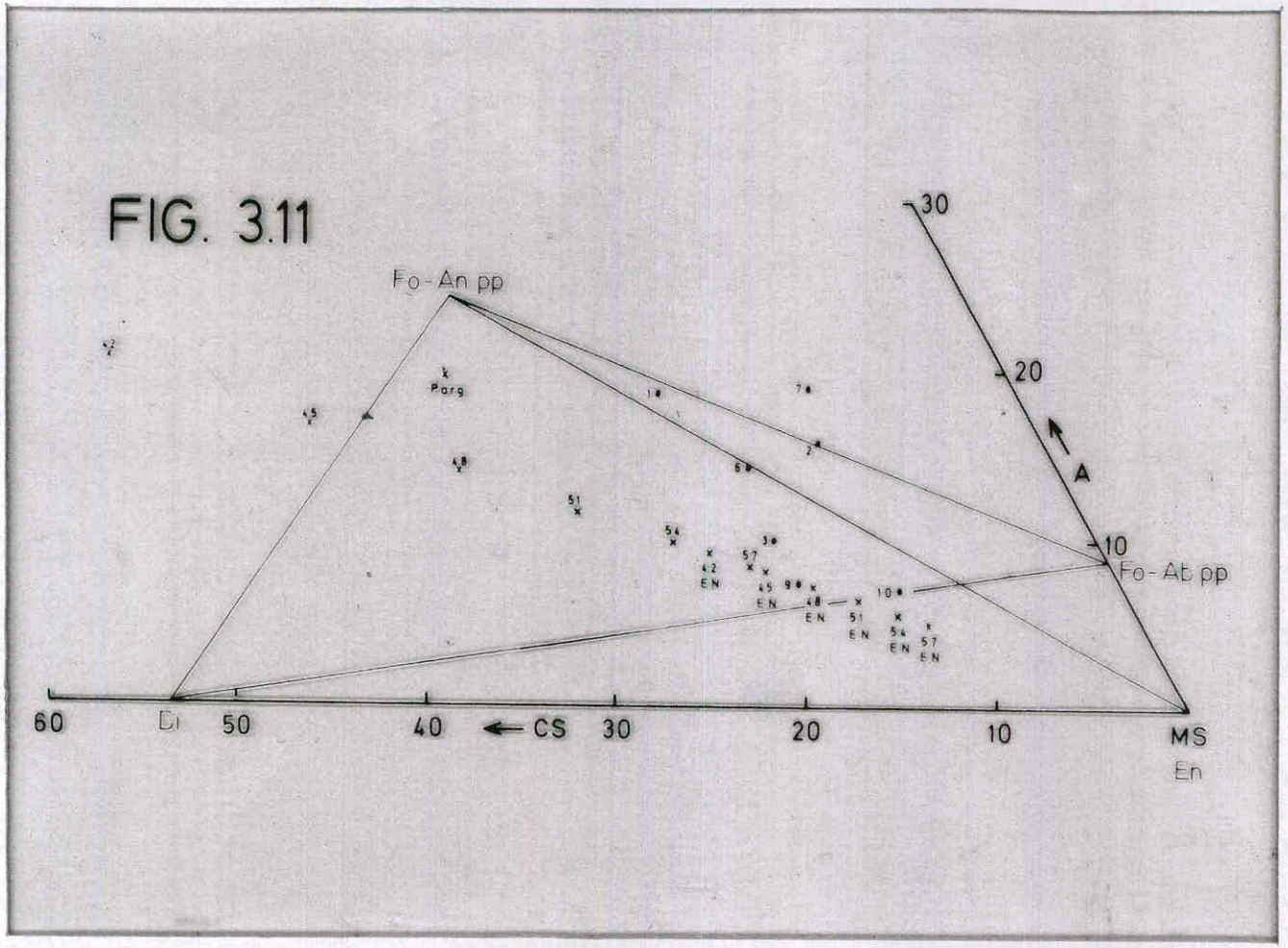

FIG. 3.13

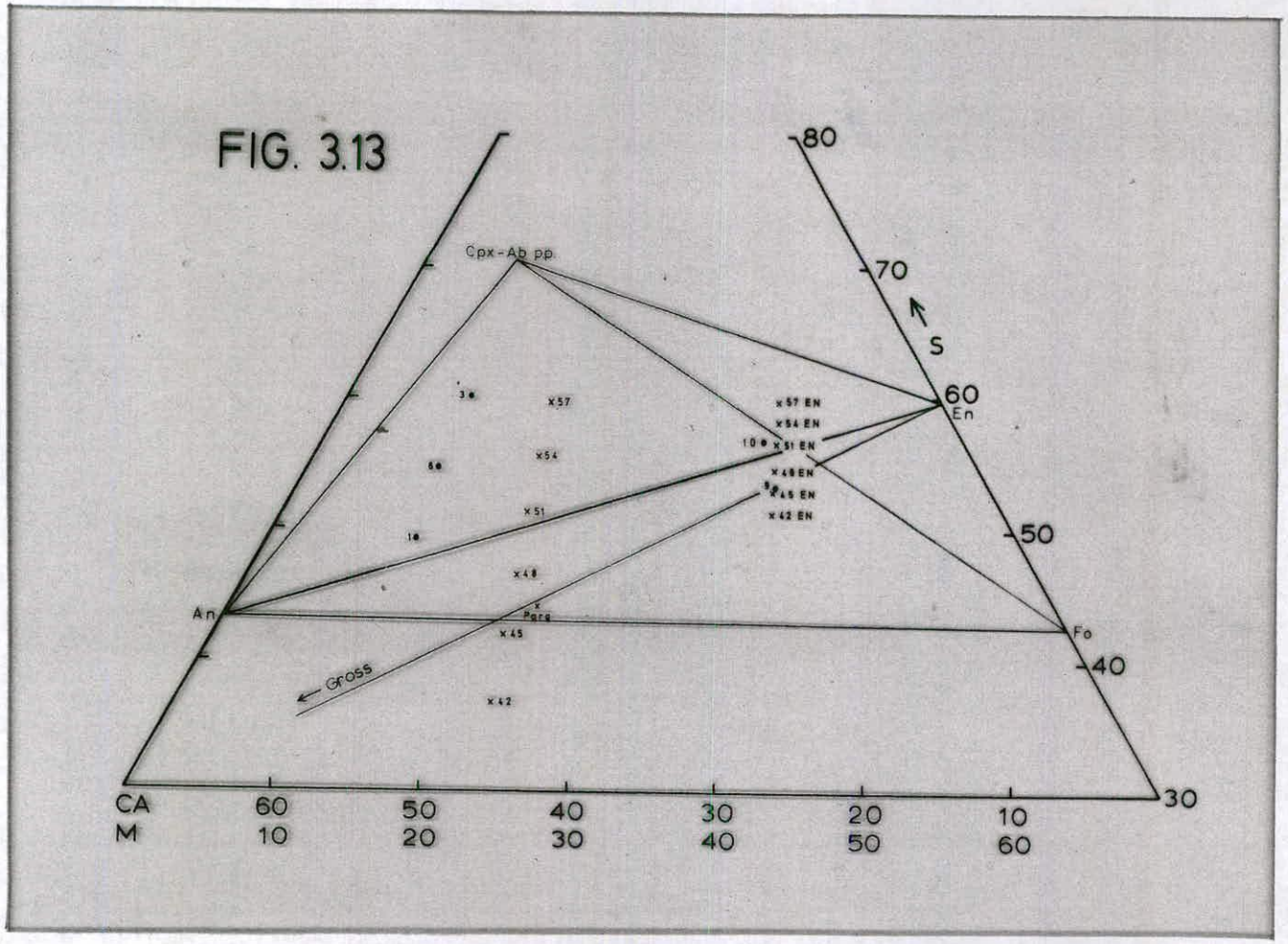
Cpx-Ab pp
80
70
S
60
En
50
40
30
Fo
An
Gross
Parg
x57
x54
x51
x48
x45
x42
x57 EN
x54 EN
x51 EN
x48 EN
x45 EN
x42 EN
CA 60 50 40 30 20 10
M 10 20 30 40 50 60